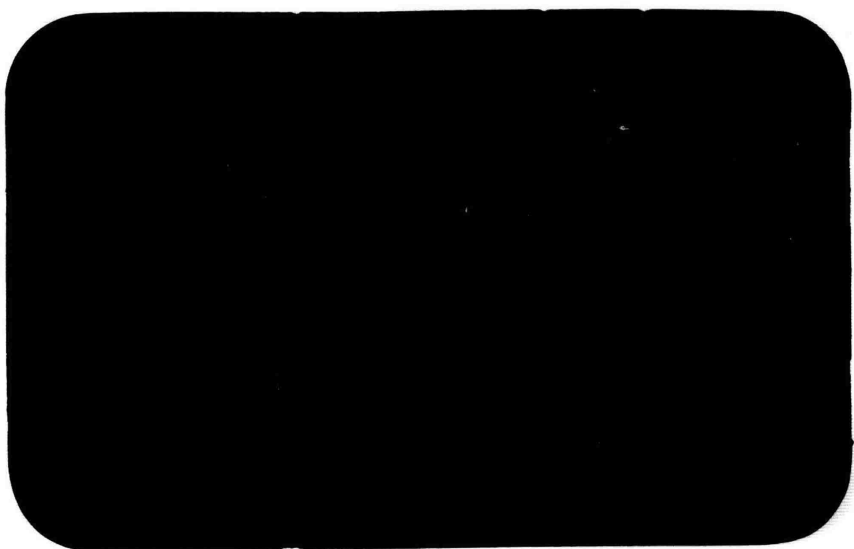


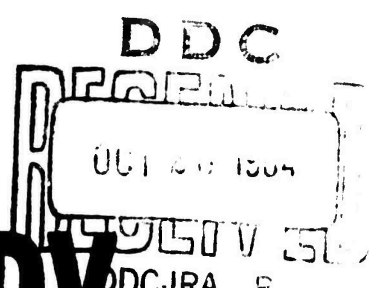
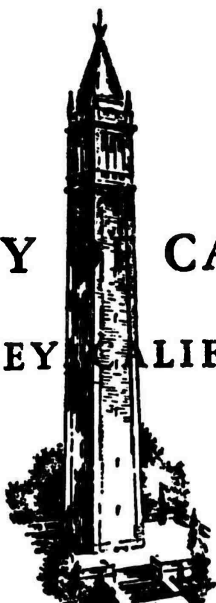
AD 607380

SPACE SCIENCES LABORATORY



COPY	/	OF	1	ent
HARD COPY	\$.	4.00		
MICROFICHE	\$.	0.75		

UNIVERSITY CALIFORNIA
BERKELEY CALIFORNIA



ARCHIVE COPY

CLEARINGHOUSE FOR FEDERAL SCIENTIFIC AND TECHNICAL INFORMATION CFSTI
DOCUMENT MANAGEMENT BRANCH 410.11

LIMITATIONS IN REPRODUCTION QUALITY

ACCESSION # AD 607380

1. WE REGRET THAT LEGIBILITY OF THIS DOCUMENT IS IN PART UNSATISFACTORY. REPRODUCTION HAS BEEN MADE FROM BEST AVAILABLE COPY.
2. A PORTION OF THE ORIGINAL DOCUMENT CONTAINS FINE DETAIL WHICH MAY MAKE READING OF PHOTOCOPY DIFFICULT.
3. THE ORIGINAL DOCUMENT CONTAINS COLOR, BUT DISTRIBUTION COPIES ARE AVAILABLE IN BLACK-AND-WHITE REPRODUCTION ONLY.
4. THE INITIAL DISTRIBUTION COPIES CONTAIN COLOR WHICH WILL BE SHOWN IN BLACK-AND-WHITE WHEN IT IS NECESSARY TO REPRINT.
5. LIMITED SUPPLY ON HAND: WHEN EXHAUSTED, DOCUMENT WILL BE AVAILABLE IN MICROFICHE ONLY.
6. LIMITED SUPPLY ON HAND: WHEN EXHAUSTED DOCUMENT WILL NOT BE AVAILABLE.
7. DOCUMENT IS AVAILABLE IN MICROFICHE ONLY.
8. DOCUMENT AVAILABLE ON LOAN FROM CFSTI (TT DOCUMENTS ONLY).
- 9.

PROCESSOR: cat

SPACE SCIENCES LABORATORY
and
INSTITUTE OF ENGINEERING RESEARCH
University of California
Berkeley 4, California

COMPUTATION OF
GASEOUS DETONATION PARAMETERS

by
C.W. Busch
A. J. Laderman
A.K. Oppenheim
Faculty Investigator

SSL Technical Note #6 on Contract NAS8-2634

Series No. 5
Issue No. 42

IER Report No. 64-12 on Grant AFOSR-AF-129-64

August, 1964

COMPUTATION OF
GASEOUS DETONATION PARAMETERS *
by
C.W. Busch, A.J. Laderman and A.K. Oppenheim
University of California, Berkeley

ABSTRACT

This report describes the development of a method programmed for a digital computer to evaluate one-dimensional detonation parameters in gaseous media. The calculations are based on the assumptions that the mixture is comprised of ideal gas constituents and that the wave process is governed by equilibrium end conditions.

Details of the analytical method of solution are presented including the IBM 7090 computer program, described in Fortran language. Sample input and output data with instructions for preparing the input data are given.

Finally, computations are performed for a number of hydrogen-oxygen mixtures from H_2+O_2 to $3H_2+O_2$ at several initial conditions covering a range in pressure from 0.1 to 760 mm Hg and in temperatures from -180 to +200°F and a comparison is made with calculations of other investigators for a stoichiometric mixture initially at NTP.

*This research was supported by the United States Air Force, through the Air Force Office of Scientific Research of the Air Research and Development Command under Grant AFOSR 129-64 and the National Aeronautics and Space Administration under Contract No. NAS8-2634.

C O N T E N T S

ABSTRACT

TABLE OF CONTENTS	i
NOMENCLATURE	ii
TABLE CAPTIONS	iv
FIGURE CAPTIONS	v
1. INTRODUCTION	1
2. DETERMINATION OF THE HUGONIOT CURVE	5
3. DETERMINATION OF THE CHAPMAN-JOUQUET STATE	10
4. DETERMINATION OF THE VON NEUMANN SPIKE	11
5. DETERMINATION OF THE POINT ON THE HUGONIOT CURVE AT $V = 1.0$	13
6. EVALUATION OF EQUILIBRIUM COMPOSITION AND EQUILIBRIUM THERMODYNAMIC DERIVATIVES	14
7. COMPUTER PROGRAM AND DATA	23
8. DISCUSSION OF RESULTS.	28
9. REFERENCES	31
10. TABLES	
11. FIGURES	

NOMENCLATURE

Dimensional Variables:

 α - sound velocity B_{jk} - defined by eq. 6.1.17 $C_{\rho i}$ - molar specific heat of i^{th} species C_p - mass specific heat of gaseous mixture f_i - defined by eq. 6.1.13 g_i - molar Gibbs free energy at i^{th} species g° - molar Gibbs free energy at i^{th} species at one atmosphere h_i - molar enthalpy of i^{th} species h - enthalpy per unit mass of the gaseous mixture m_i - molecular weight of i^{th} species m - molecular weight of gaseous mixture n_i - number of moles of i^{th} species n - total number of moles of gaseous mixture P - pressure q_j - mole fraction of j^{th} component in hypothetical system R - universal gas constant r - specific gas constant s - molar entropy per unit mass of the gaseous mixture T - absolute temperature u - particle velocity relative to the wave v - volume per unit mass of the gaseous mixture x_i - mole fraction of i^{th} species y_i - chemical symbol denoting the i^{th} species z_j - iteration parameters defined by eq. 6.1.14 β_{ij} - stoichiometric coefficients for i^{th} chemical reaction $\Delta_i h$ - enthalpy change for the i^{th} chemical reaction defined by eq. 6.2.3 $\Delta_i g$ - Gibbs free energy change for the i^{th} chemical reaction defined by eq. 6.1.15 γ - specific heat ratio μ_i - chemical potential of i^{th} species

Subscripts:

1 - denotes initial properties upstream of the wave

2 - denotes final properties downstream of the wave

f - denotes properties based on frozen composition

e - denotes properties based on equilibrium composition

Dimensionless Variables:

 $C = c_p/R$, $\mathcal{H} = h/R, T$, $M = m_2/m_1$, $M_1 = u_1/a_1$, $M_{e,2} = u_2/a_{e,2}$ $M_{f,2} = u_2/a_{f,2}$ $P = P_2/P_1$ P_{CJ} - pressure ratio at CJ state P_{VN} - pressure ratio at von Neumann spike $P_{V_{z1}}$ - pressure ratio in Hugoniot curve where $V = 1.0$ $\Theta = T_2/T_1$ $V = v_2/v_1 = u_2/u_1$ V_H - V evaluated from Hugoniot equation at given P and approximate T V_R - V evaluated on Rayleigh line at given P V_{RH} - V evaluated on Rankine-Hugoniot curve at given P V_s - V evaluated from equation of state at given P and Θ $\Delta\Theta$ - correction to Θ at specified P on Hugoniot curve ΔP_{CJ} - correction to P_{CJ} ΔP_{VN} - correction to P_{VN} $\Delta P_{V_{z1}}$ - correction to $P_{V_{z1}}$

TABLES

1. Comparison of Various Methods of Analysis.
2. Fortran Listing - Source Program.
3. Fortran Listing - Spec(a) Subroutine; Hugoniot Curve Calculations.
4. Fortran Listing - Spec(b) Subroutine; CJ Calculations.
5. Fortran Listing - Spec(c) Subroutine; Shock Conditions At Given Mach Number.
6. Fortran Listing - Main Subroutine.
7. Fortran Listing - Brink Subroutine.
8. Thermodynamic Data: Coefficients of Polynomial Expansions for Entropy at One Atmosphere, Specific Heat, and Enthalpy of Constituents of Hydrogen-Oxygen System.
9. Sample Input Data for Computer Program for $2H_2 + O_2$ Mixture Initially at $60^{\circ}F$ and 760 mmHg .
10. Sample Output: Hugoniot Curve Computed Using Spec(a) Subroutine and Input Data in Table 9.
11. Sample Output. Calculation of CJ State Using Spec(b) Subroutine and Input Data in Table 9.
12. Sample Output: Calculation of Shock Wave Parameters for Mach No. = 5.0 Using Spec(c) Subroutine and Input Data in Table 9.
13. Computed Properties of CJ Detonations in Hydrogen-Oxygen Mixtures.
14. Computed Properties at the Von Neumann Spike Corresponding to CJ States Listed in Table 13.
15. Stoichiometric Hydrogen-Oxygen Detonation Parameters.

FIGURE CAPTIONS

- 1) Determination of a Point on the Hugoniot Curve in the V-P Plane.
- 2) Determination of a Point on the Hugoniot Curve in the V-θ Plane.
- 3) P-V Diagram Showing Hugoniot Curve, Rankine-Hugoniot Curve, and CJ Rayleigh Line for $2\text{H}_2 + \text{O}_2$ Mixture at 60°F , 760 mmHg.
- 4) Determination of the CJ State in the M_e -P Plane.
- 5) Flow Diagram of Computer Program.
- 6) Hugoniot Curves for $3\text{H}_2 + \text{O}_2$ Mixture Initially at 200°F
- 7) Hugoniot Curves for Hydrogen-Oxygen Mixtures Initially at 60°F .
- 8) Hugoniot Curves for $3\text{H}_2 + \text{O}_2$ Mixture Initially at -50°F .
- 9) Hugoniot Curves for Hydrogen-Oxygen Mixtures Initially at -180°F .
- 10) Hugoniot Curve in Dimensionless Temperature-Entropy Diagram for $2\text{H}_2 + \text{O}_2$ Mixture Initially at 60°F , 760 mmHg.
- 11) Hugoniot Curve in Dimensionless Pressure-Entropy Diagram for $2\text{H}_2 + \text{O}_2$ Mixture Initially at 60°F , 760 mmHg.
- 12) Influence of Initial Pressure on CJ Pressure Ratio.
- 13) Influence of Initial Temperature on CJ Pressure Ratio for $3\text{H}_2 + \text{O}_2$ Mixture.
- 14) Influence of Initial Pressure on CJ Temperature Ratio.
- 15) Influence of Initial Pressure on CJ Detonation Velocity.
- 16) Influence of Initial Temperature on CJ Detonation Velocity for $3\text{H}_2 + \text{O}_2$ Mixture.
- 17) Influence of Initial Pressure on CJ Detonation Mach Number.
- 18) Influence of Initial Pressure on Equilibrium Composition of Product Gases for $3\text{H}_2 + \text{O}_2$ Mixture Initially at 200°F .
- 19) Influence of Initial Pressure on Equilibrium Composition of Product Gases for $3\text{H}_2 + \text{O}_2$ Mixture Initially at 60°F .
- 20) Influence of Initial Pressure on Equilibrium Composition of Product Gases for $3\text{H}_2 + \text{O}_2$ Mixture Initially at -50°F .
- 21) Influence of Initial Pressure on Equilibrium Composition of Product Gases for $3\text{H}_2 + \text{O}_2$ Mixture at -180°F .

FIGURE CAPTIONS - Continued

- 22) Influence of Initial Pressure on Equilibrium Composition of Product Gases for $2H_2+O_2$ Mixture Initially at $60^{\circ}F$.
- 23) Influence of Initial Pressure on Equilibrium Composition of Product Gases for $2H_2+O_2$ Mixture Initially at $-180^{\circ}F$.
- 24) Influence of Initial Pressure on Equilibrium Composition of Product Gases for H_2+O_2 Mixture Initially at $60^{\circ}E$
- 25) Influence of Initial Pressure on Equilibrium Composition of Product Gases for H_2+O_2 Mixture Initially at $-180^{\circ}F$.
- 26) Influence of Initial Pressure on Specific Heat at Constant Pressure. of Products at CJ State. Initial Temperature $60^{\circ}F$.
- 27) Influence of Initial Pressure on Specific Heat at Constant Pressure. of Products at CJ State. Initial Temperature $-180^{\circ}F$.
- 28) Influence of Initial Pressure on Specific Heat Ratio of Products at CJ State.
- 29) Influence of Initial Pressure on von Neumann Spike Pressure Ratio.
- 30) Influence of Initial Pressure on von Neumann Spike Temperature Ratio.
- 31) Influence of Initial Pressure on von Neumann Spike Velocity Ratio.

1. INTRODUCTION

The calculations of detonation parameters have been made by several investigators, notably Lewis and Friauf (1), Berets et al (2), Edse (3), Wolfson and Dunn (4), Luker et al (5), Eisen et al (6), Bollinger and Edse (7), Barrere's (8), Gordon and Zeleznik (9), and Bird et al (10).

The distinguishing features of the various analyses are summarized in Table 1. All have in common two basic assumptions, namely that complete thermodynamic and chemical equilibrium is established immediately downstream of the wave, so that dissipative effects and variations in chemical reaction rates can be disregarded, and that the constituents of both reactants and products behave as perfect gases.

The work in references (1), (2), (4), and (5) followed similar approaches and in particular, specified the CJ state as that for which the final Mach number, based on the frozen sound speed, was equal to unity. Lewis and Friauf made use of this condition in their equations and proceeded to calculate detonation properties by determining successive corrections to the assumed initial values of the independent variables, T_2 and ν_2 using an iterative technique. Berets et al (2) used the same method, while Wolfson and Dunn (3) and Luker et al (4) performed the calculations in a similar manner but with T_2 and p_2 as the independent variables.

It was subsequently shown, however, that the correct specification of the CJ state must be based on the equilibrium sound speed. This problem was circumvented by Edse (3) and Bollinger and Edse (7) who determined the CJ state from the condition that the corresponding wave Mach number is a minimum. An initial estimate was made for the CJ value of the final temperature in both cases, the corresponding properties on the Hugoniot curve evaluated, and then corrections to the CJ temperature found. This is essentially the approach used by Eisen et al (6) who chose, however, M_1 as the independent

parameter. The latter method gave double-valued solutions for each value of M_1 , and the CJ state was determined when both solutions converged, yielding the minimum wave Mach number. In addition, Eisen et al (6) were the first to evaluate the final equilibrium Mach number as a check on their CJ calculations.

Barrere (8) developed a graphical method for calculating detonation properties which gave results in good agreement with those of Eisen et al (6). The CJ state in this instance was defined as the point on the Hugoniot curve at which the entropy was a minimum. Incorporating this into the conservation equations, T_2 and p_2 were used as the independent variables to evaluate the CJ properties.

Zeleznik et al (9) were the first to actually utilize in their computations the principle that at the CJ state the equilibrium Mach number is unity. On this basis initial estimates were made for the independent variables β_2 and T_2 and corrections found until the Hugoniot equation and equation of state were satisfied.

Bird et al (10) computed the CJ properties by finding the point of minimum wave Mach number. Since the thermodynamic properties are functions of the final temperature, T_2 , alone, this parameter was chosen as the independent variable, eliminating the need for re-evaluation of these properties at each iteration. The program is generalized to include the presence of condensed phases in the products of reaction.

In the present work, a method was developed for the determination of detonation and deflagration parameters including, in addition to the CJ state, solutions on both the deflagration and detonation branches of the Hugoniot curve. The procedure was programmed for an IBM 7090 digital computer in Fortran language. For detonations the calculations are terminated when states with pressure ratios corresponding to the von Neumann spike on the one end,

and the condition that the density ratio is equal to unity on the other, are attained. For deflagrations, the calculations are restricted, of course, to values of the pressure ratio equal to and less than unity. It should be noted also that since the allowable chemical reactions are specified in the input data, the parameters for other processes, such as non-reactive or dissociative waves, may be easily determined.

During the initial phases of this study, the wave velocity was chosen as the independent variable, following the approach used by several other investigators. For each specification of the velocity, then, solutions on both the strong and weak branches of the Hugoniot curve were obtained and the CJ state determined when the solutions converged at the minimum value of wave velocity. However, difficulties in obtaining convergence within a desired accuracy were encountered and it has been then found that the most convenient independent variable is the pressure ratio.

Since the thermodynamic properties of each constituent are uniquely functions of the temperature alone, the temperature ratio suggests itself as a convenient independent variable. However, as shown in Figs. 10 and 11, where temperature and pressure ratios are plotted respectively against the dimensionless entropy, the variation in the pressure ratio is about ten times greater than that in the temperature ratio along the Hugoniot curve, so that choosing the pressure ratio as the independent variable allows greater latitude in making an initial estimate of its value at the CJ state.

The CJ state was specified by the condition that the local equilibrium Mach number is equal to unity which, within the accuracy of calculations, corresponds exactly to the state of minimum wave velocity.

Calculations of detonation parameters were carried out for several hydrogen-oxygen mixtures over the range of initial conditions as follows:

Composition	Initial Pressure mmHg	Initial Temperature °F
$H_2 + O_2$	760	-180
		-50
		+60
		+200
$2H_2 + O_2$	100	-180
		+60
$3H_2 + O_2$	10	-180
		+60
	1	-180
		+60
	0.1	-180
		+60

The best available source of thermodynamic data, namely the JANAF Tables (11) prepared by the Dow Chemical Company, was used in the calculations. Within the accuracy of these data, the results for the CJ wave were found to be in good agreement with those of references 6, 8, and 9 obtained for similar conditions. In addition the CJ wave velocity exhibits an increase, independently of composition, of approximately 15 percent as the initial pressure was increased from 0.1 to 760 mmHg, and a decrease of approximately 3 percent as the initial temperature was increased from -180 to +200°F. Over the same range of initial conditions, the CJ pressure and temperature ratios were found to be more sensitive functions of the initial temperature than of the initial pressure.

2. DETERMINATION OF THE HUGONIOT CURVE

The detonation wave is considered to be a one-dimensional front and the process to take place in the absence of dissipative effects so that the simple continuity, momentum, and energy equations apply. The conditions of the initial gas mixture, including its composition, are assumed to be known, while the thermodynamic properties of each constituent of both the initial mixture and final products must be specified as input data. Each gas species is assumed to obey the ideal gas law so that the thermodynamic data of each species can be expressed conveniently in the form of a polynomial expansion in terms of the temperature. Any number of chemical reactions may be considered in the equilibrium system, including the case of no chemical reaction, corresponding to the Rankine-Hugoniot curve.

The final conditions of the wave are determined from a solution to the conservation equations and the equilibrium equation of state. The equations expressing conservation of mass, momentum, and energy respectively are:

$$\frac{u_1}{v_1} = \frac{u_2}{v_2} \quad 2.1$$

$$p_2 - p_1 = \frac{u_1^2}{v_1} - \frac{u_2^2}{v_2} \quad 2.2$$

$$h_2 - h_1 = \frac{1}{2}(u_1^2 - u_2^2) \quad 2.3$$

where u is the particle velocity, v the specific volume, p the pressure, and h the enthalpy while subscripts 1 and 2 denote initial and final states of the wave, respectively. The enthalpies in the energy equation are evaluated by means of a simple summation procedure:

$$h = \sum_i x_i h_i / m \quad 2.4$$

where the x_i , the mole fractions of the i^{th} species, are determined for state 1 from the specified composition of the initial mixture and for state 2 from the composition corresponding to local thermodynamic equilibrium. The mean molecular weight is a weighted average of the molecular weights, m_i , of the i^{th} species given by the relation:

$$m = \sum_i x_i m_i \quad 2.5$$

and h_i , the molar enthalpy of the i^{th} species, can be expressed as:

$$h_i = h_i^{\circ} + \int_{T_0}^{T_2} c_{p_i} dT \quad 2.6$$

where h_i° is the enthalpy of formation at a reference temperature T_0 and c_{p_i} is the specific heat of the i^{th} species.

The conservation equations, eqs. (2.1), (2.2) and (2.3), can be combined to yield the well-known Hugoniot equation:

$$h_2 - h_1 = \frac{1}{2} (P_2 - P_1) (V_2 + V_1) \quad 2.7$$

which, expressed in dimensionless terms, has the form:

$$\mathcal{H}_2 - \mathcal{H}_1 = \frac{1}{2} (P - 1) (V + 1) \quad 2.8$$

where P is the pressure ratio, P_2/P_1 , V the volume ratio, V_2/V_1 and \mathcal{H} is the dimensionless enthalpy defined as:

$$\mathcal{H} = \frac{h}{R V} = \frac{h}{R_1 T_1} \quad 2.9$$

where T is the temperature and R , the specific gas constant, is expressed in terms of the universal gas constant R and the mean molecular weight:

$$R = R/m \quad 2.10$$

The equation of state of the medium behind the wave can be written as:

$$P_2 V_2 = R_2 T_2 \quad 2.11$$

In dimensionless form, eq. (2.11) becomes

$$PV = \Theta/m \quad 2.12$$

where Θ and m are respectively the temperature and molecular weight ratios, T_2/T_1 and m_2/m_1 , across the wave.

Since it is most convenient to work in the specific volume-temperature plane, eqs. (2.8) and (2.12) can be rearranged to yield the following expressions:

$$V = 2(\gamma_2 - \gamma_1)/(P - 1) - 1 \quad 2.13$$

$$V = \Theta/(PM) \quad 2.14$$

Both γ_2 and m can be determined, of course, once P and Θ are known; hence, by specifying a value of P , solutions to eqs. (2.13) and (2.14) can be found as shown in Fig 1. The intersection of the equation of state (2.14) and the Hugoniot equation (2.13), which represents a solution point, i.e., a point on the Hugoniot curve corresponding to final conditions of the wave, is found in the following manner. An initial choice is made for Θ and, at the specified P , the equilibrium composition and corresponding thermodynamic properties are calculated. If the initial choice of Θ was correct, then eqs. (2.13) and (2.14) would be satisfied simultaneously within the prescribed accuracy. If not, a correction to Θ , $\Delta\Theta$, is obtained by expansion of eqs. (2.13) and (2.14) in terms of a Taylor series about the initial approximation to Θ . Equating the resulting expansions and retaining only first order terms, we obtain then:

$$\Delta\Theta = (V_H - V_S)/[(\frac{\partial V}{\partial \Theta})_{P,S} - (\frac{\partial V}{\partial \Theta})_{P,H}] \quad 2.15$$

where V_H and V_S are the volume ratios evaluated from the Hugoniot equation and equation of state respectively at the specified P and previous value of Θ . Differentiating eqs. (2.13) and (2.14) with respect to Θ at constant P yields, respectively:

$$\left(\frac{\partial V}{\partial \Theta}\right)_{P,H} = \frac{2C}{P-1} \quad 2.16$$

$$\left(\frac{\partial V}{\partial \Theta}\right)_{P,S} = \frac{m}{P} \left\{ 1 - \left(\frac{\partial \log m}{\partial \log \Theta} \right)_P \right\} \quad 2.17$$

where $C = \frac{C_p}{R_1}$ is the non-dimensional equilibrium specific heat at constant P and the subscripts H and S denote differentiation in the $V-\Theta$ plane along the path of the Hugoniot equation and along the path of the equation of state respectively. The derivation of equation (2.17) is given in section 6.5. Successive corrections are made to the temperature, Θ , until the values of V computed from eqs. (2.13) and (2.14) agree within a prescribed accuracy.

Eqs. (2.13) and (2.14) can also be solved by choosing Θ as the independent variable and iterating for the correct value of P .

Eq. (2.15) then becomes

$$\Delta\Theta = (V_H - V_S) / \left[\left(\frac{\partial V}{\partial P} \right)_{\Theta,S} - \left(\frac{\partial V}{\partial P} \right)_{\Theta,H} \right] \quad 2.18$$

where the subscripts H and S now refer to differentiation in the $V-P$ plane along the Hugoniot equation and the path of the equation of state respectively. For this case eqs. (2.16) and (2.17) become respectively

$$\left(\frac{\partial V}{\partial P} \right)_{\Theta,H} = 2 \left[(P-1) \left(V - \frac{\partial V}{\partial \ln \Theta} \right) - (\chi_2 - \chi_1) \right] / (P-1)^2 \quad 2.19$$

$$\left(\frac{\partial V}{\partial P} \right)_{\Theta,S} = - \frac{V}{P} \left\{ 1 + \left(\frac{\partial \log m}{\partial \log P} \right)_\Theta \right\} \quad 2.20$$

Eq. (2.19) is obtained by straightforward differentiation of eq. (2.13), while eq. (2.20) is derived in section 6.5. Fig. 2 shows the solution for a point on the Hugoniot curve in the V-P plane. The initial conditions are the same as those of Fig. 1 and the value of Θ , Fig. 2, was chosen so that both solutions correspond to some point on the Hugoniot curve. A comparison of Figs. 1 and 2 shows that the Hugoniot equation and equation of state are nearly orthogonal in the V- Θ (constant pressure) plane while in the V-P (constant temperature) plane they are almost parallel. Hence, in addition to a wider latitude for the initial choice of the independent parameter, choosing P, rather than Θ , as the dependent variable should minimize problems associated with convergence.

For purposes of illustration, Fig. 3 shows the Hugoniot curve for a $2\text{H}_2 + \text{O}_2$ mixture initially at 60°F and 1 atmosphere in the P-V plane. Shown also is the CJ Rayleigh line whose intersection with the Rankine-Hugoniot curve defines the von Neumann spike.

3. DETERMINATION OF THE CHAPMAN JOUGUET STATE

The CJ state is defined as that state at which the final equilibrium Mach number is equal to unity. It is determined by finding the intersection of the Hugoniot curve with the line $M_{e,2} = 1$, in the $M_{e,2}$ - P plane. Fig. 4 shows the Hugoniot curve in the $M_{e,2}$ - P plane for a $2H_2+O_2$ mixture initially at 60°F and 1 atmosphere, and the line $M_{e,2} = 1$. The CJ state is determined by making an initial guess for the CJ pressure, P_{CJ} , linearizing the Hugoniot curve in the $M_{e,2}$ - P plane, and solving for corrections in the initial choice of P_{CJ} . At each approximate value of P_{CJ} , the corresponding properties on the Hugoniot curve are evaluated by the method described in the previous section.

While previously it was possible to find analytical expressions for the derivatives of the governing equations, a numerical method must be used here. The derivative of the Hugoniot curve in the $M_{e,2}$ - P plane is found by taking a small increment, δP , in the previous estimate of P_{CJ} and evaluating the corresponding incremental change in $M'_{e,2}$, $\delta M_{e,2}$. Hence, to a good approximation, the derivative of the Hugoniot curve in the $M_{e,2}$ - P plane is given by $\frac{\delta M_{e,2}}{\delta P}$, and it can be easily verified that the correction ΔP_{CJ} is given by

$$\Delta P_{CJ} = (1 - M_{e,2}) / (\delta M_{e,2} / \delta P) \quad 3.1$$

It is advisable to overestimate the initial approximation to P_{CJ} in order to insure that the corresponding value of V on the Hugoniot curve will be less than one. The stability of the iteration procedure is improved by requiring that

$$|\Delta P_{CJ}| < 1 \quad 3.2$$

which should prevent the new approximation to P_{CJ} from becoming too small and yielding an imaginary wave velocity. The iteration is continued until the value of $M_{e,2}$ is sufficiently close to one, so that ΔP_{CJ} is less than a prescribed value.

4. DETERMINATION OF THE VON NEUMANN SPIKE

The von Neumann spike conditions correspond to the properties behind a non-reactive shock wave which propagates at a Mach number equal to that of the CJ detonation. In this report the von Neumann spike is used to establish the upper limit to the Hugoniot curve. The state in the P-V plane corresponding to the von Neumann spike is determined by the intersection of the Rayleigh line, which emanates from the initial state and is tangent to the Hugoniot curve, with the Rankine-Hugoniot curve. Fig. 3 illustrates the solution for the case of a $2\text{H}_2\text{O} + \text{O}_2$ mixture initially at 60°F and 1 atmosphere. The iterative technique used in the method of solution is similar to that outlined in section 3. An initial guess is made for P_{VN} , the von Neumann spike pressure ratio and the equations of the Rayleigh line and Rankine-Hugoniot curve are linearized permitting corrections to be found to the initial choice of P_{VN} .

It is necessary to know the value of the derivatives, $\frac{\partial V}{\partial P}$, along both the Rankine-Hugoniot curve and the Rayleigh line in the P-V plane, in order to linearize the equations describing these curves. The first, $\frac{\partial V}{\partial P}_{RH}$, is found by taking a small increment in P , δP , and evaluating the corresponding increment in V , δV ; the ratio $\frac{\delta V}{\delta P}$, yields, then, a sufficiently good approximation to the derivative, $\frac{\partial V}{\partial P}_{RH}$. The second, $\frac{\partial V}{\partial P}_R$, is invariant and may be found analytically. The dimensionless Rayleigh line equation is given by:

$$(P-1) = \gamma_1 M_1^2 (1-V) \quad 4.1$$

where γ_1 , and M_1 are, respectively, the initial specific heat ratio and Mach number. Since both γ_1 and M_1 remain constant along the Rayleigh line, differentiation of eq. (4.1) yields:

$$\frac{\partial V}{\partial P}_R = - \frac{1}{\gamma_1 M_1^2} \quad 4.2$$

An initial approximation to the von Neumann spike pressure, P_{VN} , is made and at this pressure, the required derivatives are evaluated as outlined above. It can easily be verified that the correction to the approximation of P_{VN} is given by:

$$\Delta P_{VN} = (V_R - V_{RH}) / \left(\left(\frac{\delta V}{\delta P} \right)_{RH} + \frac{1}{k_1 M_1^2} \right) \quad 4.3$$

where V_{RH} and V_R are, respectively, the values of the volume ratio evaluated from the equations for the Rankine-Hugoniot curve and Rayleigh line at the previous value of P_{VN} . The iteration is continued until V_{RH} is sufficiently close to V_R so that ΔP_{VN} is less than a prescribed value.

5. DETERMINATION OF THE POINT ON THE HUGONIOT CURVE AT V = 1.0

The pressure ratio, $P_{V=1}$, corresponding to the point on the Hugoniot curve where $V=1$ is used to establish the lower limit of the Hugoniot curve. It is determined by the intersection, in the $H-P$ plane, of the Hugoniot curve with a line of 45° slope passing through the point $H=H_1, P=0$, corresponding to the Hugoniot equation with $V=1.0$. The two equations are then:

$$H_2 = H_1 + \frac{1}{2}(P - 1)(V + 1) \quad 5.1$$

$$H_2 = H_1 + (P - 1) \quad 5.2$$

Similar techniques are employed to solve eqs. (5.1) and (5.2) as that used in sections 2, 3, and 4. An initial approximation is made for $P_{V=1}$, the two equations (5.1) and (5.2) are linearized at this value of $P_{V=1}$, and a correction found for the initial guess.

The derivative of eq. (5.1) in the $H-P$ plane is found by taking a small increment δP in the approximate $P_{V=1}$ and evaluating the corresponding increment in H_2 , δH_2 . Hence a good approximation to the derivative of eq. (5.1) is given by $\frac{\delta H_2}{\delta P}$. The derivative of eq. (5.2) is obviously equal to one. It can be easily verified then that the correction to the initial approximation of $P_{V=1}$ is given by:

$$\Delta P_{V=1} = (H_{2_H} - H_{2_{V=1}}) / \left(1 - \frac{\delta H_2}{\delta P}\right) \quad 5.3$$

where H_{2_H} and $H_{2_{V=1}}$ are evaluated from eqs. (5.1) and (5.2) respectively at the approximate $P_{V=1}$.

The iteration is continued again until $H_{2_{V=1}}$ is sufficiently close to H_{2_H} , that $\Delta P_{V=1}$ is less than a prescribed value.

6. EVALUATION OF EQUILIBRIUM COMPOSITION AND EQUILIBRIUM THERMODYNAMIC DERIVATIVES

The preceding analysis requires the evaluation of the equilibrium composition of a multicomponent mixture of gases at a specified temperature and pressure. Brinkley (12) has developed a convenient method for equilibrium calculations for use in machine computation, and this procedure has been adopted for our work.

6.1 Equilibrium Composition

Following Brinkley (12) and Obert (14), we shall consider the products to consist of a certain number of species, referred to as constituents, of which a certain minimum number are components. The distinction between constituents and components is derived from the fact that in a closed system at a given pressure and temperature in which departures from equilibrium are considered, a component is defined as an independent variable while a constituent is defined as a dependent variable. (In an equilibrium system at a given pressure and temperature, the composition is fixed and hence the components may not be varied independently). For example, consider a closed system in which H_2 , O_2 , and H_2O are present at a given pressure and temperature. Any two of the three constituents may be considered as components. Formal rules for selecting components were given by Brinkley (13).

The constituents of the equilibrium system can be expressed symbolically in terms of the components in the following form:

$$Y_i = \sum_j \beta_{ij} Y_j$$

6.1.1

where Y_i designates the chemical symbol of the i^{th} constituent, Y_j - the chemical symbol of the j^{th} component, and β_{ij} are the stoichiometric coefficients. In this section, i subscripts refer to constituents and j and k

subscripts refer to components. For example, consider the hydrogen-oxygen system in which six constituents are assumed present, namely, H_2 , O_2 , H_2O , OH , H , and O , and let the components be H_2O and O_2 . Then the matrix formed by the β_{ij} 's is:

↓ Constituents	Components →	
	H_2O	O_2
H_2	1.00	-0.50
O_2	0.00	1.00
H_2O	1.00	0.00
OH	0.50	0.25
H	0.50	0.25
O	0.00	0.50

The composition of the initial mixture determines the mole fraction of each component in a hypothetical system consisting of components only. The mass balance between the hypothetical system and the equilibrium constituents is expressed then by the relationship:

$$\sum_i \beta_{ij} n_i = q_j \quad 6.1.2$$

where n_i is the number of moles of the i^{th} constituent in the equilibrium system derived from the hypothetical system. The mass action relations for the system under consideration can be expressed as:

$$\mu_i = \sum_j \beta_{ij} \mu_j \quad 6.1.3$$

where μ_i and μ_j are the chemical potentials of the i^{th} constituent and j^{th} component respectively.

Dividing eq. (6.1.2) by n , where

$$n = \sum_i n_i \quad 6.1.4$$

leads to:

$$\sum_j \beta_{ij} x_i = q_j/n \quad 6.1.5$$

which, when summed over the j components, becomes after rearrangement:

$$\frac{1}{n} = 1 + \sum_i (\beta_i - 1)x_i \quad 6.1.6$$

where β_i is defined by the relation:

$$\beta_i = \sum_j \beta_{ij} \quad 6.1.7$$

Substituting eq. (6.1.6) into eq. (6.1.5) yields finally:

$$\sum_i (\beta_{ij} - (\beta_i - 1)q_j)x_i = q_j \quad 6.1.8$$

A quantity G_j can be defined now as the residue of eq. (6.1.8), i.e.,

$$G_j = \sum_i (\beta_{ij} - (\beta_i - 1)q_j)x_i - q_j \quad 6.1.9$$

where G_j is identically zero when the correct set of x_i are substituted into eq. (6.1.9).

The chemical potential of the i^{th} ideal gas constituent may be written in the form:

$$\mu_i = \mu_i^\circ + RT \log(p x_i) \quad 6.1.10$$

where μ_i° is the chemical potential of the i^{th} constituent at the temperature in question and one atmosphere. Note that the chemical potential of a pure species is equal to the Gibbs free energy per mole. Hence, for this case:

$$\mu_i^\circ = g_i^\circ$$

6.1.11

where g_i° is the molar Gibbs free energy of the i^{th} constituent. Substituting eq. (6.1.10) into eq. (6.1.3) and rearranging terms yields:

$$\log(x_i) = f_i(p, T) - \sum_j \beta_{ij} z_j \quad 6.1.12$$

where

$$f_i(p, T) = -\log(p) - \Delta_i g^\circ / RT \quad 6.1.13$$

and z_j , the iteration parameter, has the formal definition:

$$z_j = -\log(p) - \log(x_j) \quad 6.1.14$$

The quantity, $\Delta_i g^\circ$, used in eq. (6.1.13) is defined by the relation:

$$\Delta_i g^\circ = g_i^\circ - \sum_j \beta_{ij} g_j^\circ \quad 6.1.15$$

Now an initial guess must be made for z_j . Then substituting the value of x_i from eq. (6.1.12) into eq. (6.1.9), expanding the resulting equation in a Taylor series about the approximate set of z_j , and retaining only first order terms, one obtains a set of linear equations of the form:

$$\sum_k B_{jk} \Delta z_k = G_j \quad 6.1.16$$

where

$$B_{jk} = \sum_i (\beta_{ij} - (\beta_i - 1) q_j) \beta_{ik} x_i \quad 6.1.17$$

and Δz_k are the correction terms for the initial choice of z_j . With the new values of z_j , the procedure is repeated and the iteration continued to the desired accuracy.

6.2 Evaluation of the Derivatives $\left(\frac{\partial \log x_i}{\partial \log T}\right)_P$ and $\left(\frac{\partial \log x_i}{\partial \log P}\right)_T$

Differentiating eq. (6.1.12) with respect to $\log(T)$ at constant P one obtains:

$$\left(\frac{\partial \log x_i}{\partial \log T}\right)_P = \frac{\Delta_i h}{RT} - \sum_j \beta_{ij} \left(\frac{\partial z_j}{\partial \log T}\right)_P \quad 6.2.1$$

where we have made use of the thermodynamic relation

$$\left(\frac{\partial \Delta_i g^o}{\partial \log T}\right)_P = - \frac{\Delta_i h}{T} \quad 6.2.2$$

and $\Delta_i h$ is defined as:

$$\Delta_i h = h_i - \sum_j \beta_{ij} h_j \quad 6.2.3$$

Taking the derivative of eq. (6.1.8) with respect to $\log(T)$ at constant P , where the correct set of x_i have been used, and substituting eq. (6.2.1) into the resulting expression yields:

$$\sum_k B_{jk} \left(\frac{\partial z_k}{\partial \log T}\right)_P = \sum_i (\beta_{ij} - (\beta_i - 1)q_j) x_i \Delta_i h / (RT) \quad 6.2.4$$

which gives a set of simultaneous equations from which the set of derivatives $\left(\frac{\partial z_k}{\partial \log T}\right)_P$ may be determined, allowing, finally, the evaluation of the set of derivatives $\left(\frac{\partial \log x_i}{\partial \log T}\right)_P$ from eq. (6.2.1)

The set of derivatives $\left(\frac{\partial \log x_i}{\partial \log P}\right)_T$ may be derived in a similar manner.

Differentiating eq. (6.1.12) with respect to $\log(P)$ at constant T we have now:

$$\left(\frac{\partial \log x_i}{\partial \log P}\right)_T = -1 - \sum_j \beta_{ij} \left(\frac{\partial z_j}{\partial \log P}\right)_T \quad 6.2.5$$

while taking the derivative of eq. (6.1.8) with respect to P at constant T , where again the correct set of x_i have been used, and substituting eq. (6.2.5) into the resulting expression we obtain finally:

$$\sum_k B_{jk} \left(\frac{\partial z_k}{\partial \log P}\right)_T = - q_j \quad 6.2.6$$

This provides a set of simultaneous equations from which the set of derivatives $\left(\frac{\partial z_i}{\partial \log p}\right)_T$ may be determined. Consequently, the derivatives $\left(\frac{\partial \log x_i}{\partial \log p}\right)_T$ may be evaluated from eq. (6.2.5).

6.3 Partial Derivatives of Molecular Weight

The partial derivatives of the molecular weight can be expressed most conveniently in terms of the partial derivatives of the mole fractions. Making use of a mathematical identity, we can write:

$$\left(\frac{\partial \log m}{\partial \log T}\right)_P = \frac{1}{m} \left(\frac{\partial m}{\partial \log T}\right)_P \quad 6.3.1$$

With the use of eq. (2.5), where m_i is, of course, a constant, we obtain:

$$\left(\frac{\partial \log m}{\partial \log T}\right)_P = \sum_i \frac{m_i x_i}{m} \left(\frac{\partial \log x_i}{\partial \log T}\right)_P \quad 6.3.2$$

Similarly, it can be shown that:

$$\left(\frac{\partial \log m}{\partial \log P}\right)_T = \sum_i \frac{m_i x_i}{m} \left(\frac{\partial \log x_i}{\partial \log P}\right)_T \quad 6.3.3$$

6.4 Evaluation of Equilibrium Specific Heat

The equilibrium specific heat per unit mass is denoted by the expression $\left(\frac{\partial h}{\partial T}\right)_P$ where

$$h = \sum_i \frac{x_i h_i}{m} \quad 6.4.1$$

Performing the indicated differentiation yeilds then:

$$C_{pe} = \sum_i \frac{x_i}{m} \left(\frac{\partial h_i}{\partial T}\right)_P + \sum_i h_i x_i \left(\frac{\partial \frac{1}{m}}{\partial T}\right)_P + \sum_i \frac{h_i}{m} \left(\frac{\partial x_i}{\partial T}\right)_P \quad 6.4.2$$

where the first term on the right hand side represents the frozen composition specific heat per unit mass, C_{pf} . Expressing the derivatives in logarithmic form we have:

$$C_{pe} = C_{pf} - \sum_i \frac{h_i x_i}{m T} \left(\frac{\partial \log m}{\partial \log T}\right)_P + \sum_i \frac{h_i x_i}{m T} \left(\frac{\partial \log x_i}{\partial \log T}\right)_P \quad 6.4.3$$

Note that for the case of frozen composition, the derivatives on the right hand side of eq. (6.4.3) vanish, leading to the identity that $C_{pe} = C_{pf}$.

6.5 Evaluation of Thermodynamic Derivatives $(\frac{\partial V}{\partial T})_P$ and $(\frac{\partial V}{\partial P})_T$

Differentiation of the ideal gas equation of state with varying molecular weight yields:

$$(\frac{\partial V}{\partial T})_P = \frac{R}{\rho m} \left(1 - (\frac{\partial \log m}{\partial \log T})_P \right) \quad 6.5.1$$

and

$$(\frac{\partial V}{\partial P})_T = -\frac{V}{P} \left(1 + (\frac{\partial \log m}{\partial \log P})_T \right) \quad 6.5.2$$

These relations are necessary to evaluate the equilibrium sound velocity and specific heat ratio, while eq. (6.5.1) has already been used in section 2.

The derivatives on the right hand side of the equations have been determined already in section 6.3.

6.6 Evaluation of the Equilibrium Specific Heat Ratio

The equilibrium specific heat ratio, γ_e , is defined as:

$$\gamma_e = \frac{C_{pe}}{C_{ve}} \quad 6.6.1$$

which upon substituting the well-known specific heat equation:

$$C_{pe} - C_{ve} = -T \left(\frac{\partial V}{\partial T} \right)_P^2 / \left(\frac{\partial V}{\partial P} \right)_T \quad 6.6.2$$

becomes:

$$\gamma_e = \frac{C_{pe}}{C_{pe} + T \left(\frac{\partial V}{\partial T} \right)_P^2 / \left(\frac{\partial V}{\partial P} \right)_T} \quad 6.6.3$$

Substituting now eqs. (6.5.1) and (6.5.2) into (6.6.3) and rearranging terms we obtain finally:

$$\gamma_e = \frac{C_{pe}}{C_{pe} - \frac{R}{m} \left[1 - \left(\frac{\partial \log m}{\partial \log T} \right)_P \right]^2 / \left[1 + \left(\frac{\partial \log m}{\partial \log P} \right)_T \right]} \quad 6.6.4$$

Note that for frozen composition, the derivatives of the molecular weight, M , vanish so that

$$\gamma_e = \gamma_f = \frac{c_{p_f}}{c_{p_f} - R/M} \quad 6.6.5$$

6.7 Evaluation of Equilibrium Sound Velocity

The equilibrium sound velocity is given by:

$$a_e^2 = \left(\frac{\partial p}{\partial v}\right)_S \quad 6.7.1$$

The above can be expressed in terms of p , v , and T and the specific heat data by a number of ways. One is by the use of the specific heat ratio

$$\gamma_e = \frac{c_{p_e}}{c_{v_e}} \quad 6.7.2$$

Now $c_{p_e} = T \left(\frac{\partial S}{\partial T} \right)_P$ and $c_{v_e} = T \left(\frac{\partial S}{\partial T} \right)_V$ so that eq. (6.7.2) becomes

$$\gamma_e = \left(\frac{\partial S}{\partial T} \right)_P / \left(\frac{\partial S}{\partial T} \right)_V \quad 6.7.3$$

Since, by the partial derivative relation between three variables,

$$\left(\frac{\partial S}{\partial T} \right)_P = - \left(\frac{\partial T}{\partial P} \right)_S \left(\frac{\partial S}{\partial P} \right)_T \quad 6.7.4$$

and

$$\left(\frac{\partial S}{\partial T} \right)_V = - \left(\frac{\partial V}{\partial T} \right)_S \left(\frac{\partial S}{\partial V} \right)_T \quad 6.7.5$$

Substituting eqs. (6.7.4) and (6.7.5) into eq. (6.7.3) and simplifying gives:

$$\gamma_e = \frac{\left(\frac{\partial T}{\partial P} \right)_S \left(\frac{\partial S}{\partial P} \right)_T}{\left(\frac{\partial V}{\partial T} \right)_S \left(\frac{\partial S}{\partial V} \right)_T} = \frac{\left(\frac{\partial T}{\partial P} \right)_S \left(\frac{\partial T}{\partial V} \right)_S}{\left(\frac{\partial P}{\partial S} \right)_T \left(\frac{\partial V}{\partial S} \right)_T} = \left(\frac{\partial P}{\partial V} \right)_S / \left(\frac{\partial P}{\partial V} \right)_T \quad 6.7.6$$

Hence

$$\left(\frac{\partial P}{\partial V} \right)_S = \gamma_e \left(\frac{\partial P}{\partial V} \right)_T \quad 6.7.7$$

Therefore the equilibrium sound velocity is given by the expression

$$a_e^2 = -v^2 \gamma_e \left(\frac{\partial P}{\partial V} \right)_T \quad 6.7.8$$

Substituting eqs. (6.5.2) and (6.6.4) into (6.7.8) yields after rearrangement

$$\alpha_e^2 = \frac{RT/m}{\left[1 + \left(\frac{\partial \log m}{\partial \log P}\right)_T\right] - \frac{R/m}{c_{p_e}} \left[1 - \left(\frac{\partial \log m}{\partial \log T}\right)_P\right]^2} \quad 6.7.9$$

for frozen composition, $\left(\frac{\partial \log m}{\partial \log P}\right)_T = \left(\frac{\partial \log m}{\partial \log T}\right)_P = 0$ and eq. (6.7.9) reduces to the classical thermodynamic relation

$$\alpha_f^2 = \gamma_f RT/m \quad 6.7.10$$

It should be noted that the equilibrium velocity of sound is not equal to $\gamma_e RT/m$. If one wishes to use a similar expression it can be done by introducing a quantity Γ such that

$$\alpha_e^2 = \Gamma RT/m \quad 6.7.11$$

Then by comparing eqs. (6.7.9) and (6.7.11)

$$\Gamma = \frac{1}{\left[1 + \left(\frac{\partial \log m}{\partial \log P}\right)_T\right] - \frac{R/m}{c_{p_e}} \left[1 - \left(\frac{\partial \log m}{\partial \log T}\right)_P\right]^2} \quad 6.7.12$$

Clearly, if the molar mass m is constant

$$\Gamma = \frac{c_{p_f}}{c_{p_e} - R/m} = \gamma_f \quad 6.7.13$$

However if the molar mass is varying,

$$\alpha_e^2 = \left(\frac{\partial P}{\partial \rho}\right)_S = \frac{P \left(\frac{\partial \log P}{\partial \log \rho}\right)_S}{\rho \left(\frac{\partial \log \rho}{\partial \log P}\right)_S} = \left(\frac{\partial \log P}{\partial \log \rho}\right)_S RT/m$$

while from the temperature-entropy relations, with e the internal energy

$$\left(\frac{\partial h}{\partial e}\right)_S = - \left(\frac{\partial \log P}{\partial \log \nu}\right)_S = \left(\frac{\partial \log P}{\partial \log \rho}\right)_S \quad 6.7.14$$

Hence

$$\Gamma = \left(\frac{\partial h}{\partial e}\right)_S$$

which should be contrasted to γ_e used in eq. (6.7.8).

7. COMPUTER PROGRAM AND DATA

The program written for the IBM 7090 digital computer at the Computer Center, University of California, Berkeley, to evaluate the detonation parameters of gaseous mixtures consists of four programs and subprograms. The Fortran listings are given in Tables 2 - 7 which are discussed below. A flow diagram illustrating the operations performed by the four sub-routines and their interdependence is shown in Fig. 5.

Table 2 Source Program

This program loads the initial data into the computer and evaluates the upstream thermodynamic properties. These initial conditions are then printed out, and several constants are evaluated from the input data which are used later in the program.

Tables 3, 4, 5 Subroutine Spec

There are three Spec subroutines which shall be denoted by Spec(a), Spec(b), and Spec(c). The purpose of the subroutine in all three cases is either to specify the pressure at which properties are to be evaluated on the Hugoniot or Rankine-Hugoniot curve, or to converge to a particular pressure, e.g. P_{cJ} , P_{VN} , or $P_{V=1}$.

The thermodynamic properties and equilibrium composition are printed out for each solution in this subroutine.

Table 6 Subroutine Main

Subroutine main is called by the Spec subroutine to determine the correct value of temperature on the Hugoniot (or Rankine-Hugoniot) curve corresponding to the given value of P . After converging to the correct Θ , the equilibrium sound velocity and specific heat ratio are evaluated and the subroutine returns to subroutine spec.

Table 7 Subroutine Brink

This subroutine is called by the subroutine main at each approximate value of T and P to evaluate the equilibrium composition and several thermodynamic properties.

Table 5 Input Data

The input data is given to the computer on IBM data cards. Instructions for putting the required data on the cards are given below. The format statement is given by each data card and the numbers on the left indicate the spaces on the card where the data must be inserted.

Data 1: 1 card (7E10. 3)

1-10:	P_i , atmospheres
11-20:	T_i , degrees Kelvin
21-30:	convergence criterion for ΔZ_j
31-40:	convergence criterion for ΔT , ΔP_{CJ} , ΔP_{VN} and ΔP_{Vz}
41-50:	increment of P for Spec(a) blank for Spec(b) and Spec(c)
51-60:	initial value at P for Spec(a) initial approximation of P_{CJ} for Spec(b) initial approximation of P_{VN} for Spec(c)
61-70:	initial approximation for T corresponding to the initial P

Data 2: 1 card (7E10. 3)

1-10:	blank
11-20:	initial approximation for P_{Vz} for Spec(b) blank for Spec(a) and Spec(c)

Data 3: 1 card (7I10)

1-10: number of pressures to be evaluated on Hugoniot curve
 for Spec(a)
 blank for Spec(b)and Spec(c)

11-20: number of constituents in downstream equilibrium system

21-30: number of components in downstream equilibrium system

31-40: number of species in upstream mixture

41-50: 1 if $P_{Y=1}$ is to be computed for Spec(b)
 0 if $P_{Y=1}$ is not to be computed for Spec(b)
 blank for Spec(a)and Spec(c)

Data 4: 1 or more cards (7I10)

1-10: subscripts of constituents appearing in initial mixture

Data 5

11-20: subscripts of constituents appearing in lists of components

Data 6: twice the number of cards as the number of constituents in downstream system

1-70: Data on each card is a line from Table 8: i. e., each card has coefficients for one species and for one temperature range. The cards with the coefficients for the constituents must appear in the order that the constituents appear in the β_{ij} , i. e., Data 8. The low temperature range coefficients must appear first followed by the high temperature range coefficients.

Data 7: 1 or more cards

10 spaces per data: molecular weights of components in order

Data 8: 1 or more cards (7E10.3)

The matrix of the stoichiometric coefficients, β_{ij} , with one or more cards for each i . If j becomes greater than 7, use two cards for each i .

Data 9: 1 or more cards

10 spaces

per data: relative composition of upstream mixture in order of Data 4.

Data 10: 1 or more cards (7A10)

10 spaces

per data: symbols of constituents

Data 11: 1 or more cards (7E10.3)

Approximate mole fractions of components in equilibrium products.

Data 12: 1 card

blank for Spec(a) and Spec(b)

value of Mach number at which shock wave properties are to be computed for Spec(c)

Table 8 Preparation of Thermodynamic Data

A fifth degree polynomial was fitted to the specific heat data of each species so that the molar specific heats were given by:

$$\frac{C_{pi}}{R} = \sum_{n=0}^5 a_{ni} (T \cdot 10^{-3})^n \quad 100 \leq T \leq 1500$$

$$\frac{C_{pi}}{R} = \sum_{n=0}^5 b_{ni} (T \cdot 10^{-3})^n \quad 1500 \leq T \leq 5100 \quad 7.6.1$$

where two series expression were used to obtain a more accurate fit over the entire temperature range. The molar enthalpy of the i^{th} species was found then by integration of eq. (7.6.1), yielding thus:

$$\frac{h_i}{RT} = \sum_{n=0}^5 a_{ni} (T \cdot 10^{-3})/(n+1) + a_{6i}/(T) \quad 100 \leq T \leq 1500$$

$$\frac{h_i}{RT} = \sum_{n=0}^5 b_{ni} (T \cdot 10^{-3})/(n+1) + b_{6i}/(T) \quad 1500 \leq T \leq 5100 \quad 7.6.2$$

where the constants of integration a_{6i} and b_{6i} were adjusted so that the enthalpy computed from both eqs. (7.6.2) were identical to the value listed in the JANAF tables at 1500°K.

Dividing eq. (7.6.1) by the temperature and integrating the resulting expression yielded finally an equation for the molar entropy:

$$\frac{S_i}{R} = a_{oi} \log T + \sum_{n=1}^{\infty} a_{ni} (T \cdot 10^{-3})^{n/2} / (n+1) + a_{7i} \quad 100 \leq T \leq 1500 \quad 7.6.3$$

$$\frac{S_i}{R} = b_{oi} \log T + \sum_{n=1}^{\infty} b_{ni} (T \cdot 10^{-3})^{n/2} / (n+1) + b_{7i} \quad 1500 \leq T \leq 5100$$

where again the constants a_{7i} and b_{7i} were adjusted to provide an identical fit with the JANAF data at 1500°K.

Table 9 lists three sets of sample input data for the computer program using Spec(a), Spec(b), and Spec(c) respectively where each set is for a 2H₂+O mixture initially at 1 atm and 288.72°K (60°F). The corresponding computer output is then listed in Tables 10 - 12.

8. DISCUSSION OF RESULTS

Detonation parameters for the forty different initial conditions listed on page 4 were calculated using the computer program and the results are presented in Figs. 6 - 31.

Figs. 6 - 9 show the P-V representation of the Hugoniot curves computed for initial pressures of .1 and 760 mm Hg. Fig. 6 presents the Hugoniot curves for a $3H_2+O_2$ mixture initially at $200^{\circ}F$, Fig. 7 shows the Hugoniot curves for all three compositions at an initial temperature of $60^{\circ}F$, Fig. 8 illustrates the results for a $3H_2+O_2$ mixture initially at $-50^{\circ}F$ while, finally Fig. 9 displays the Hugoniot curves for all compositions at an initial temperature of $-180^{\circ}F$. It is of interest to note that the Hugoniot curves are relatively independent of initial composition, and further that the CJ state in all cases has a volume, or velocity, ratio of approximately 0.54.

Figs. 10 and 11 show dimensionless temperature-entropy and pressure-entropy diagrams for the case of a $2H_2+O_2$ mixture initially at 1 atm and $60^{\circ}F$. They illustrate the classical condition that the entropy is a minimum at the CJ state. Further they indicate that the pressure variation is greater than that of the temperature over a given portion on the Hugoniot curve.

The effect of initial pressure on the CJ pressure and temperature ratios are shown respectively in Figs. 12 and 14. Fig. 13 is a cross plot of Fig. 12 for the $3H_2+O_2$ composition and illustrates the obviously greater effect of initial temperature on the CJ pressure ratio.

Figs. 15 and 17 show the effect of initial pressure on the CJ wave velocity and Mach number respectively. It is interesting to note that the CJ wave velocity is comparatively independent of initial temperature, while the Mach number is relatively independent of composition. Fig. 16, obtained from a

cross plot of Fig. 15 for the $3H_2 + O_2$ composition demonstrates the effect of initial temperature on wave velocity.

Figs. 18 - 25 show the equilibrium composition at the CJ state as a function of initial pressure for each initial composition and temperature. They reveal the interesting result that the equilibrium composition of H_2O is approximately the same for all conditions.

Figs. 26 and 27 indicate the effect of initial pressure on both frozen and equilibrium CJ specific heats for all three compositions at $-180^{\circ}F$ and $60^{\circ}F$. The frozen specific heat is seen to be independent of initial composition. More interesting yet is the comparison between the equilibrium and frozen specific heat, the former being about five times larger than the latter.

Fig. 28 illustrates the dependence of both frozen and equilibrium CJ specific heat ratios on the initial pressure. The equilibrium specific heat ratio, γ_e , is nearly independent of initial pressure and temperature, but shows a significant dependence on composition. The frozen composition specific heat ratio, γ_f , on the other hand, shows an obvious dependence on initial pressure, although it is relatively independent of initial temperature and composition.

The von Neumann spike values of P , Θ , and V are shown in Figs. 29, 30, and 31 as a function of initial pressure. It is interesting to note that the ratio of the VN pressure and temperature to the corresponding CJ values is nearly independent of the initial conditions.

The CJ properties for the initial conditions considered are tabulated in Table 13, while the von Neumann spike properties are presented in Table 14.

Finally, it is of interest to compare results of the present calculations with those obtained by other investigators together with some experimental

results. The data for CJ detonations presented in Table 15 indicate a good agreement between the various results based on the use of the equilibrium sound speed, which in general are slightly larger than both experimental measurements and those results based on frozen sound speed. The present results also agree quite well with those of Bollinger and Edse (7), which were obtained at 313°K.

REFERENCES

- 1) Lewis, B., and Friauf, J. B., Journal of the American Chemical Society 52, 1930.
- 2) Berets, D. J., Green, E. F., and Kistiakowsky, G. B., Journal of the American Chemical Society, 72, pp 1080-1086, March 1950.
- 3) Edse, R., Proceedings of the Propellant Thermodynamics and Handling Conference, Special report 12, Eng. Exp. Station, Ohio State University, June 1960.
- 4) Wolfson, B. T., and Dunn, G., Proceedings of the Propellant Thermodynamics and Handling Conference, Special Report 12, Eng. Exp. Station, Ohio State University, June 1960.
- 5) Luker, J. A., McGill, P. L., and Adler, L. B., Journal of Chemical and Engineering Data 4, pp 136-142, April 1959.
- 6) Eisen, C. L., Gross, R. A., and Rivlin, T. J., Combustion and Flame 4, pp 137-149, June 1960.
- 7) Bollinger, L. E., and Edse, R., ARS Journal 31, pp 251-256, February 1961.
- 8) Barrere S., and Barrere, M., La Recherche Aeronautique 87, pp 23-31, Mars-April, 1962.
- 9) Zeleznik, F. J., and Gordon, S., ARS Journal 32, pp 606-615, April 1962.
- 10) Bird, P. F., Duff, R. E., and Schott, G. L., A FORTRAN-FAP Code for Computing Normal Shock and Detonation Wave Parameters in Gases, Los Alamos Scientific Laboratory, University of California, September 11, 1963.
- 11) JANAF Thermochemical Data, compiled and calculated by the Dow Chemical Company, 1961.

- 12) Brinkley, S. R., "Calculation of the Thermodynamic Properties of Multi-component Systems and Evaluation of Propellant Performance Parameters" published in Kinetics, Equilibria and Performance of High Temperature Systems, The Proceedings of the First Conference, Western States Section, Combustion Institute, Butterworth and Co., London, 1959.
- 13) Brinkley, S. R., Journal of Chemical Physics 14, pp 563-565, 1946.
- 14) Obert, E. F., Concepts of Thermodynamics, McGraw-Hill, New York, 1960.

TABLE 1. Comparison of Various Methods of Analysis

<u>AUTHOR</u>	<u>SYSTEM</u>	<u>SCOPE</u>	<u>INDEPENDENT VARIABLES</u>	<u>METHOD</u>	<u>REMARKS</u>
Lewis & Friauf (1)	Hydrogen-Oxygen with inerts	CJ state	T_2, V_2	Iteration on T_2, V_2 , to satisfy conservation equations with CJ state determined from condition $M_2 = M_{2f} = 1$	Atomic oxygen not considered in the equilibrium system
Berets, et al (2)	Hydrogen, Oxygen	CJ state	T_2, V_2	Same as Lewis and Friauf	
Edse (3)	Arbitrary	Hugoniot curve and CJ state	T_2	Hugoniot curve determined by selecting arbitrary T_2 and iterating for the corresponding value of P_2 . CJ state determined when slope of Hugoniot curve is identical to slope of Rayleigh line.	
Wolfson & Dunn (4)	Arbitrary	CJ state	T_2, P_2	Iterations on T_2 and P_2 to satisfy conservation equation with CJ point determined from condition $M_2 = M_{2f} = 1.0$	
Luker et al (5)	Hydrogen, Oxygen and Steam	CJ state	T_2, P_2	Same method as Reference 1	Van de Waal equations of state used for H_2O
Eisen et al (6)	C,H,O,N,A	Hugoniot curve and CJ state	M_1	For selected values of M_1 , iterations are preformed to determine points along Hugoniot curve. CJ state specified by condition that M_1 is a minimum.	First to check CJ state with $M_{2,e} = 1$
Bollinger & Edse (7)	Hydrogen-Oxygen	CJ state	T_2	Hugoniot curve found by selecting arbitrary T_2 , and determining corresponding P_2 by iteration. The CJ state is determined by finding the value of minimum M_1 .	Equilibrium equations are incorporated directly in the conservation equations
Barrera et al (8)	Arbitrary	CJ state	P_2, T_2	Computes equilibrium composition for several values of P and T in the neighborhood of the CJ state. Values of γ_e and h are then evaluated from both the conservation equations and the equation of state. A cross plot technique yields the solution to the CJ state. The criteria for the CJ state is that of minimum entropy.	Graphical method
Zeleznik & Gordon (9)	Arbitrary	CJ state	P_2, T_2	Iteration on P_2 and T_2 with condition $M_2 = M_{2e}$ incorporated in conservation equations	Sound speed of products expressed by $c_e^2 = \Gamma R T$ where $\Gamma = \frac{P_{e,1}}{m_{e,1} h_{e,1}}$, $C_{pe} = C_{ve}$
Bird et al (10)	Arbitrary including condensed phase	Hugoniot curve & CJ state	T_2	P_2 is determined iteratively for specified T_2 to satisfy Hugoniot equation and equation of state. CJ state evaluated for M_1 minimum.	May include more than one phase in the chemical system
Present Work	Arbitrary	CJ state, von Neumann spike and Hugoniot curve	P_2	T_2 is determined iteratively for specified P_2 to satisfy Hugoniot equation and equation of state. CJ state evaluated for $M_{e,2} = 1$.	Sound speed of products expressed by $c_e^2 = V_e \frac{\partial P}{\partial V} T$ where $V_e = \frac{C_{pe}}{C_{ve}}$

TABLE 2. Fortran Listing - Source Program

```

* LIST
* LABEL
* FORTRAN
      DIMENSION A(10,10),B(20,10),BB(20),BC(20,10),C(30,10),COMP(20),
      1CPM(20),AEQ(10,10),DZ(20),G(20),GG(10),H(20),HF(20),Q(10),UU(20),
      2UB(10),WMM(20),NB(10),NX(20),X(20),Z(10),WMC(10),WMP(20),CP(20),
      3STORE(50,20),BETA(20),DH(20)
      COMMON A,AA,AAA,B,BB,BBB,BC,C,CC,COMP,CDZ,CDV,CPM,CP1,CP2,D,DP,DT,
      1DT2,DZ,G,GAMMA1,GG,H,HF,H1,H2,MM,MP,NB,NCM,NCOM,NCON,NGO,NN,NX,P,
      2P1,P2,Q,QQ,R,SONIC,T,T1,T2,U1,UU,UB,V,V1,V2,WM,WMM,WMO,X,XN,Z,ZZ,
      3E,WM1,WMC,WMP,CONV,CON,CP,EMACH2,FMACH2,XMCH1,FRSON,EQSON,GAMM2R,
      4GAMM2E,CPR,CPE,H2,STORE,U2,CVE,CVR,BETA,DH,LSMFT,DS,DU,DELP,XX,YY,
      5LX,LY,LZ,LW,LV,LU,LT,LS,LR,LD,QLOSS,SOUND,CHECKV,CHECK,N,RR,RRM,SS
1000 FORMAT (7E10.6)
1001 FORMAT (7I10)
1003 FORMAT (7A10)
1004 FORMAT (6E12.5)
1005 FORMAT (8E10.3)
      R=1.98726
      CONV=4184.
      CON=41.84/1.0139
1050 READ 1000,P1,T1,CDZ,CDV,DP,P,T,QLOSS,CHECK
      NGO=0
      NN=0
      IF(P1) 1100,2000,1055
1100 PRINT 1110
1110 FORMAT (7H STOP 1)
      CALL EXIT
1055 PRINT 1060
      ARG6=0
1060 FORMAT (56H1HUGONIOT CURVE CALCULATIONS FOR GASEOUS MIXTURES---PROP
      162HULSION DYNAMICS LABORATORY--UNIVERSITY OF CALIFORNIA--BERKELEY)
1150 READ 1001,MP,NCON,NCOM,NCM,LR
      READ 1001, (NX(I),I=1,NCM)
      READ 1001, (NB(J),J=1,NCOM)
      N=NCON
      DO 1160 I=1,NCM
      IF (N-NX(I)) 1155,1160,1160
1155 N=NX(I)
1160 CONTINUE
      MC=2*N
      READ 1005,((C(I,J),J=1,8),I=1,MC)
1200 READ 1000, (WMC(J),J=1,NCOM)
      DO 1250 I=1,N
1250 READ 1000,(B(I,J),J=1,NCOM)
      READ 1000,(X(I),I=1,NCM)
      READ 1003,(COMP(J),J=1,N)
      QQ=0.0
      DO 1300 I=1,NCM
1300 QQ=QQ+X(I)
      DO 1350 I=1,NCM
1350 X(I)=X(I)/QQ
      QQ=0.0
      DO 1500 J=1,NCOM
      Q(J)=0.0
      DO 1450 K=1,NCM

```

TABLE 2 - Continued

```

I=NX(K)
1450 Q(J)=Q(J)+B(I,J)*X(K)
1500 QQ=QQ+Q(J)
DO 1550 J=1,NCOM
1550 Q(J)=Q(J)/QQ
WMO=0
DO 1560 J=1,NCOM
1560 WMO=WMO+WMC(J)*Q(J)
WM1=WMO*QQ
RR=R/WM1
RRM=RR*T1
DO 1690 I=1,NCON
WMP(I)=0.
DO 1690 J=1,NCOM
1690 WMP(I)=WMP(I)+B(I,J)*WMC(J)
DO 1700 I=1,NCON
BB(I)=0.0
DO 1700 J=1,NCOM
1700 BB(I)=BB(I)+B(I,J)
DO 1750 I=1,NCON
DO 1750 J=1,NCOM
1750 BC(I,J)=B(I,J)-(BB(I)-1.)*Q(J)
TK=T1/1000.
1760 IF(T1-1500.) 1770,1770,1772
1770 DO 1771 K=1,NCM
I=NX(K)
1771 CPM(K)=((((C(I,6)*TK+C(I,5))*TK+C(I,4))*TK+C(I,3))*TK+C(I,2))*TK+
IC(I,1))*R
GO TO 1780
1772 DO 1773 K=1,NCM
I=NX(K)
J=I+N
1773 CPM(K)=((((C(J,6)*TK+C(J,5))*TK+C(J,4))*TK+C(J,3))*TK+C(J,2))*TK+
IC(J,1))*R
1780 CP1=0.
DO 1800 I=1,NCM
1800 CP1=CP1+CPM(I)*X(I)
GAMMA1=CP1/(CP1-R)
CP1=CP1/WM1
SONIC=GAMMA1*R*T1/WM1
U1=SQRTF(SONIC*CONV)
V1=R*T1/(WM1*R1)
V=V1*CON
IF(T1-1500.) 1810,1810,1812
1810 DO 1811 K=1,NCM
I=NX(K)
HF(K)=((((C(I,6)*TK/5.+C(I,5)/4.)*TK+C(I,4)/3.)*TK+C(I,3)/2.)*TK+
IC(I,2))*TK+C(I,1)*LOGF(T1))*R+C(I,8)*R
1811 H(K)=((((C(I,6)*TK/6.+C(I,5)/5.)*TK+C(I,4)/4.)*TK+C(I,3)/3.)*TK+
IC(I,2)/2.)*TK+C(I,1))*T1*R+C(I,7)*R
GO TO 1850
1812 DO 1813 K=1,NCM
I=NX(K)
J=N+I
HF(K)=((((C(J,6)*TK/5.+C(J,5)/4.)*TK+C(J,4)/3.)*TK+C(J,3)/2.)*TK+
IC(J,2))*TK+C(J,1)*LOGF(T1))*R+C(J,8)*R
1813 H(K)=((((C(J,6)*TK/6.+C(J,5)/5.)*TK+C(J,4)/4.)*TK+C(J,3)/3.)*TK+
IC(J,2)/2.)*TK+C(J,1))*T1*R+C(J,7)*R
1850 H1=0.
SS=0.

```

TABLE 2 - Continued

```
DO 1900 J=1,NCM
SS=SS+ X(J)*(HF(J)-R*LOGF(P1*X(J)))
1900 H1=H1+H1(J)*X(J)
H1=H1/WM1
SS=SS/R
HH=H1/RRM
HC=CP1/RR
PRINT 1950
1950 FORMAT(30HO INITIAL CONDITION OF MIXTURE)
PRINT 1960,P1,T1,HH,U1
1960 FORMAT(4HOP1=E12.5, 14HATM      TEMP=F10.4,16H DEGK  ENTHALPY=F10
,1.2,16H          SD VEL=F10.4,5HM/SEC)
PRINT 1961,V , HC,GAMMA1,WM1
1961 FORMAT(4H V1=E10.5,16HCM3/GM      CP1=F10.3,16H           GAMMA1=F10
,1.3,16H          WM1=F10.3/)
PRINT 1959,SS
1959 FORMAT(9H ENTROPY=F10.4)
PRINT 1962
1962 FORMAT(23HOCOMPOSITION OF MIXTURE/)
DO 1965 J=1,NCM
I=NXT(J)
PRINT 1963,COMP(I),X(J)
1963 FORMAT(A7,2H =E12.5)
1965 CONTINUE
READ 1000, (X(J),J=1,NCOM)
1980 CONTINUE
CALC SPEC
GO TO 1050
2000 CALI. EXIT
END
```

**TABLE 3. Fortran Listing - Spec(a) Subroutine;
Hugoniot Curve Calculations**

```

* LIST
* LABEL
* FORTRAN
SUBROUTINE SPEC
DIMENSION A(10,10),B(20,10),BB(20),BC(20,10),C(30,10),COMP(20),
1CPM(20),AEQ(10,10),DZ(20),G(20),GG(10),H(20),HF(20),Q(10),UU(20),
2UB(10),WMM(20),NB(10),NX(20),X(20),Z(10),WMC(10),WMP(20),CP(20),
3STORE(50,20),BETA(20),DH(20)
COMMON A,AA,AAA,B,BB,BBB,BC,C,CC,COMP,CDZ,CDV,CPM,CP1,CP2,D,DP,DT,
1DT2,DZ,G,GAMMA1,GG,H,HF,H1,H2,MM,MP,NB,NCM,NCOM,NCON,NGO,NN,NX,P,
2P1,P2,Q,QQ,R,SONIC,T,T1,T2,U1,UU,UB,V,V1,V2,WM,WMM,WMO,X,XN,Z,ZZ,
3E,WMI,WMC,WMP,CONV,CON,CP,EMACH2,FMACH2,XMCH1,FRSON,EQSON,GAMM2R,
4GAMM2E,CPR,CPE,H2,STORE,U2,CVE,CVR,BETA,DH,LSMFT,DS,DU,DELP,XX,YY,
5LX,LY,LZ,LW,LV,LU,LT,LS,LR,LD,QLOSS,SOUND,CHECKV,CHECK,N,RR,RRM,SS
1 FORMAT(1H )
2 FORMAT(47H1THERMODYNAMIC PROPERTIES ON THE HUGONIOT CURVE)
3 FORMAT(56HO PRESS R TEMP R VEL R MACH1 FMACH2 FMACH2 FSDVEL2
165HESDVEL2 FGAMM2 EGAMM2 FSPHT ESPHT ENTH2 MOLWT ENTROP
2Y )
4 FORMAT(F9.4,F8.4,F7.4,3F7.4,2F9.3,2F7.4,2F8.4,F10.3,F8.3,F9.4)
5 FORMAT(F10.4,9E12.5)
6 FORMAT(46H1EQUILIBRIUM COMPOSITION ON THE HUGONIOT CURVE)
7 FORMAT(10HO PRESS R 9A12)
NGO=0
2000 MM=5
LSMFT=0
K=NCON+1
LV=0
PRINT 2
PRINT 1
PRINT 3
GO TO 2250
2200 P=P+DP
2250 P2=P*P1
I2=1*T1
CALL MAIN
XX=XX/RR
H2=H2/RRM
CPE=CPE/RR
CPR=CPR/RR
IFTMM=5) 2300,2275,2275
2275 PRINT 1
MM=0
2300 PRINT 4,P,T,V,XMCH1,FMACH2,EMACH2,FRSON,EQSON,GAMM2R,GAMM2E,
1CPR,CPE,H2,WM,XX
MM=MM+1
NGO=NGO+1
LSMFT=LSMFT+1
STORE(LSMFT,1)=P
DO 2700 I=1,NCON
L=I+1
2700 STORE(LSMFT,L)=X(I)
IF(MP-NGO) 2800,2800,2750
2750 IF(40-LSMFT) 2800,2800,2200
2800 MM=5
PRINT 6

```

TABLE 4 Fortran listing - Spec(b) Subroutine; CJ Calculations

```

*      LIST
*      LABEL
*      FORTRAN
      SUBROUTINE SPEC
      DIMENSION A(10,10),B(20,10),BB(20),BC(20,10),C(30,10),COMP(20),
1CPM(20),AEQ(10,10),DZ(20),G(20),GG(10),H(20),HF(20),Q(10),UU(20),
2UB(10),WMM(20),NB(10),NX(20),X(20),Z(10),WMC(10),WMP(20),CP(20),
3STORE(50,20),BETA(20),DH(20)
      COMMON A,AA,AAA,B,BB,BBB,BC,C,CC,COMP,CDZ,CDV,CPM,CP1,CP2,D,DP,DT,
1DT2,DZ,G,GAMMA1,GG,H,HF,H1,H2,MM,MP,NB,NCM,NCOM,NCON,NGO,NN,NX,P,
2P1,P2,Q,QQ,R,SONIC,T,T1,T2,U1,UU,UB,V,V1,V2,WM,WMM,WMO,X,XN,Z,ZZ,
3E,WMM1,WMC,WMP,CONV,CON,CP,EMACH2,FMACH2,XMCH1,FRSON,EQSON,GAMM2R,
4GAMM2E,CPR,CPE,H2,STORE,U2,CVE,CVR,BETA,DH,LSMFT,DS,DU,DELP,XX,YY,
5LX,LY,LZ,LW,LV,LU,LT,LS,LR,LD,QLOSS,SOUND,CHECKV,CHECK,N,RR,RRM,SS
      IF (LR) 5,5,4
4      PX=0.
      GO TO 2100
5      PP=P
      TT=T
      P=CHECK
      P2=P*P1
      T2=T*T1
      LV=1
10     CALL MAIN
      DS=H2
      DD=H2
      BBBB=H1+V1*(P2-P1)+QLOSS
      P=P+.05
      P2=P*P1
      CALL MAIN
      DS=(H2-DS)
      AAA=V1*P1
      CC=DS/.05
      DELP=(DD-BBBB)/(AAA-CC)
      IF(ABSF(DELP)-1.) 14,12,12
12     DELP=DELP/ABSF(DELP)
14     CONTINUE
      P=P-.05+DELP
      IF(ABSF(BBBB-DD)-CDV)20,20,10
20     IF(ABSF(DELP)-CDV) 21,21,10
21     PX=P
      PRINT 22, PX
22     FORMAT(63HO THE PRESSURE RATIO OF THE HUGONIOT CURVE AT V2=V1 IS E
1QUAL TO F9.4)
      IF(PX-1.) 23,23,28
23     PRINT 25
25     FORMAT(48H THERE IS NO CHAPMAN-JOUQUET POINT FOR THIS DATA)
      GO TO 3270
28     P=PP
      T=TT
      DO 2000 I=1,NCM
      K=NX(I)
2000  DH(I)=X(K)
      DO 2050 I=1,NCM
2050  X(I)=DH(I)
2100  PRINT 2200
2200  FORMAT(1H //)
      PRINT 2250
2250  FORMAT(54H THERMODYNAMIC PROPERTIES AT THE CHAPMAN-JOUQUET POINT)
      P2=P*P1
      T2=T*T1

```

TABLE 4 - Continued

LV=0
2300 CALL MAIN
DU=EMACH2
PP=P
P=P+.05
P2=P#P1
SOUND=EMACH2
CALL MAIN
DU=+EMACH2-DU+.05
DELP=(1.-SOUND)/DU
IF(ABSF(DELP)-1.) 2310,2308,2308
2308 DELP=DELP/ABSF(DELP)
2310 CONTINUE
P=PP+DELP
P2=P#P1
IF(ABSF(SOUND-1.) -CDV) 2350,2350,2300
2350 IF(ABSF(DELP)-CDV) 2500,2500,2300
2500 CONTINUE
CALL MAIN
T=T2/T1
PRINT 2520
2520 FORMAT(56H0 PRESS R TEMP R VEL R MACH1 FMACH2 EMACH2 FSDVEL2
165HESDVEL2 FGAMM2 EGAMM2 FSPHT ESPHT ENTH2 MOLWT ENTROP
2Y)
PRINT 2560
XX=XX/RR
H2=H2/RRM
CPE=CPE/RR
CPR=CPR/RR
PRINT 2550,P,T,V,XMCH1,FMACH2,EMACH2,FRSON,EQSON,GAMM2R,GAMM2E,
1CPR,CPE,H2,WM,XX
2550 FORMAT(F9.4,F8.4,F7.4,3F7.4,2F9.3,2F7.4,2F8.4,F10.3,F8.3,F9.4)
2560 FORMAT(1H)
PRINT 2560
PRINT 2600
2600 FORMAT(54H0 EQUILIBRIUM COMPOSITION AT THE CHAPMAN-JOUQUET POINT)
PRINT 2560
LFIRST=1
IF(NCON-9) 3000,3000,2950
2950 LPRINT=9
GO TO 3050
3000 LPRINT=NCON
3050 PRINT 3060,(COMP(J),J= LFIRST,LPRINT)
3060 FORMAT(9A12)
PRINT 2560
PRINT 3070,(X(I),I=LFIRST,LPRINT)
IF(NCON-LPRINT) 3270,3270,3260
3070 FORMAT(9E12.5)
3260 LFIRST=LFIRST+9
IF(NCON-LPRINT-9) 3262,3262,3264
3262 LPRINT=NCON
GO TO 3266
3264 LPRINT=LPRINT+9
3266 PRINT 2560
GO TO 3050
3270 RETURN
END

TABLE 5. Fortran Listing - Spec (c) Subroutine, Shock Conditions at Given Mach Number

* LIST
 * LABEL
 * FORTRAN

SUBROUTINE SPEC

```

DIMENSION A(10,10),B(20,10),BB(20),BC(20,10),C(30,10),COMP(20),
1CPM(20),AEQ(10,10),DZ(20),G(20),GG(10),H(20),HF(20),Q(10),UU(20),
2UB(10),WMM(20),NB(10),NX(20),X(20),Z(10),WMC(10),WMP(20),CP(20),
3STORE(50,20),BETA(20),DH(20)
COMMON A,AA,AAA,B,BB,BBB,BC,C,CC,COMP,CDZ,CDV,CPM,CP1,CP2,D,DP,DT,
1DT2,DZ,G,GAMMA1,GG,H,HF,H1,H2,MM,MP,NB,NCM,NCON,NGO,NN,NX,P,
2P1,P2,Q,QQ,R,SONIC,T,T1,T2,U1,UU,UB,V,V1,V2,WM,WMM,WMO,X,XN,Z,ZZ,
3E,WM1,WMC,WMP,CONV,CON,CP,EMACH2,FMACH2,XMCH1,FRSON,EQSON,GAMM2R,
4GAMM2E,CPR,CPE,H2,STORE,U2,CVE,CVR,BETA,DH,LSMFT,DS,DU,DELP,XX,YY,
5LX,LY,LZ,LW,LV,LU,LT,LS,LR,LD,GLOSS,SOUND,CHECKV,CHECK,N,RR,RRM,SS

1 FORMAT(8E10.3)
LV=0
READ 1,XMCH1
ALPHA=GAMMA1*XMH1**2
T2=T*T1
9000 P2=P#P1
CALL MAIN
VRH=V
VALPH=1.-(P-1.)/ALPHA
P=P+.05
P2=P#P1
CALL MAIN
DVDP=(V-VRH)/.05
DELP=(VALPH-VRH)/(DVDP+1./ALPHA)
IF(ABSF(DELP)-1.) 9100,9100,9050
9050 DELP=DELP/ABSF(DELP)
9100 P=P-.05+DELP
IF(ABSF(DELP)-CDV) 9200,9200,9000
9200 P2=P#P1
CALL MAIN
PRINT 9400
9400 FORMAT(29H0PROPERTIES BEHIND SHOCK WAVE)
PRINT 9410
9410 FORMAT(16H0 PRESS R TEMP R VEL R MACH1 FMACH2 EMACH2 FSDVEL1
165HESDVEL2 FGAMM2 EGAMM2 FSPHT ESPHT ENTH2 MOLWT ENTROP
2Y.)
PRINT 9430
PRINT 9420,P,T,V,XMCH1,FMACH2,EMACH2,FRSON,EQSON,GAMM2R,GAMM2E,
1CPR,CPE,H2,WM,XX
9420 FORMAT(F9.4,F8.4,F7.4,3F7.4,2F9.3,2F7.4,2F8.4,F10.3,F8.3,F9.4)
PRINT 9430
9430 FORMAT(1H )
PRINT 9440
9440 FORMAT(30H0COMPOSITION BEHIND SHOCK WAVE//)
LFIRST=1
IF(NCON-91 9500,9500,9450
9450 LPRINT=9
GO TO 9550
9500 LPRINT=NCON
9550 PRINT 9560,(COMP(J),J=LFIRST,LPRINT)
9560 FORMAT(9A12)
PRINT 9430
PRINT 9570,(X(I),I=LFIRST,LPRINT)
9570 FORMAT(9E12.5)
IF(NCON-LPRINT) 9770,9770,9760
9760 LFIRST=LFIRST+9

```

TABLE 5 - Continued

```
IF(NCON-LPRINT-9) 9762,9762,9764
9762 LPRINT=NCON
GO TO 9766
9764 LPRINT=LPRINT+9
9766 PRINT 9768
9768 FORMAT(1H //)
GO TO 9550
9770 RETURN
END
```

TABLE 6. Fortran Listing - Main Subroutine.

```

*      LIST
*      LABEL
*      FORTRAN
      SUBROUTINE MAIN
      DIMENSION A(10,10),B(20,10),BB(20),BC(20,10),C(30,10),COMP(20),
1CPM(20),AEQ(10,10),DZ(20),G(20),GG(10),H(20),HF(20),Q(10),UU(20),
2UB(10),WMM(20),NB(10),NX(20),X(20),Z(10),WMC(10),WMP(20),CP(20),
3STORE(50,20),BETA(20),DH(20)
      COMMON A,AA,AAA,B,BB,BB,B,C,CC,COMP,CDZ,CDV,CPM,CP1,CP2,D,DP,DT,
1DT2,DZ,G,GAMMA1,GG,H,HF,H1,H2,MM,MP,NB,NCM,NCUM,NCON,NGO,NN,NX,P,
2P1,P2,Q,QQ,R,SONIC,T,T1,T2,U1,UU,UB,V,V1,V2,WM,WMM,WMO,X,XN,Z,ZZ,
3E,WMC,WMP,CONV,CON,CP,EMACH2,FMACH2,XMCH1,FRSON,EQSON,GAMM2R,
4GAMM2E,CPR,CPE,H2,STORE,U2,CVE,CVR,BETA,DH,LSMFT,US,DU,DELP,XX,YY,
5LX,LY,LZ,LW,LV,LU,L1,LS,LR,LD,QLOSS,SOUND,CHECKV,CHECK,N,RR,RRM,SS
4000 CALL BRINK
      PVPT=0.
      DO 4005 I=1,NCON
4005 PVPT=PVPT+WMP(I)*X(I)*BETA(I)
      PVPT=(1.-PVPT/WM)*R/(WM*P2)
      AAA=2.*CP2/(V1*(P2-P1))
      BBB=2.*(H2-H1-QLOSS)/((P2-P1)*V1)-1.
      CC=PVPT/V1
      D=R*T2/(V1*P2*WM)
      DT2=(BBB-D)/(CC-AAA)
      IF(ABSF(DT2)-400.) 4008,4008,4007
4007 DT2=400.*(DT2/(ABSF(DT2)))
4008 T2=T2+DT2
      IF(ABSF(BBB-D)-CDV) 4010,4000,4000
4010 DT2=DT2/T1
      IF(ABSF(DT2)-CDV) 4150,4000,4000
4150 V=BBB
      T=T2/T1
      IF(LV) 4200,4200,4500
4200 U1=2.*(H2-H1-QLOSS)/(1.-V**2)
      U2=(V**2)*U1
      XMCH1=SQRTF(U1/SONIC)
      GAMM2R=CPR/(CPR-R/WM)
      FRSON=GAMM2R*R*T2/WM
      FMACH2=SQRTF(U2/FRSON)
      FRSON=SQRTF(FRSON*CONV)
      DO 4300 J=1,NCOM
4300 GG(J)=-Q(J)
      ARG6=0
      LLL=ISIMEQ(10,NCOM,1,A,GG,ARG6,DZ)
      IF(LLL-1) 4320,4320,4310
4310 PRINT 4311
4311 FORMAT(7H STOP 5)
      CALL EXIT
4320 DO 4350 I=1,NCON
      BETA(I)=0.
      DO 4340 J=1,NCOM
4340 BETA(I)=BETA(I)-B(I,J)*A(J,1)
4350 BETA(I)=BETA(I)-1.
      PVPT=0.
      DO 4400 I=1,NCON
4400 PVPT=PVPT+WMP(I)*X(I)*BETA(I)

```

TABLE 6 - Continued

```
PVPT=(1.+PVPT/WM)
GAMM2E=PVTP**2*WM*R2**2/(R*PVPT*CPE)
GAMM2E=1./(1.-GAMM2E)
EQSON=GAMM2E*R*T2/(PVPT*WM)
EMACH2=SQRTF(U2/EQSON)
EQSON=SQRTF(EQSON*CONV)
XX=0.
DO 4450 I=1,NCON
  IF(X(I)*10.**10-1.) 4450,4450,4430
4430 XX=XX+X(I)*(HF(I)-R*LOGF(X(I)*P2))
4450 CONTINUE
  XX=XX/WM
4500 RETURN
END
```

TABLE 7. Fortran Listing - Brink Subroutine.

```

*      LIST
*      LABEL
*      FORTRAN
      SUBROUTINE BRINK
      DIMENSION A(10,10),B(20,10),BB(20),BC(20,10),C(30,10),COMP(20),
1CPM(20),AEQ(10,10),DZ(20),G(20),GG(10),H(20),HF(20),Q(10),UU(20),
2UB(10),WMM(20),NB(10),NX(20),X(20),Z(10),WMC(10),WMP(20),CP(20),
3STORE(50,20),BETA(20),DH(20)
      COMMON A,AA,AAA,B,BB,BBC,C,CC,COMP,CDZ,CDV,CPM,CP1,CP2,D,DP,DT,
1DT2,DZ,G,GAMMA1,GG,H,HF,M1,H2,MM,MP,NB,NCM,NCOM,NCON,NGO,NN,NX,P,
2P1,P2,Q,QQ,R,SONIC,T,T1,T2,U1,UU,UU,V,V1,V2,W,WMM,WMO,X,XN,Z,ZZ,
3E,WM1,WMC,WMP,CONV,CON,CP,EMACH2,FMACH2,XMCH1,FRSON,EQSON,GAMM2R,
4GAMM2E,CPR,CPE,H2,STORE,U2,CVE,CVR,BETA,DH,LSMFT,DS,DU,DELP,XX,YY,
5LX,LY,LZ,LW,LV,LU,LT,LS,LR,LD,QLOSS,SOUND,CHECKV,CHECK,N,RR,RRM,SS
      L=0
      TK=T2/1000.
      IF(T2-1500.) 500,500,502
 500  DO 501 I=1,NCON
      CP(I)=((((((C(I,6)*TK+C(I,5))*TK+C(I,4))*TK+C(I,3))*TK+C(I,2))*TK+
1C(I,1))*R
      H(I)=((((((C(I,6)*TK/6.+C(I,5)/5.)*TK+C(I,4)/4.)*TK+C(I,3)/3.)*TK+
1C(I,2)/2.)*TK+C(I,1))*T2*R+C(I,7)*R
      HF(I)=((((((C(I,6)*TK/5.+C(I,5)/4.)*TK+C(I,4)/3.)*TK+C(I,3)/2.)*TK+
1C(I,2))*TK+C(I,1))*LOGF(T2))*R+C(I,8)*R
 501  UU(I)=H(I)-T2*HF(I)
      GO TO 504
 502  DO 503 I=1,NCON
      J=I+N
      CP(I)=((((((C(J,6)*TK+C(J,5))*TK+C(J,4))*TK+C(J,3))*TK+C(J,2))*TK+
1C(J,1))*R
      H(I)=((((((C(J,6)*TK/6.+C(J,5)/5.)*TK+C(J,4)/4.)*TK+C(J,3)/3.)*TK+
1C(J,2)/2.)*TK+C(J,1))*R*T2+C(J,7)*R
      HF(I)=((((((C(J,6)*TK/5.+C(J,5)/4.)*TK+C(J,4)/3.)*TK+C(J,3)/2.)*TK+
1C(J,2))*TK+C(J,1))*LOGF(T2))*R+C(J,8)*R
 503  UU(I)=H(I)-T2*HF(I)
 504  DO 505 J=1,NCOM
      I=NB(J)
 505  UB(J)=UU(I)
      DO 520 I=1,NCON
      G(I)=0.0
      DO 510 J=1,NCOM
 510  G(I)=B(I,J)*UB(J)/(R*T2)+G(I)
 520  G(I)=G(I)-LOGF(P2)-UU(I)/(R*T2)
      IF(NN) 523,523,521
 521  DO 522 J=1,NCOM
 522  X(J)=WMM(J)
 523  DO 531 J=1,NCOM
 531  Z(J)=-LOGF(X(J))-LOGF(P2)
      NN=1
 540  DO 560 I=1,NCON
      X(I)=0.0
      DO 550 J=1,NCOM
 550  X(I)=X(I)-B(I,J)*Z(J)
      X(I)=X(I)+G(I)
 560  X(I)=EXP(X(I))
 564  IF(L) 565,565,610

```

TABLE 7 - Continued

```
565 DO 575 J=1,NCOM
      GG(J)=0.0
      DO 570 I=1,NCON
      570 GG(J)=GG(J)+BC(I,J)*X(I)
      575 GG(J)=GG(J)-Q(J)
      DO 580 J=1,NCOM
      DO 580 K=1,NCOM
      A(J,K)=0.0
      DO 580 I=1,NCON
      A(J,K)=A(J,K)+BC(I,J)*B(I,K)*X(I)
      580 AEQ(J,K)=A(J,K)
      ARG6=0
      LLL=ISIMEQ(10,NCOM,1,AEQ,GG,ARG6,DH)
      IF(LLL-1) 585,585,583
583 PRINT 584
584 FORMAT(6H STOP 5)
585 ZZ=0.0
      DO 590 J=1,NCOM
      Z(J)=Z(J)+AEQ(J,1)
      590 ZZ=ZZ+ABSF(AEQ(J,1))
      IF (ZZ-CDZ) 600,600,540
600 L=1
      GO TO 540
610 XN=0.
      DO 620 J=1,NCOM
      I=Nb(J)
      620 WMM(J)=X(I)
      DO 630 I=1,NCON
      630 XN=XN+BB(I)*X(I)
      XN=1./XN
      WM=WMO/XN
      H2=0.0
      DO 640 I=1,NCON
      640 H2=H2+H(I)*X(I)
      H2=H2/WM
      CPR=0.
      DO 710 I=1,NCON
      710 CPR=CPR+CP(I)*X(I)
      DO 730 I=1,NCON
      DH(I)=0.
      DO 720 J=1,NCOM
      K=Nb(J)
      720 DH(I)=DH(I)-B(I,J)*H(K)
      730 DH(I)=DH(I)+H(I)
      DO 750 J=1,NCOM
      GG(J)=0.
      DO 750 I=1,NCON
      750 GG(J)=GG(J)+BC(I,J)*X(I)*DH(I)/(R*T2)
      DO 752 I=1,NCOM
      DO 752 J=1,NCOM
      752 AEQ(I,J)=A(I,J)
      ARG6=0
      LLL=ISIMEQ(10,NCOM,1,AEQ,GG,ARG6,DZ)
      IF(LLL-1) 760,760,758
758 PRINT 759
759 FORMAT(7H STOP 5)
    CALL EXIT
760 DO 775 I=1,NCON
      BETA(I)=0.
      DO 774 J=1,NCOM
```

TABLE 7 - Contined

```
774 BETA(I)=BETA(I)-B(I,J)*AEQ(J,1)
775 BETA(I)=BETA(I)+DH(I)/(R*T2)
CPR=CPR/WM
CPE=CPR
PLNM=0.
DO 777 I=1,NCON
777 PLNM=PLNM-WMP(I)*X(I)*BETA(I)
PLNM=PLNM/(T2*WM**2)
DO 780 I=1,NCON
780 CPE=CPE+H(I)*X(I)*BETA(I)/(WM*T2)+H(I)*X(I)*PLNM
CP2=CPE
RETURN
END
```

TABLE 8. THERMODYNAMIC DATA: COEFFICIENTS

TABLE 9. Sample Input Data for Computer Program for
at 60° F and 760 mmHg.

Mixture Initially

Data for Spec(a) Subroutine

1.	288.72	.000001	.00001		20.	15.		
10.								
	6	2	2					
1	2							
3	2							
1.7747952	12.496609	-33.09569940	.682321	-23.2940095	.0387882	-863.800883	.0137790	
3.3965745	-.304322673	.4248489	-3.43487621	.2359846	-.11996245	-1023.48725	.2713790	
4.0821991	-1.11136904	.0978967	-3.05819011	.1289416	-.18128401	-30285	.013	-.380000032
4.0067420	-2.41251144	.5443704	-4.07081442	.0592515	-.440107533574	.8129	-.017819557	
2.4999245						25472.761	-.043940595	
3.0439461	-2.25985073	.9647901	-3.48223001	.5042257	-.2541731729134	.002	2.05385942	
2.8699448	.72232810	.063994338	-.09072252	.020446865	-.00147682	-741.174	.1-0.57067450	
5.8411221	-3.04058982	.2486945	-.72166208	.11018010	-.00652828	-2228.2782	-8.9705383	
8.0282346	-6.47261295	.5982138	-1.9865405	.32350238	-.01997535	-52297.751	-23.324212	
4.3902840	-1.71685631	.6660167	-.60766657	.10002323	-.00619887	.9223.8187	-2.8644487	
2.4999245						25472.761	-.043940595	
3.5206998	-1.76641331	.1796127	-.38134480	.060163981	-.0036775628790	.139	-.09613732	
18.016	32.							
1.	-.5							
1.	1.							
1.								
.5	.25							
.5	-.25							
	.5							
2.	1.							
	H2	O2	H2O	OH	H	O		
.45		.08						

Data for Spec(b) Subroutine

1.	288.72	.000001	.00001		10.	10.	
10.							
	2	2	2				
1	2						
1	2						
1.7747952	12.496609	-33.09569940	.682321	-23.2940095	.0387882	-863.800883	.0137790
3.3965745	-.304322673	.4248489	-3.43487621	.2359846	-.11996245	-1023.48725	.2713790
2.8699448	.72232810	.063994338	-.09072252	.020446865	-.00147682	-741.174	.1-0.57067450
5.8411221	-3.04058982	.2486945	-.72166208	.11018010	-.00652828	-2428.2782	-8.9705383
2.016	32.						
1.							
	1.						
2.	1.						
	H2	O2					
.666		.333					
5.							

TABLE 9 - Continued

Data for Spec(c) Subroutine

1.	288.72	.000001	.000001	1.	10.	10.	
	40	6	2	2			
	1	2					
	3	2					
1.7747952	12.426609	-33.09569940	.682327	-23.2540095	.0387882	-863.800883	.0137796
3.3965745	-.304322673	.4248489	-3.43487621	.2359846	-.11996245	-1023.48725	.2713998
4.0821991	-1.11136904	.0978967	-3.05815011	.1289416	-.18128481	-30283.013	-.38880032
4.0067420	-2.41251144	.5443704	-4.07081442	.0592515	-.440107533574	.8129	-.17879530
2.4999245						25472.761	-.45946595
3.0439461	-2.25985073	.9647901	-3.48223001	.5042257	-.2541731729134	.002	2.5385942
2.8699448	.72232810	.003974338	-.09072252	.020446865	-.00147682	-741.17471	-.57067420
5.8411221	-3.04058982	.2486945	-.72166209	.11018010	-.00552828	-2228.2782	-.8.9783383
8.0282346	-6.47261295	.5982138	-1.9865405	.32350238	-.01995635	-32297.791	-23.324212
4.3902840	-1.71685631	.6660167	-.60766657	.10002323	-.006198873223	.8187	-2.8644487
2.4999245						25472.761	-.45946595
3.5206998	-1.76641331	.1796127	-.38134430	.050163981	-.0036775628790	.139	-.59613732
18.016	32.						
1.	-.5						
	1.						
1.							
.5	.25						
.5	-.25						
	.5						
2.	1.						
	H2	O2	H2O	OH	H	O	
	.45	.08					

NOMENCLATURE FOR TABLES 10, 11, and 12

Initial Condition of Mixture

P₁ - p_1 , atm
TEMP - T_1 , °K
ENTHALPY - \mathcal{H}_1
SD VEL - a_1 , m/sec
V₁ - v_1 , cm³/gm
CP₁ - c_{p1}/R_1
GAMMA 1 - γ_1
WM₁ - m
ENTROPY - s_1/R_1

Properties Downstream of Wave

PRESS R - P
TEMP R - Θ
VEL R - V
MACH 1 - M₁
EMACH 2 - M_{e,2}
F MACH 2 - M_{f,2}
ESDVEL 2 - $a_{e,2}$, m/sec
FSDVEL 2 - $a_{f,2}$, m/sec
F GAMM 2 - γ_f
E GAMM 2 - γ_e
FSPHT - c_{p_f}/R_1
ESPHT - c_{p_e}/R_1
ENTH 2 - \mathcal{H}_2
MOLWT - m_2
ENTROPY - s_2/R_1

**Table 10: Sample Output: Hugoniot Curve Computed Using Spec(a)
Subroutine and Input Data in Table 9**

HUGONIOT CURVE CALCULATIONS FOR GASCUS FIXTURES---PROPELLUTION DYNAMICS LABORATORY--UNIVERSITY OF CALIFORNIA--HERKHEY

INITIAL CONDITION OF FIXTURE

PIN 0-1GECE .1ATM	TEMPA 280.72J0 CEGK ENTHALPYA -3.12	SD VELA 529.7653M/SEC
V1=19729E-00CP3/GP	CPI= 5.476	GAMPB1= 1.464
ENTHCV= 19.2081		WP1= 12.011

COMPOSITION OF FIXTURE
H2 = C.686887E C0
O2 = C.393333E-C0

THERMOEQUATIC PROPERTIES ON THE HUGONIOT CURVE

PRESS R	TEMP R	VEL R	MACH1	FRAHC2	ENHALP2	FSCVCL2	ESDVEL2	FGAPP2	EGAPP2	FSRPT	SSPHT	ENTH2	MCLT	ENTHCPY
10.0000	12.1512	5.994032.582711.J359511.4791	1594.7 0	1496.823	1.2107	1.2123	4.5933	24.1019	0.655	14.633	24.2279			
11.0000	12.2489	5.9115 8.9196 2.7566 2.E866 1504.795	1525.733	1.2126	1.2134	4.5967	24.0514	9.435	14.665	24.1975				
12.0000	12.3323	0.8647 7.3121 1.9938 2.0733 1506.476	1506.597	1.2135	1.2145	4.6230	23.9463	12.000	14.666	24.177				
13.0000	12.3726	0.7815 6.2536 1.4469 1.7122 1522.070	1512.257	1.2137	1.2151	4.6231	23.8573	11.571	14.627	24.1534				
14.0000	12.4356	0.7316 5.8622 1.4382 1.4963 1517.593	1517.746	1.2148	1.2166	4.6236	23.7866	11.131	14.566	24.1371				
15.0000	12.5024	0.6864 5.6383 1.2932 1.3460 1502.863	1521.088	1.2177	1.2187	4.6285	23.7298	11.687	14.579	24.122				
16.0000	12.5666	0.6476 5.5558 1.1494 1.2359 1528.395	1528.394	1.2176	1.2187	4.6116	23.6495	12.233	14.564	24.1178				
17.0000	12.6234	0.6133 5.4785 1.1071 1.1502 1593.214	1593.612	1.2185	1.2198	4.8163	23.5676	12.783	14.561	24.1116				
18.0000	12.6810	0.5828 5.3870 1.0426 1.0811 1598.762	1593.619	1.2183	1.223	4.4173	23.0253	13.336	14.517	24.1076				
19.0000	12.7373	0.5554 5.3699 0.9854 1.0230 1630.237	1634.363	1.2219	1.2219	4.6195	23.078	13.001	14.476	24.1022				
2.0000	12.7915	0.5218 5.3701 0.3390 0.3753 1620.160	1598.191	1.2188	1.2230	4.6272	23.5973	14.425	14.472	24.1074				
21.0000	12.8446	0.5084 5.3853 0.8989 0.9336 1619.301	1592.971	1.2191	1.2241	4.6265	23.5029	14.469	14.469	24.1173				
22.0000	12.8966	0.4881 0.8639 0.8973 0.9197 1617.823	1557.607	1.2194	1.2251	4.8269	23.3840	15.517	14.425	24.1116				
23.0000	12.9476	0.4495 0.4366 0.8331 0.8652 1622.537	1562.351	1.2156	1.2262	4.6293	23.3999	16.487	14.461	24.1113				
24.0000	12.9971	0.4524 0.4494 0.8258 0.8366 1627.269	1566.962	1.2221	1.2273	4.6310	23.01.3	16.582	14.376	24.1213				
25.0000	13.0560	0.4367 0.5180 0.8112 0.8112 1631.943	1571.527	1.2206	1.2266	4.6346	23.6245	17.123	14.351	24.122				
26.0000	13.0939	0.4222 0.5511 0.7587 0.7878 1636.580	1576.746	1.2226	1.2262	4.6362	23.6623	17.466	14.327	24.1171				
27.0000	13.1410	0.4087 0.5982 0.7386 0.7667 1641.186	1581.531	1.2231	1.235	4.6385	23.6632	18.196	14.322	24.116				
28.0000	13.1876	0.3962 0.6349 0.7191 0.7474 1645.759	1586.977	1.2214	1.2316	4.6607	23.6677	19.731	14.276	24.115				
29.0000	13.2330	0.3846 0.5492 0.8258 0.8258 1650.363	1589.389	1.2218	1.2326	4.6633	23.7134	19.266	14.291	24.115				
30.0000	13.2780	0.3737 0.5742 0.6870 0.7139 1654.825	1593.770	1.2221	1.2317	4.6652	23.7622	19.801	14.226	24.117				
31.0000	13.3224	0.3635 0.5793 0.6724 0.6991 1659.320	1598.122	1.2225	1.2366	4.6673	23.7721	20.335	14.227	24.119				
32.0000	13.3661	0.3539 0.6055 0.6588 0.6864 1663.794	1652.466	1.2235	1.2350	4.6695	23.8339	21.468	14.174	24.2062				
33.0000	13.4193	0.3249 0.5893 0.6461 0.6762 1668.246	1606.745	1.2232	1.2369	4.6510	23.845	21.461	14.169	24.2179				
34.0000	13.4520	0.3345 0.5913 0.6362 0.6585 1672.670	1611.027	1.2233	1.2366	4.6538	23.7677	21.934	14.123	24.2322				
35.0000	13.4941	0.3285 0.5049 0.6231 0.6469 1677.061	1615.272	1.2246	1.2350	4.6559	23.9144	22.467	14.097	24.2471				
36.0000	13.5358	0.3219 0.5180 0.6126 0.6361 1681.407	1619.503	1.2244	1.2368	4.6580	23.9534	22.399	14.071	24.2624				
37.0000	13.5770	0.3138 0.6125 0.6227 0.6258 1685.867	1623.715	1.2267	1.2412	4.6601	23.9930	23.531	14.055	24.2743				
38.0000	13.6178	0.3072 0.6165 0.5933 0.6161 1690.231	1627.997	1.2251	1.2392	4.6622	24.0349	24.302	14.119	24.295				
39.0000	13.6592	0.3016 0.6205 0.5946 0.6269 1694.900	1632.001	1.2255	1.2433	4.6642	24.0772	24.594	14.093	24.3112				
40.0000	13.6982	0.2945 0.5745 0.5972 0.5982 1699.915	1636.230	1.2259	1.2444	4.6663	24.125	25.125	13.987	24.3222				
41.0000	13.7370	0.2887 0.3282 0.5862 0.5902 1703.730	1660.380	1.2263	1.2454	4.6688	24.1645	25.658	13.941	24.3616				
42.0000	13.7770	0.2831 0.3422 0.5860 0.5921 1707.547	1684.505	1.2267	1.2465	4.6714	24.2293	26.187	13.915	24.3616				
43.0000	13.8159	0.2779 0.4359 0.5933 0.5766 1711.845	1664.617	1.2271	1.2476	4.6724	24.2546	26.717	13.887	24.3817				
44.0000	13.8544	0.2724 0.4489 0.5465 0.5475 1716.132	1657.714	1.2275	1.2466	4.6764	24.3010	27.246	13.862	24.401				
45.0000	13.8926	0.2676 0.5420 0.5399 0.5627 1727.460	1656.799	1.2275	1.2477	4.6764	24.3475	27.776	13.836	24.4119				
46.0000	13.9306	0.2636 0.5693 0.5354 0.5727 1729.676	1661.871	1.2283	1.25	4.6784	24.3966	28.304	13.811	24.4312				
47.0000	13.9682	0.2594 0.6489 0.5276 0.5479 1731.930	1666.030	1.2288	1.2610	4.6814	24.4421	28.838	13.784	24.5972				
48.0000	14.0055	0.2547 0.7017 0.5218 0.5419 1733.177	1668.978	1.2293	1.2629	4.6824	24.4900	29.368	13.756	24.6707				
49.0000	14.0429	0.2527 0.7543 0.5162 0.5361 1737.415	1673.016	1.2294	1.2719	4.6864	24.5383	29.898	13.732	24.6915				

PRESS R	H2	O2	H2C	CH	P	C
10.0000	0.15810E-00	0.48404E-01	0.95510E-00	0.12831E-00	0.75335C-01	0.34780E-01
11.0000	0.16270E-00	0.48306E-01	0.95270E-00	0.12947E-00	0.75464E-01	0.34564E-01
12.0000	0.15932E-00	0.48345E-01	0.95322E-00	0.13059E-00	0.75472E-01	0.35264E-01
13.0000	0.15995E-00	0.48339E-01	0.94702E-00	0.13156E-00	0.76520E-01	0.35028E-01
14.0000	0.16059E-00	0.48345E-01	0.94526E-00	0.13270E-00	0.77031E-01	0.35719E-01
15.0000	0.16123E-00	0.48342E-01	0.94264E-00	0.13384E-00	0.77554E-01	0.36168E-01
16.0000	0.16180E-00	0.48307E-01	0.93998E-00	0.13459E-00	0.78132E-01	0.36731E-01
17.0000	0.16254E-00	0.48441E-01	0.93727E-00	0.13552E-00	0.78741E-01	0.37170E-01
18.0000	0.16319E-00	0.48457E-01	0.93453E-00	0.13659E-00	0.79380E-01	0.37695E-01
19.0000	0.16389E-00	0.48501E-01	0.93176E-00	0.13765E-00	0.80043E-01	0.37992E-01
20.0000	0.16451E-00	0.48539E-01	0.92896E-00	0.13873E-00	0.80699E-01	0.38499E-01
21.0000	0.16517E-00	0.48600E-01	0.92614E-00	0.13984E-00	0.81164E-01	0.38719E-01
22.0000	0.16582E-00	0.48655E-01	0.92330E-00	0.14094E-00	0.81214E-01	0.39113E-01
23.0000	0.16648E-00	0.48676E-01	0.92172E-00	0.14188E-00	0.812914E-01	0.39571E-01
24.0000	0.16717E-00	0.48712E-01	0.92015E-00	0.14284E-00	0.81367E-01	0.40017E-01
25.0000	0.16777E-00	0.48743E-01	0.91846E-00	0.14380E-00	0.81445E-01	0.40555E-01
26.0000	0.16843E-00	0.48773E-01	0.91672E-00	0.14480E-00	0.81520E-01	0.41077E-01
27.0000	0.16908E					

TABLE 11. Sample Output: Calculation of CJ State Using Spec (b) Subroutine and Input Data in Table 9.

HUGONIOT CURVE CALCULATIONS FOR GASEOUS MIXTURES---PROPELLSION DYNAMICS LABORATORY---UNIVERSITY OF CALIFORNIA--BERKELEY

INITIAL CONDITION OF MIXTURE						HUGONIOT CURVE CALCULATIONS FOR GASEOUS MIXTURES---PROPELLSION DYNAMICS LABORATORY---UNIVERSITY OF CALIFORNIA--BERKELEY						
P1= 0.10000E 01ATP	TEMP= 288.71200	DEGK	ENTHALPY= /	-0.12	SD VEL= 529.7653M/SEC	V1=.19725E 04CM ³ /GM	CP1= 3.474	GAMMAL= 1.404	M1= 12.011			
V1=.19725E 04CM ³ /GM						ENTRCPY= 19.2C81						
COMPOSITION OF MIXTURE						THERMODYNAMIC PROPERTIES AT THE CHAPMAN-JOUQUET POINT						
R2 = 0.66667E CO						PRESS R . TEMP R VEL R MACH1 FMACH2 EMACH2 FSDVEL2 ESDVEL2 FGAMM2 EGAMM2 FSPPHT ESPHT						
C2 = 0.33333E-CC						19.4719 12.7629 5.3335 5.3682 0.9627 1.0000 1605.562 1345.040 1.2187 1.7224 4.6207 23.6020 14.1138 14.485 25.1053						
THE PRESSURE RATIO OF THE HUGONIOT CURVE AT V2=V1 IS EQUAL TO 9.8845						EQUILIBRIUM COMPOSITION AT THE CHAPMAN-JOUQUET POINT						
H2	O2	H2C	O+	H	O	0.16416E-00 0.48523E-01 0.53044E 00 0.13843E-00 0.80365E-01 0.38083E-01						

TABLE 12. Sample Output: Calculation of Shock Wave Parameters for Mach No. = 5.0 Using Spec (c) Subroutine and Input Data in Table 9.

HUGONIOT CURVE CALCULATIONS FOR GASEOUS MIXTURES--PROPULSION DYNAMICS LABORATORY--UNIVERSITY OF CALIFORNIA--BERKELEY

TABLE 13. Computed Properties of CJ Detonations in Hydrogen-Oxygen Mixtures.

Initial Compose Edition: 3H2402

P ₁	t ₁	a _{1,m/sec}	N ₁	u _{1,m/sec}	P	T	V	a _{f,2}	a _{e,2}	g _{3,2}	g _{5,2}	g _{f,2}
1atm	-180°F	446.16	7.2603	3239.25	36.5907	23.8059	.5393	1807.518	1746.984	1.1986	1.2189	11.475
100mm	-180°F	446.16	6.9991	3122.72	34.2422	21.6190	.5370	1751.861	1676.915	1.2009	1.2288	11.183
10mm	-180°F	446.16	6.7048	2991.41	31.6546	19.4065	.5347	1688.182	1599.612	1.2028	1.2396	10.906
1mm	-180°F	446.16	6.4249	2866.53	29.2601	17.5071	.5329	1627.183	1527.576	1.2041	1.2502	10.680
•1mm	-180°F	446.16	6.1646	2750.40	27.0963	15.8922	.5315	1570.233	1461.721	1.2051	1.2602	10.497
1atm	-50°F	532.19	6.0257	3206.81	24.6655	16.0074	.5422	1802.704	1738.678	1.2006	1.2214	11.386
100mm	-50°F	532.19	5.8026	3088.08	23.0415	14.5256	.5402	1746.150	1668.072	1.2029	1.2314	11.101
10mm	-50°F	532.19	5.5537	2955.62	21.2735	13.0406	.5383	1682.249	1590.967	1.2047	1.2422	10.832
1mm	-50°F	532.19	5.3183	2830.35	19.6491	11.7715	.5363	1621.472	1519.514	1.2059	1.2528	10.615
•1mm	-50°F	532.19	5.0999	2714.11	18.1963	10.6743	.5358	1564.921	1454.365	1.2069	1.2632	10.439
1atm	60°F	595.49	5.3471	3184.14	19.2871	12.5069	.5448	1801.025	1734.677	1.2023	1.2232	11.322
100mm	60°F	595.49	5.1447	3063.62	17.9042	11.3431	.5430	1743.856	1663.671	1.2046	1.2331	11.042
10mm	60°F	595.49	4.9204	2930.05	16.5970	10.1837	.5415	1679.744	1586.602	1.2063	1.2440	10.778
1mm	60°F	595.49	4.7080	2804.10	15.3187	9.1956	.5404	1619.025	1515.424	1.2075	1.2546	10.911
•1mm	60°F	595.49	4.5130	2687.44	14.1698	8.3577	.5398	1562.648	1450.633	1.2084	1.2650	10.394
1atm	200°F	668.056	4.7280	3158.57	15.0672	9.7704	.5483	1800.671	1731.837	1.2045	1.2252	11.250
100mm	200°F	668.056	4.3421	2900.76	12.9300	7.9504	.5458	1742.815	1660.347	1.2067	1.2351	10.735
10mm	200°F	668.056	4.1520	2773.77	11.2226	7.1379	.5452	1617.665	1512.224	1.2095	1.2567	10.508
1mm	200°F	668.056	3.9760	2656.19	11.0196	6.5292	.5450	1561.393	1447.720	1.2103	1.2671	10.340

TABLE 13 - Continued

Initial Composition: 2H₂+O₂

p ₁	t ₁	a _{1,m/sec}	u ₁	u _{1,m/sec}	P	T	V	a _{f,2}	a _{e,2}	y _{e,2}	y _{f,2}	#2
1atm	-180°F	396.175	7.3100	2896.04	37.0324	24.3919	.5379	1612.874	1557.661	1.2187	1.2141	14.702
100mm	-180°F	396.175	7.0447	2786.97	34.5105	21.9662	.5359	1560.775	1493.598	1.2216	1.2245	14.284
10mm	-180°F	396.175	6.7318	2666.97	31.8188	19.6615	.5339	1502.532	1423.938	1.2237	1.2354	13.900
1mm	-180°F	396.175	6.4474	2554.30	29.3713	17.6944	.5323	1447.493	1359.542	1.2257	1.2460	13.594
• 1mm	-180°F	396.175	6.1847	2450.22	27.1800	16.0389	.5309	1396.487	1300.903	1.2274	1.2564	13.349
1atm	60°F	529.765	5.3682	2843.88	19.4719	12.7629	.5435	1605.562	1545.640	1.2224	1.2187	14.485
100mm	60°F	529.765	5.1580	2732.53	18.1071	11.5150	.5421	1552.69	1481.19	1.2250	1.2289	14.091
10mm	60°F	529.765	4.9291	2611.26	16.6674	10.7032	.5407	1494.462	1412.029	1.2271	1.2398	13.730
1mm	60°F	529.765	4.7155	2498.11	15.3675	9.2854	.5398	1439.871	1348.540	1.2288	1.2504	13.444
• 1mm	60°F	529.765	4.5185	2393.74	14.2076	8.4293	.5393	1389.517	1290.92	1.2304	1.2607	13.213

Initial Composition: H₂+O₂

1atm	-180°F	331.505	7.1299	2363.60	34.923	22.7884	.5388	1318.225	1273.395	1.1785	1.2159	20.600
100mm	-180°F	331.505	6.8169	2286.36	32.8918	20.9133	.5366	1281.020	1226.811	1.1790	1.2241	20.154
10mm	-180°F	331.505	6.6295	2197.71	30.6036	18.9482	.5344	1237.933	1174.512	1.1802	1.2335	19.595
1mm	-180°F	331.505	6.3706	2111.89	28.4396	17.2110	.5327	1196.018	1124.932	1.1818	1.2431	19.323
• 1mm	-180°F	331.505	6.11262	2030.86	26.4501	15.7023	.5312	1156.334	1078.975	1.1837	1.2526	19.005
1atm	60°F	444.891	5.2267	2325.3	18.4466	12.0249	.5416	1314.931	1266.294	1.1810	1.2175	20.359
100mm	60°F	444.891	5.0456	2244.74	17.3177	11.0121	.5429	1276.50	1218.741	1.1819	1.2279	19.920
10mm	60°F	444.891	4.8414	2153.89	16.0712	9.9698	.5415	1232.65	1166.24	1.1834	1.2375	19.486
1mm	60°F	444.891	4.6455	2066.74	14.9074	9.0580	.5404	1190.895	1116.976	1.1853	1.2472	17.122
• 1mm	60°F	444.891	4.4617	1984.97	13.8450	8.2701	.5398	1151.42	1071.56	1.1872	1.2567	18.819

TABLE 13 - Continued

Initial Composition: 3H₂+O₂

Initial Composition: 2H₂+O₂

P ₁	t ₁	H ₂	O ₂	H ₂ O	O _H	O	P ₁	t ₁	H ₂	O ₂	H ₂ O	O _H	P ₁	t ₁	H ₂	O ₂	H ₂ O	O _H	O	
1atm	-180°F	.31933	.00665	.50747	.07179	.08414	.01062	1atm	-180°F	.15952	.046174	.55264	.13717	.070604	.033889					
10mm	-180°F	.31090	.00949	.47769	.075648	.11074	.015523	100mm	-180°F	.16628	.052092	.51396	.13233	.092943	.042401					
10mm	-180°F	.29959	.01258	.45335	.074144	.13974	.020594	10mm	-180°F	.16879	.058170	.48293	.12185	.11783	.050457					
1mm	-180°F	.28726	.01539	.43702	.068900	.16674	.024686	1mm	-180°F	.16763	.063719	.46176	.10887	.14152	.056513					
.1mm	-180°F	.27447	.017907	.42649	.061827	.19163	.027665	.1mm	-180°F	.16408	.068829	.44737	.095236	.16578	.060698					
1atm	-50°F	.31778	.00743	.49719	.074423	.09115	.012031	1atm	60°F	.16416	.048523	.53044	.13843	.080365	.038083					
100mm	-50°F	.30990	.010294	.46901	.076953	.11785	.016992	100mm	60°F	.16902	.054213	.49580	.13155	.10306	.046348					
10mm	-50°F	.29725	.013357	.44630	.074406	.14670	.021982	10mm	60°F	.16999	.060096	.46827	.11973	.12798	.053923					
1mm	-50°F	.28472	.016134	.43124	.068541	.17345	.02920	1mm	60°F	.16777	.065499	.44961	.10612	.15152	.059479					
.1mm	-50°F	.27182	.018606	.42164	.061138	.19808	.028723	.1mm	60°F	.16350	.070494	.437000	.092277	.17357	.063157					
1atm	60°F	.31671	.00799	.48981	.076281	.096122	.013077													
100mm	60°F	.30754	.010865	.46267	.077947	.12291	.018078													
10mm	60°F	.29566	.013915	.44100	.074724	.15168	.023022	1atm	-180°F	.034511	.26595	.48994	.14204	.020248	.047316					
1mm	60°F	.28298	.016673	.42673	.068452	.17829	.026864	100mm	-180°F	.043211	.26006	.46256	.14153	.031890	.060756					
.1mm	60°F	.27000	.019123	.41772	.060825	.20277	.029555	10mm	-180°F	.051053	.25660	.43792	.1336	.047005	.073633					
1atm	200°F	.31555	.0086284	.48142	.078368	.10173	.014302	1mm	-180°F	.056588	.25578	.41929	.12130	.063062	.083973					
100mm	200°F	.30625	.011512	.45535	.079127	.12861	.019349	.1mm	-180°F	.060081	.25682	.40534	.10725	.079325	.091195					
10mm	200°F	.29393	.014552	.43475	.075197	.15733	.024246	1atm	60°F	.039008	.26140	.47370	.14630	.025344	.054254					
1mm	200°F	.28110	.017291	.42131	.068492	.18382	.027993	100mm	60°F	.047215	.25651	.44795	.14282	.038071	.067431					
.1mm	200°F	.26802	.019725	.41291	.06021	.20815	.030569	10mm	60°F	.054302	.25402	.42523	.13264	.054006	.079800					
								1mm	60°F	.059089	.25394	.40823	.11910	.070550	.089089					
								.1mm	60°F	.061928	.25551	.39554	.10447	.087085	.095470					

TABLE 14. Computed Properties at the Von Neumann Spike Corresponding to CJ States Listed in Table 13.

TABLE 15. Stoichiometric Hydrogen-Oxygen Detonation Parameters
Initial Pressure 1.0 ATM

SOURCE	INITIAL TEMP. K°	MEASURED VELOCITY m/sec.	CALCULATED PARAMETERS	
			Velocity m/sec.	P ₂ atm. T ₂ °K
Lewis and Friauf (1)	291.00	2819	2806	18.05 3583
Berets et al (2)	298.16	2833	2852	18.06 3678
Luker et al (5)	298.16	---	2845	18.10 3674
Eisen et al (6)	294.00	---	2838	18.82 3675
Barrene et al (8)	298.16	---	2848	18.93 3686
Zelenik and Gordon (9)	298.15	---	2840	18.82 3681
Present Work	298.00	---	2840	18.84 3682

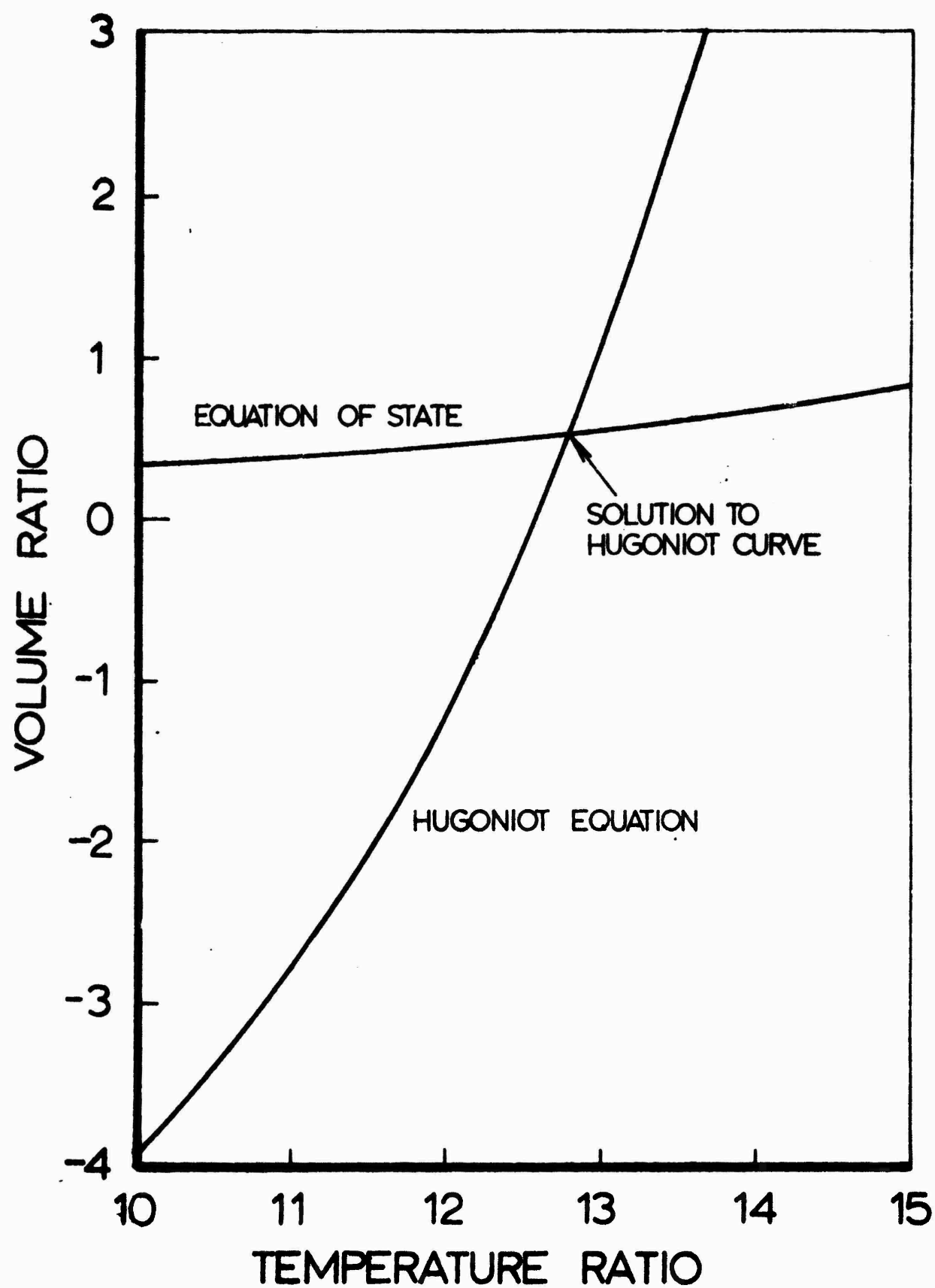


Fig. 1: Determination of a Point on the Hugoniot Curve in the V - P Plane

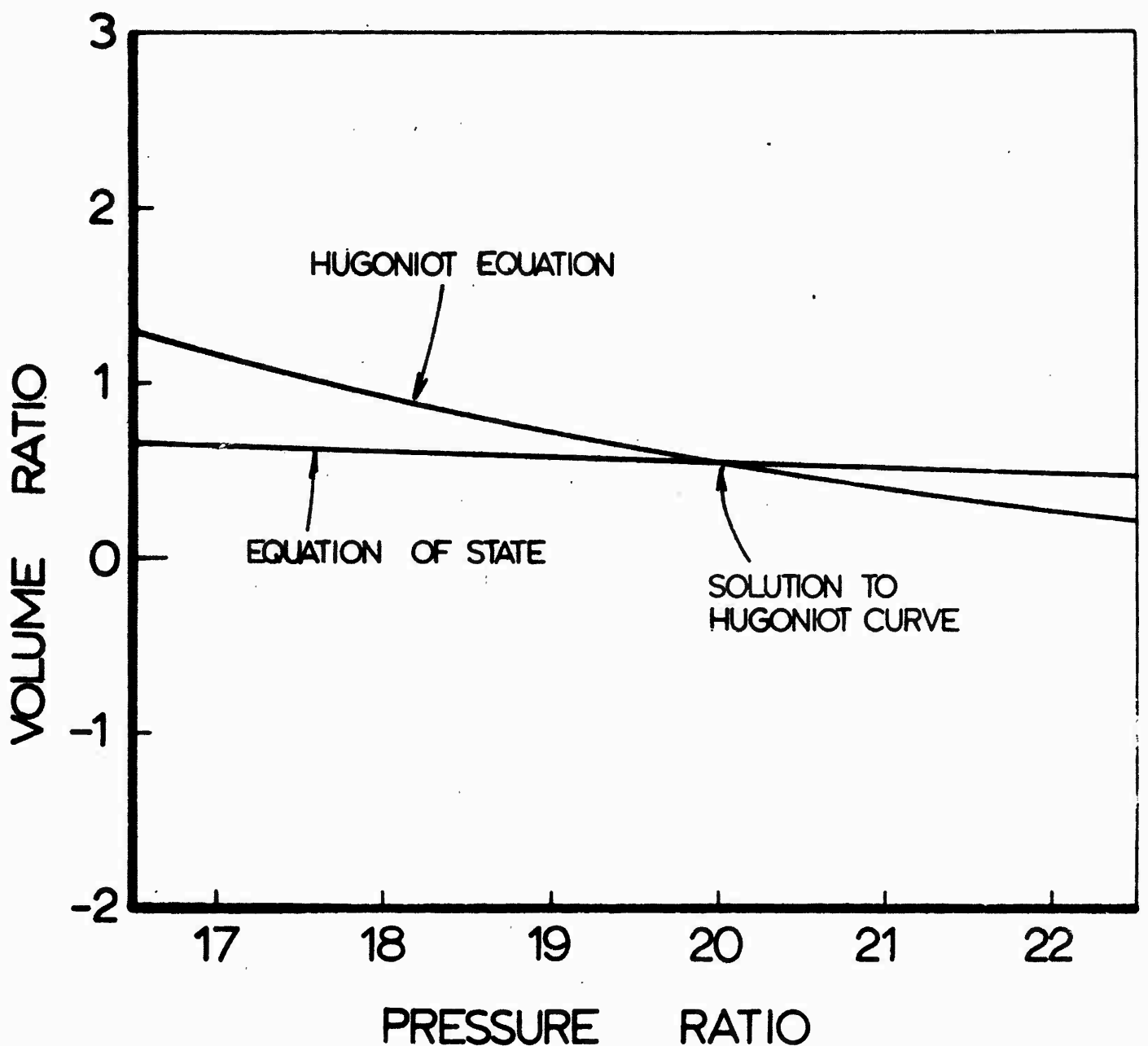


Fig. 2: Determination of a Point on the Hugoniot Curve
the $V-\theta$ Plane

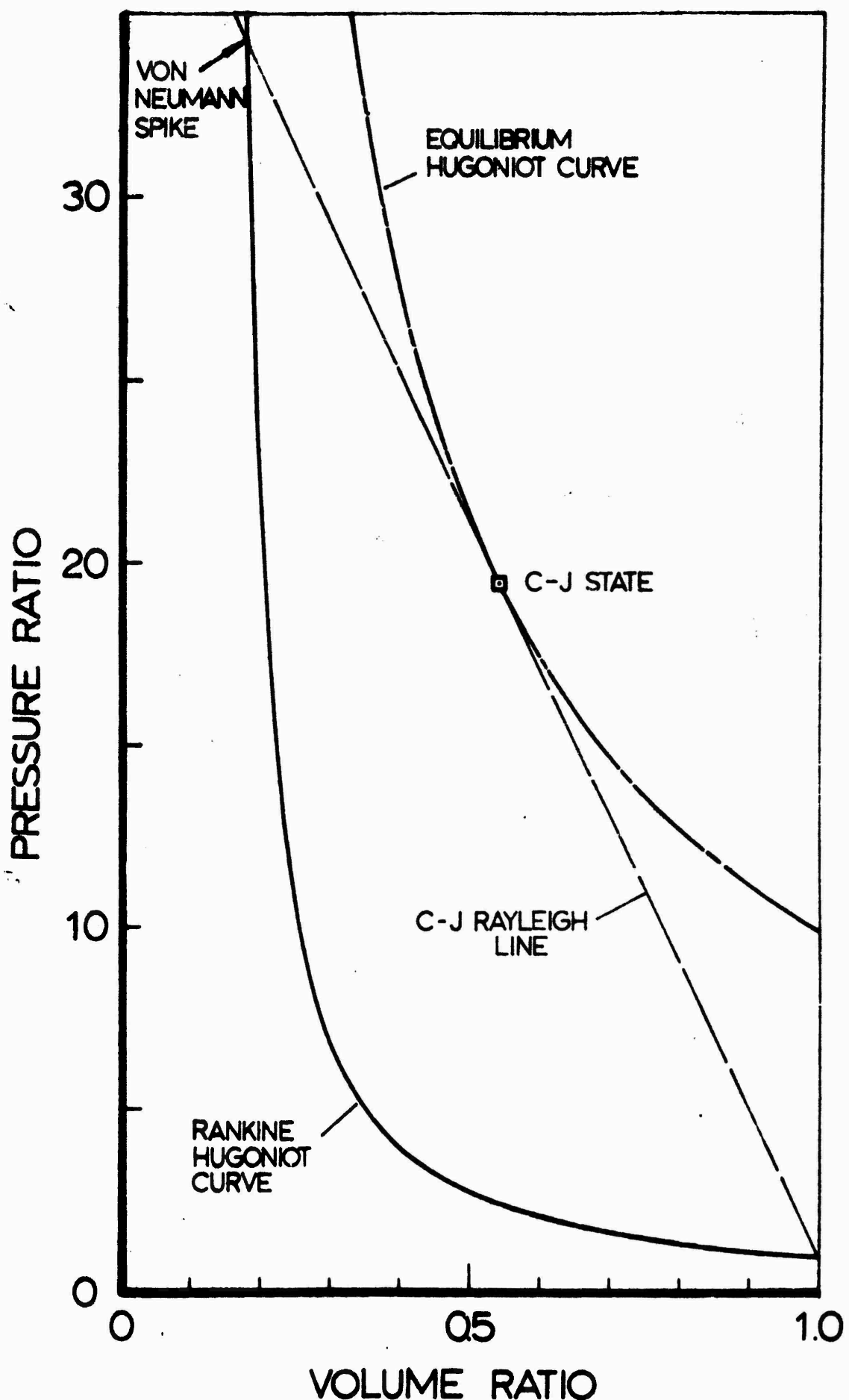


Fig. 3: Diagram Showing Hugoniot Curve, Rankine-Hugoniot Curve, and CJ Rayleigh Line for $2\text{H}_2 + \text{O}_2$ Mixture at 60°F , 760 mm Hg.

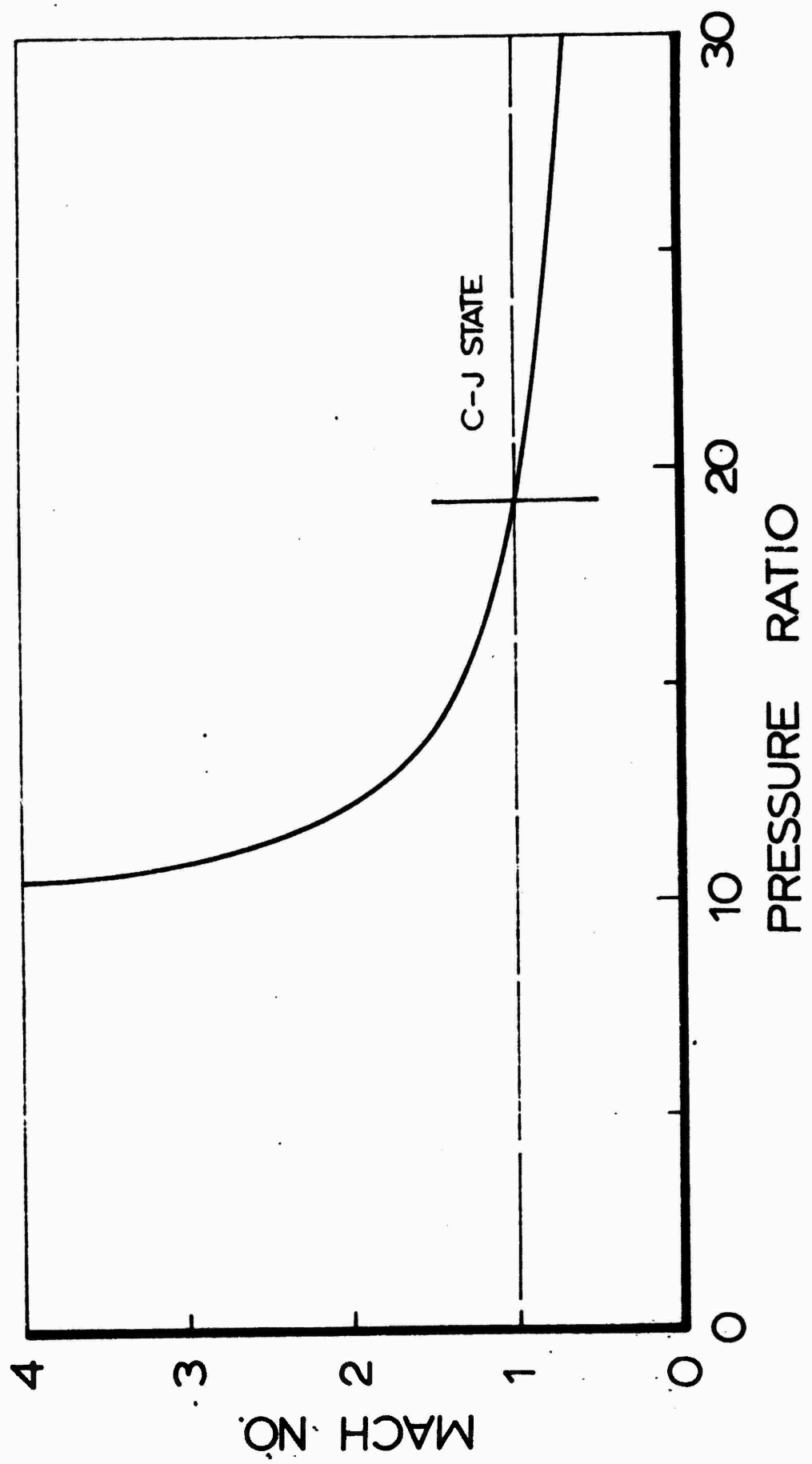


Fig. 4: Determination of the CJ State in the M_t - P Plane

FLOW DIAGRAM

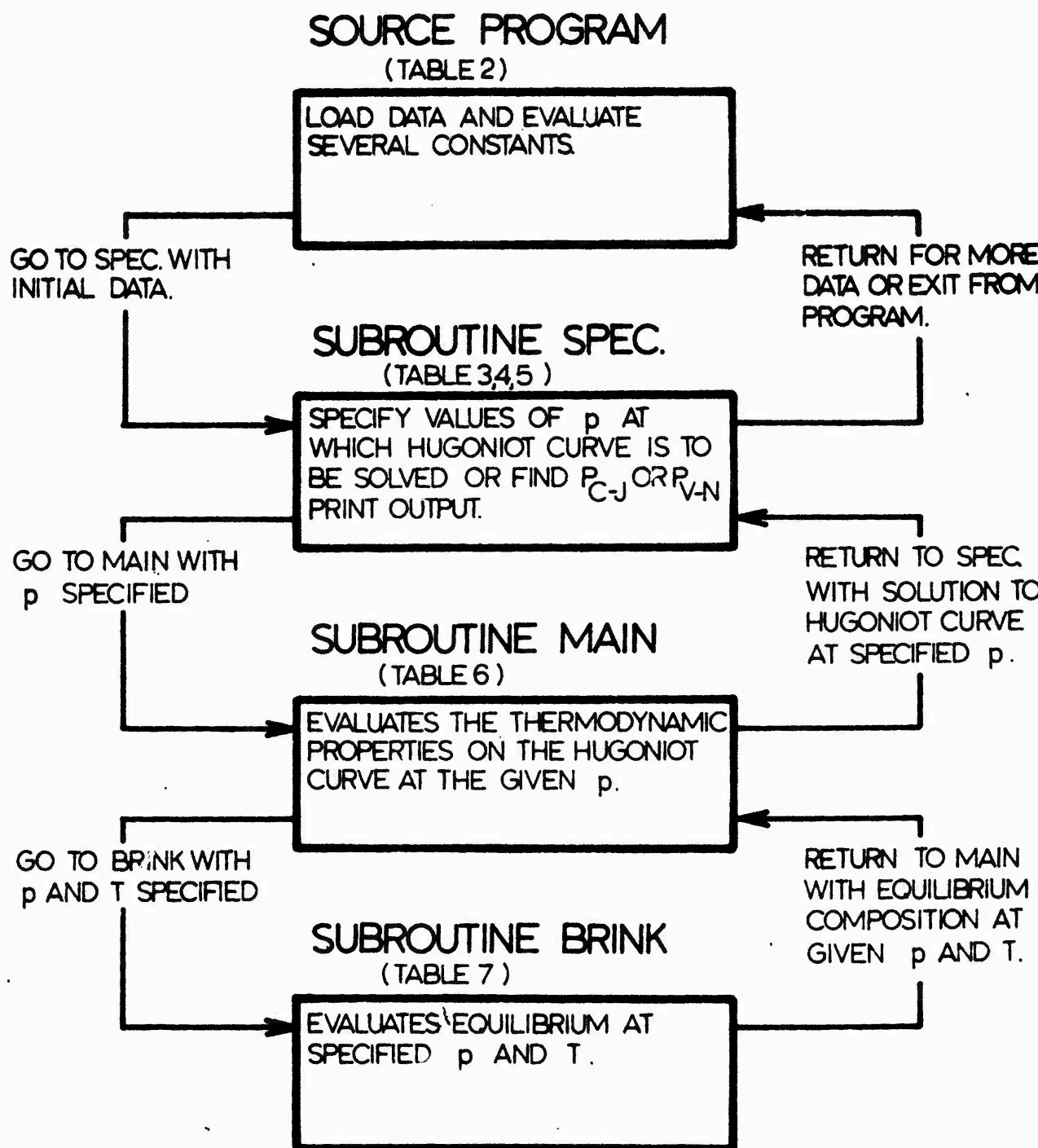


Fig. 5: Flow Diagram of Computer Program

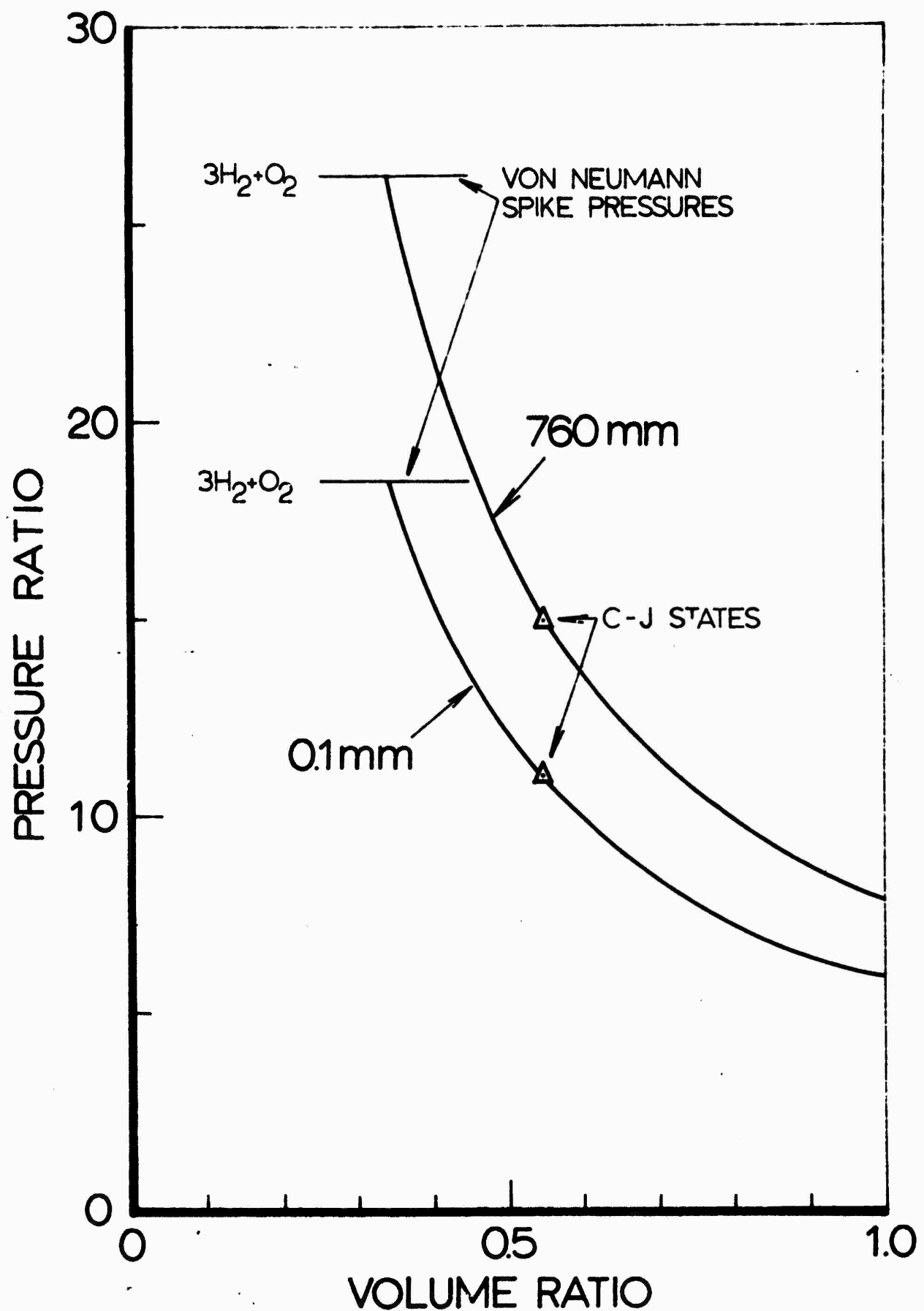


Fig. 6: Hugoniot Curves for $3\text{H}_2 + \text{O}_2$ Mixture Initially at 200°F

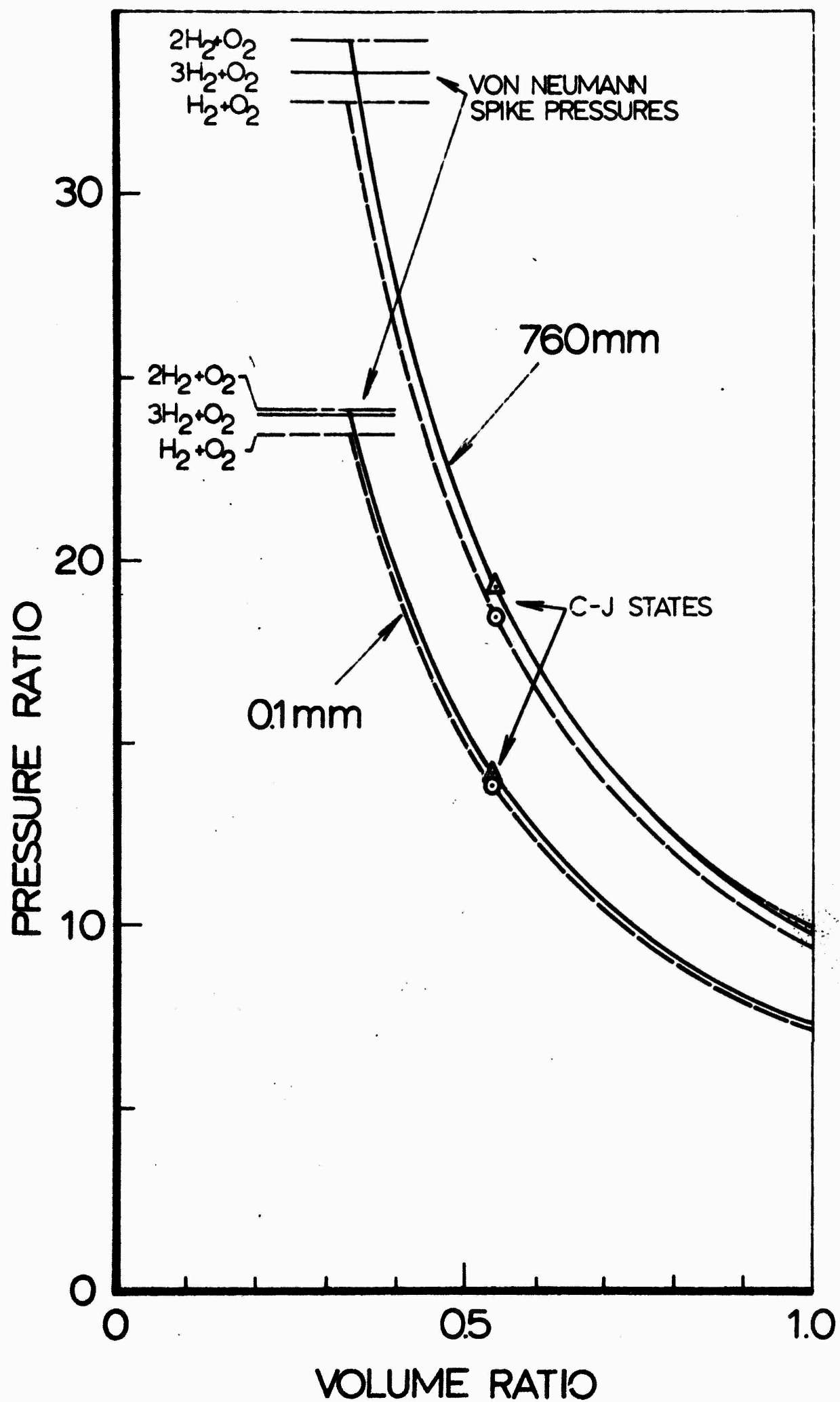


Fig. 7: Hugoniot Curves for Hydrogen-Oxygen Mixtures
Initially at 60°F

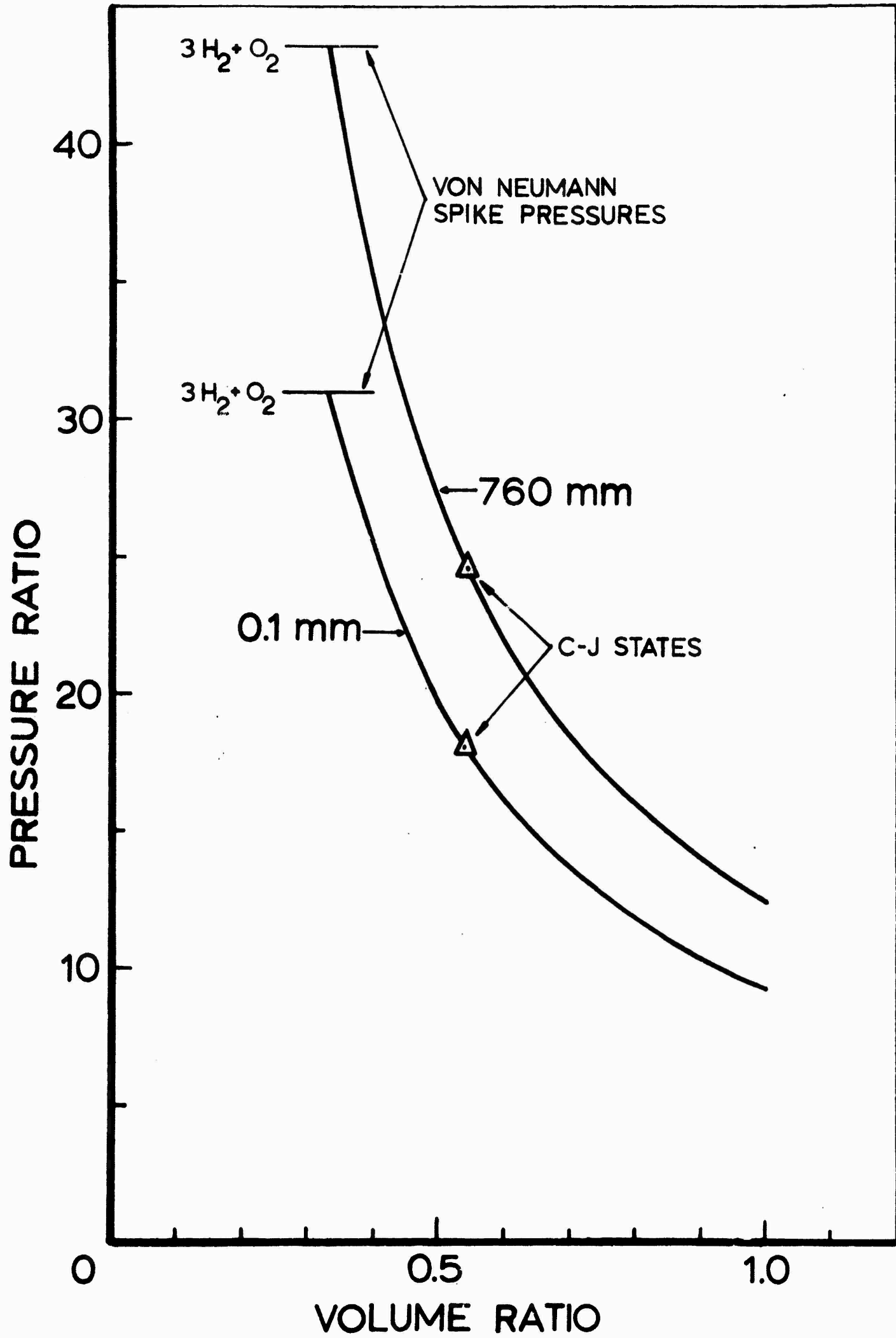


Fig. 8: Hugoniot Curves for $3\text{H}_2 + \text{O}_2$ Mixture Initially at -50°F

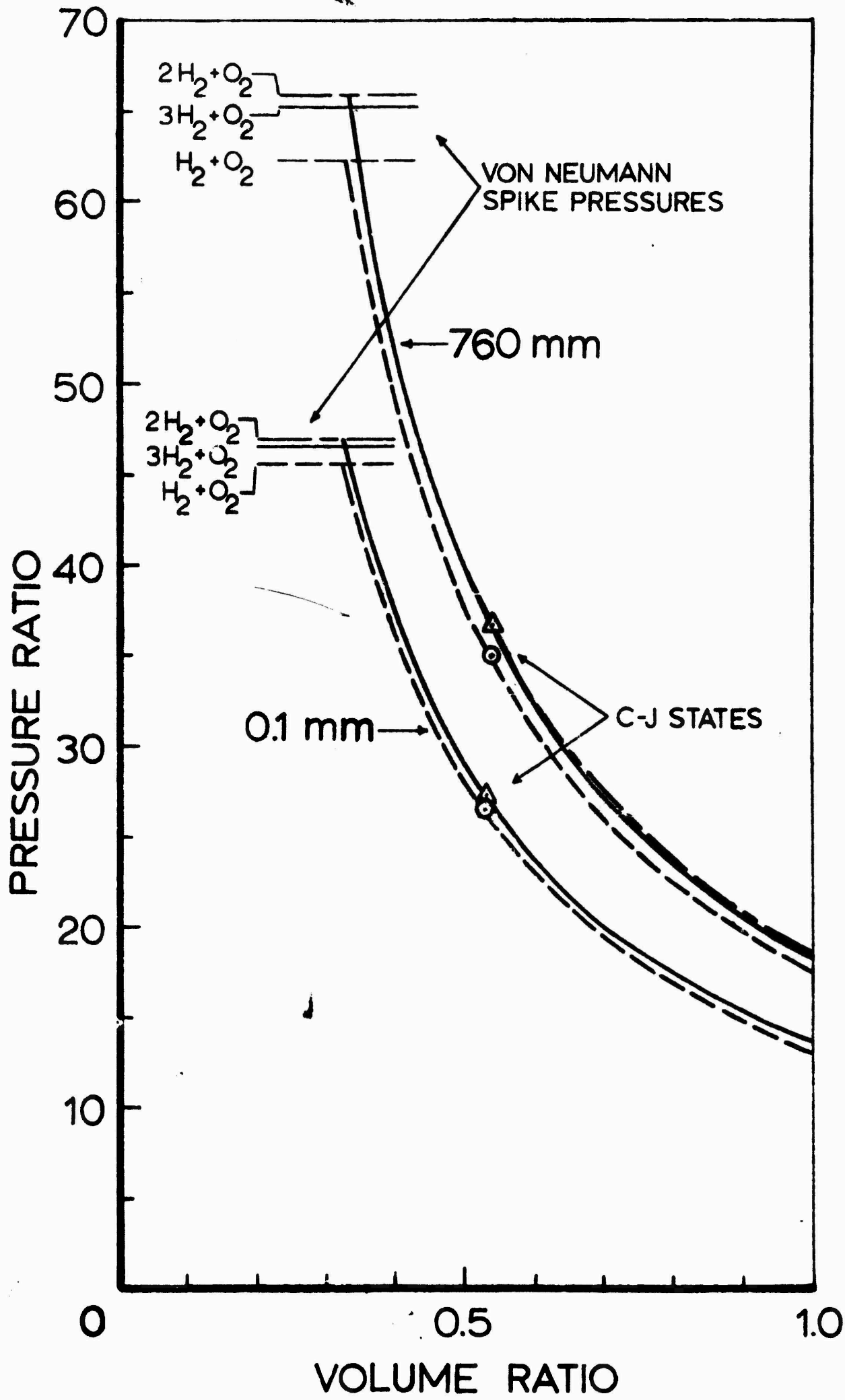


Fig. 9: Hugoniot Curves for Hydrogen-Oxygen Mixtures
Initially at -180° F

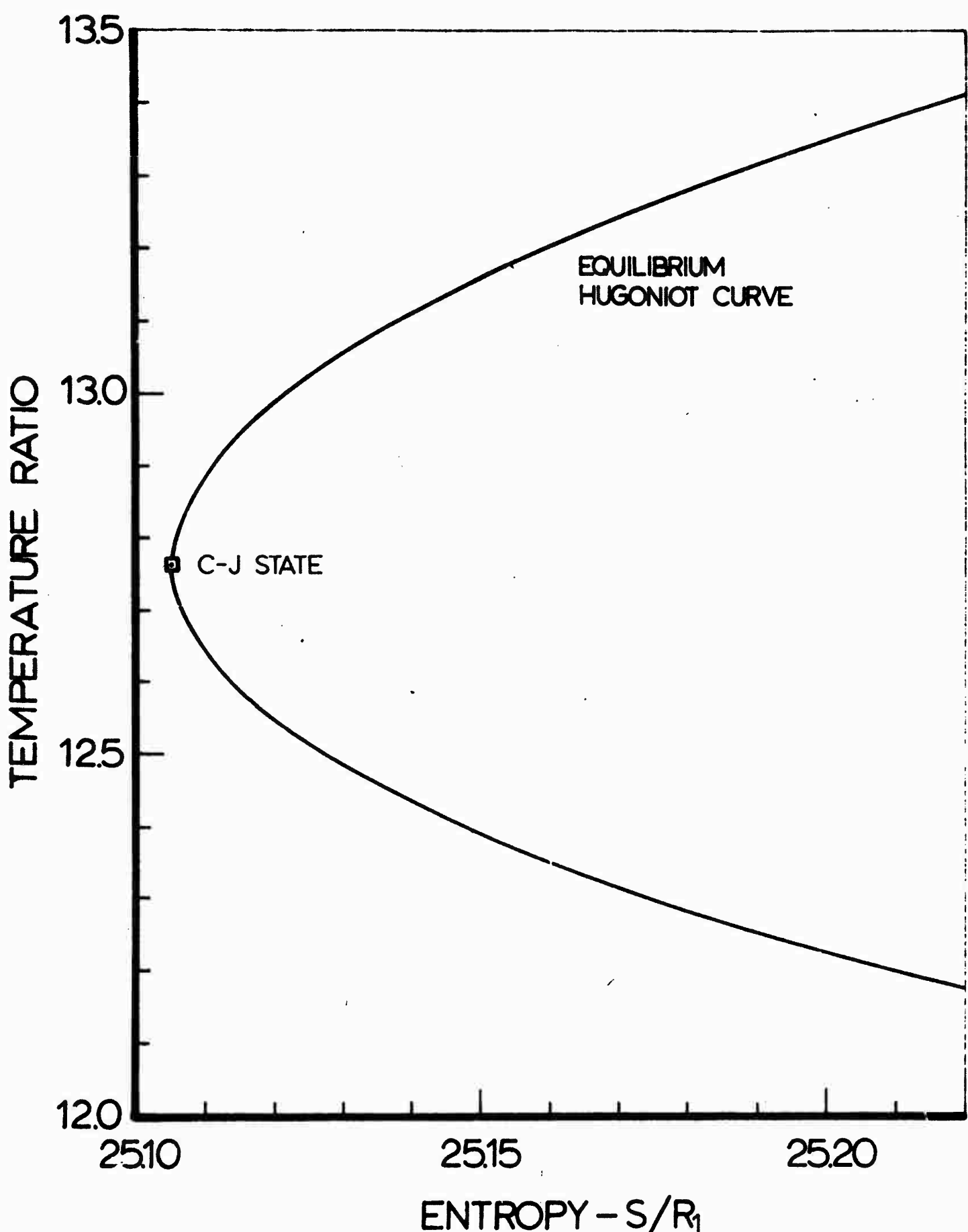


Fig. 10: Hugoniot Curve in Dimensionless Temperature-Entropy Diagram
for $2\text{H}_2 + \text{O}_2$ Mixture Initially at 60°F , 760 mmHg.

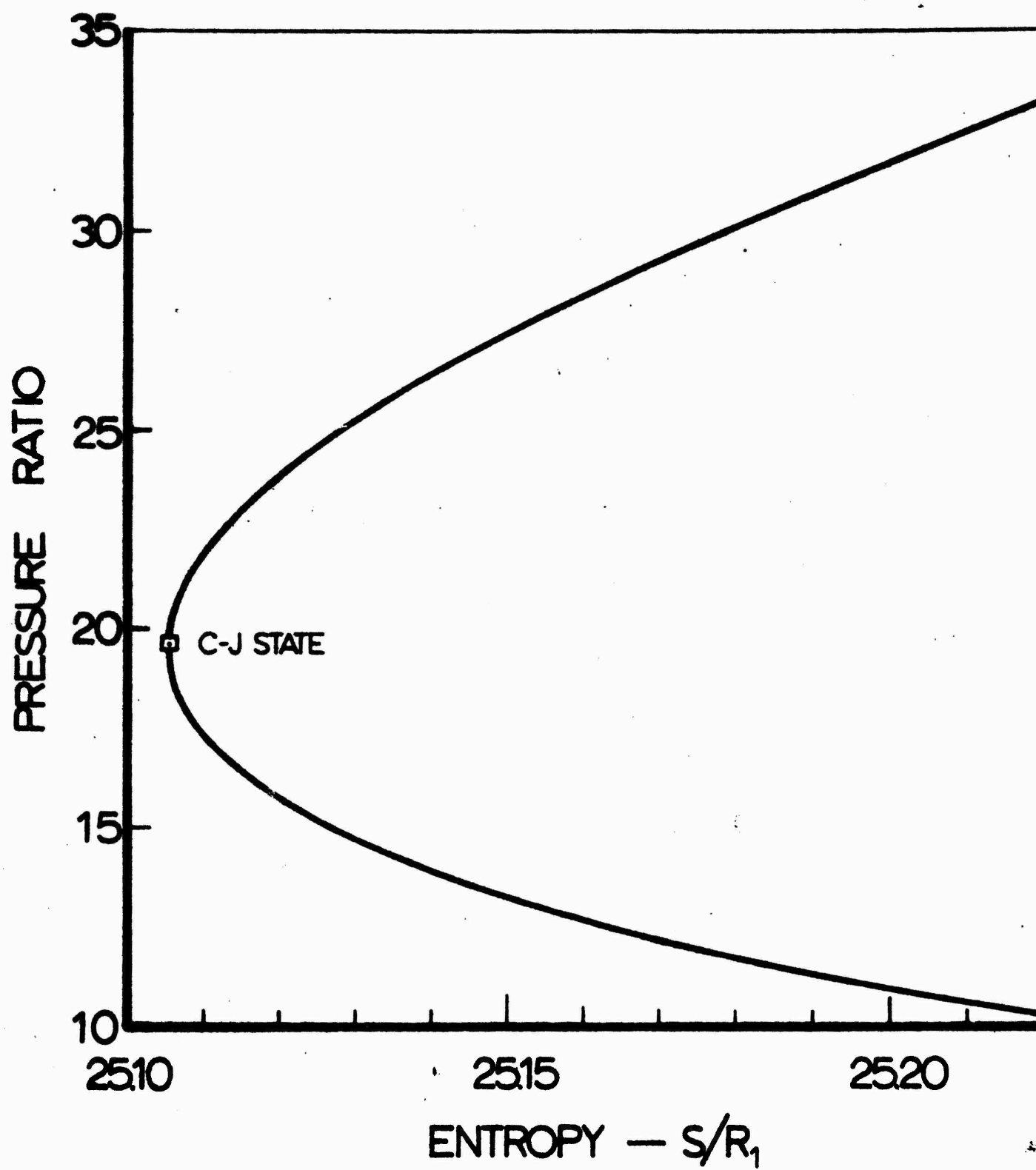


Fig. 11: Hugoniot Curve in Dimensionless Pressure-Entropy Diagram
for Mixture Initially at 60°F, 760 mmHg

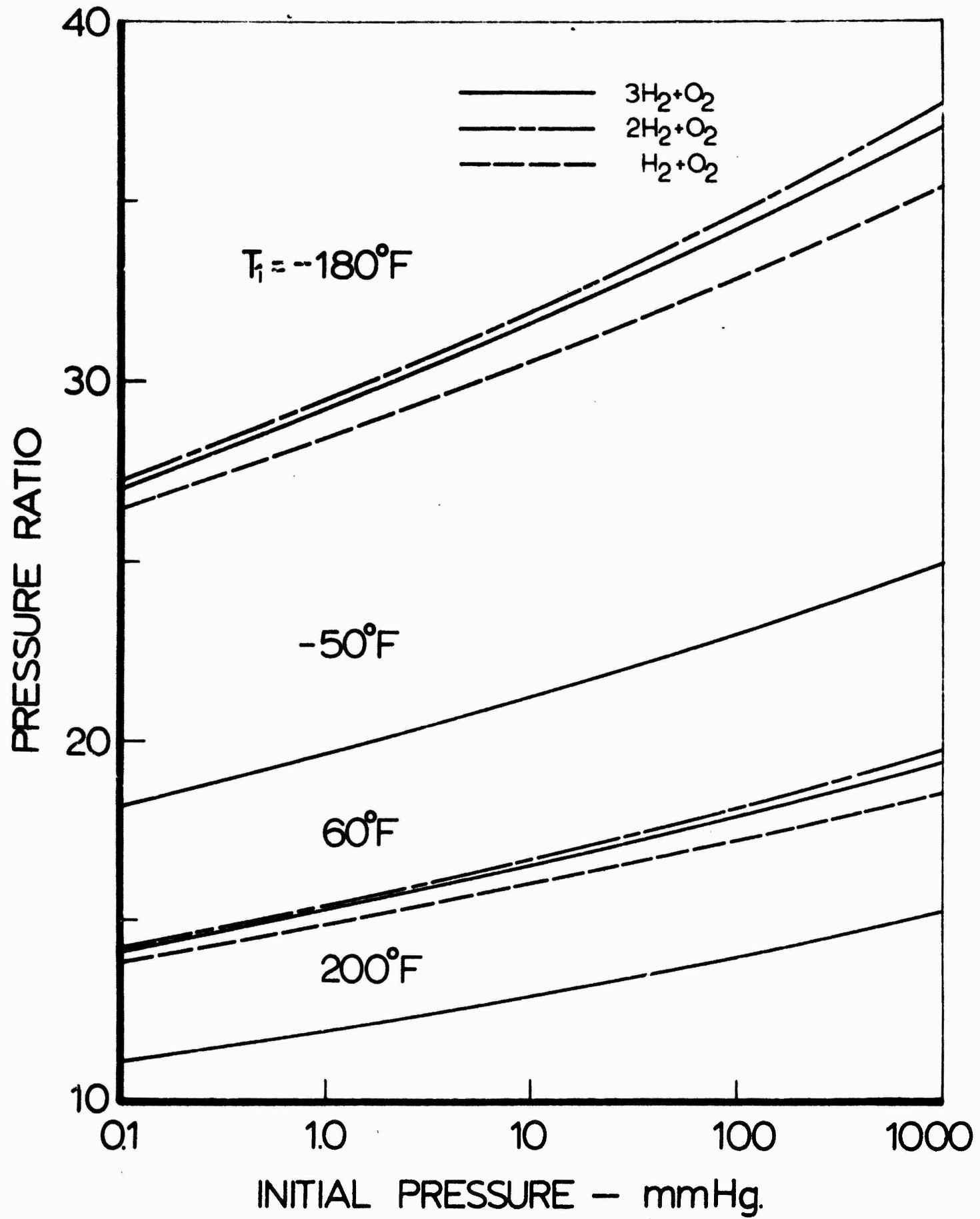


Fig. 12: Influence of Initial Pressure on CJ Pressure Ratio

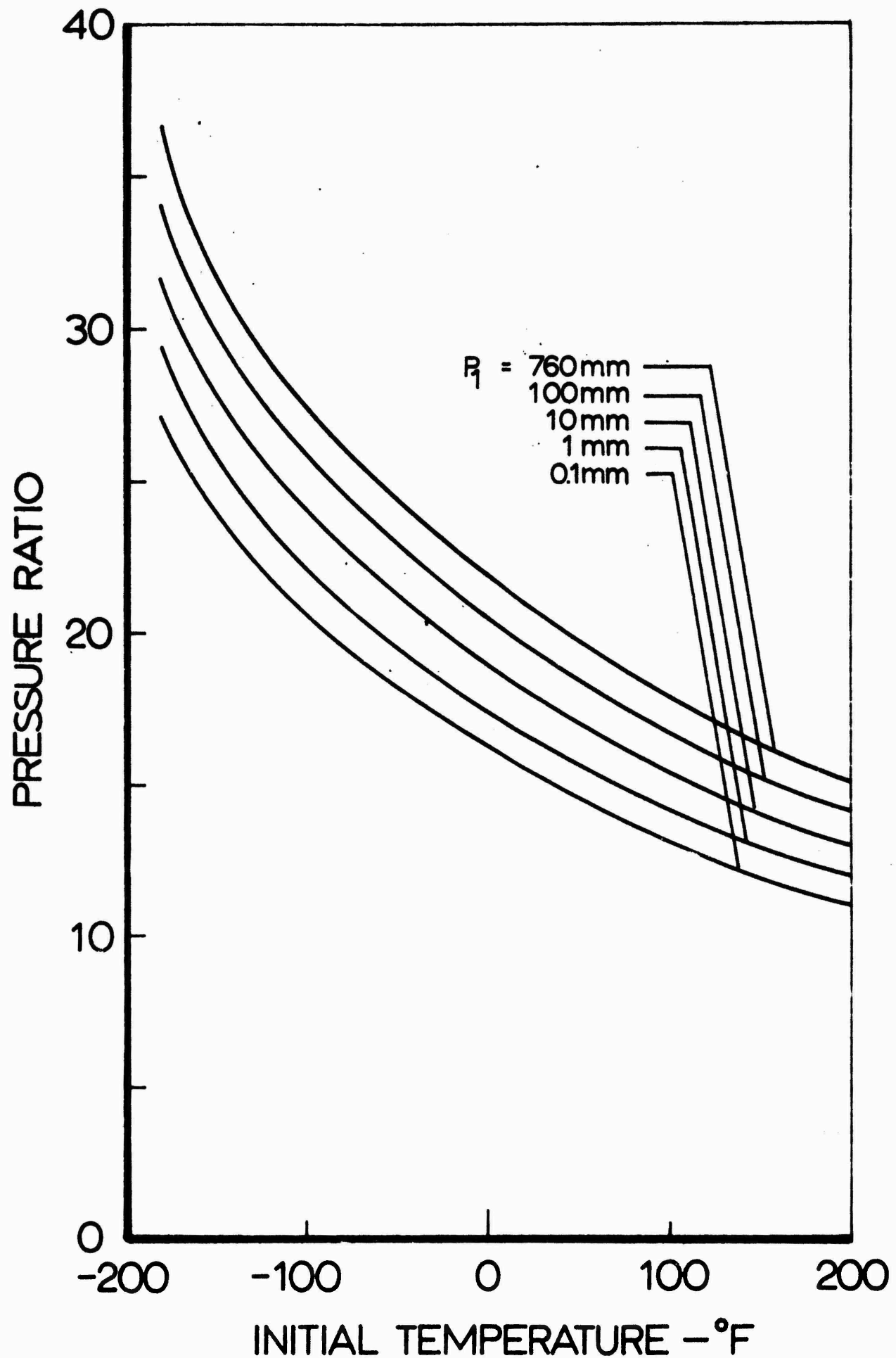


Fig. 13: Influence of Initial Temperature on CJ Pressure Ratio
for $3\text{H}_2 + \text{O}_2$ Mixture

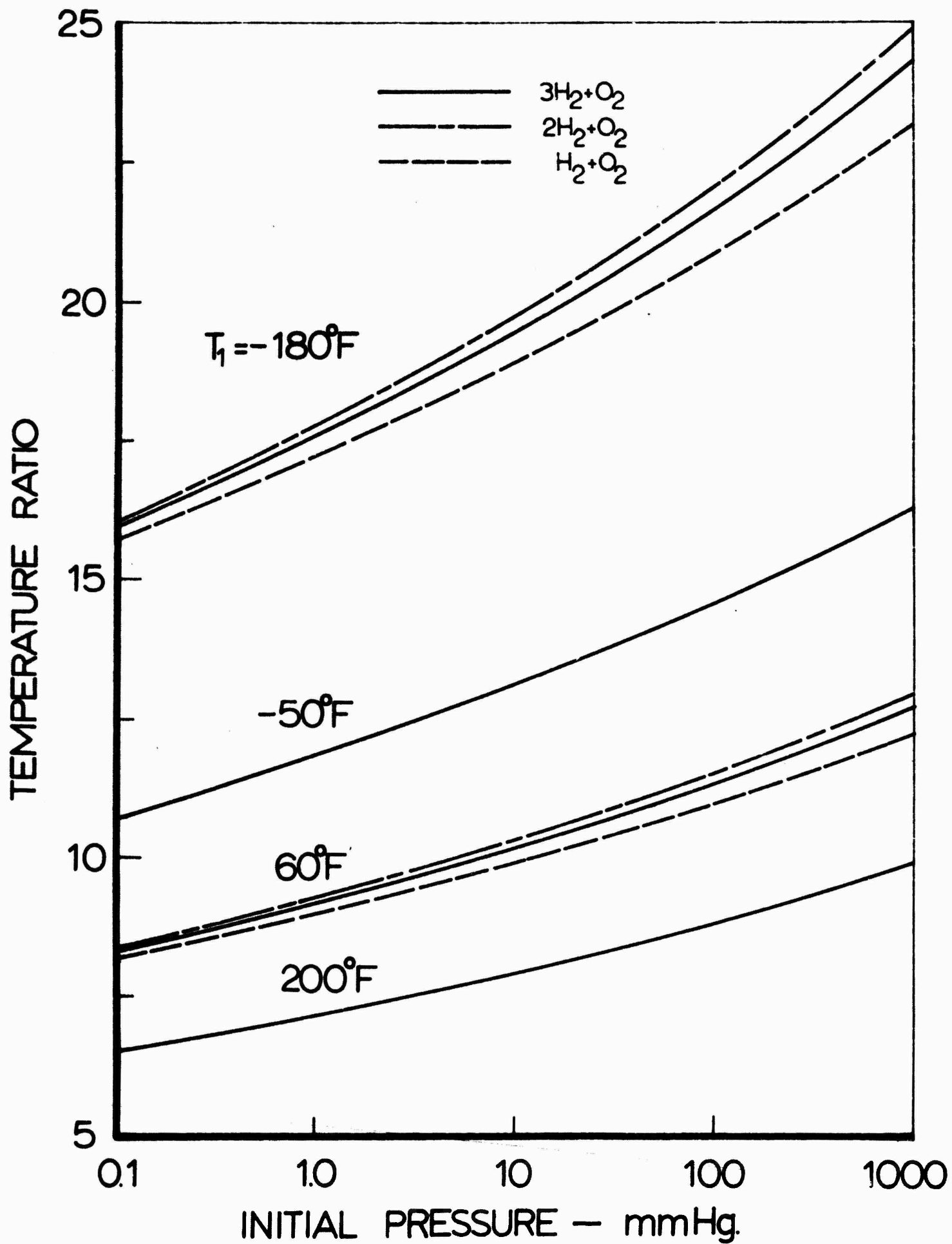


Fig. 14: Influence of Initial Pressure on CJ Temperature Ratio

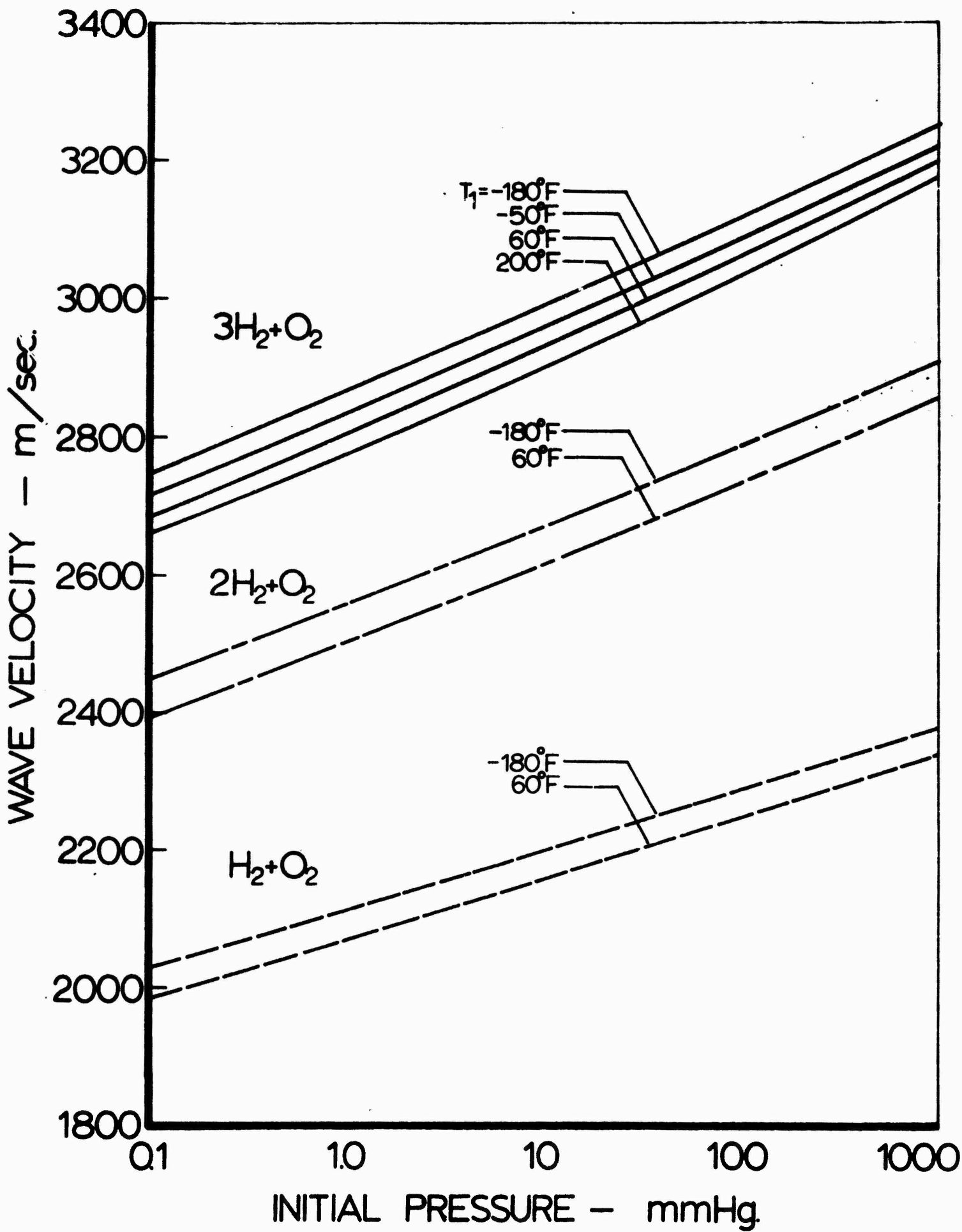


Fig. 15: Influence of Initial Pressure on CJ Detonation Velocity

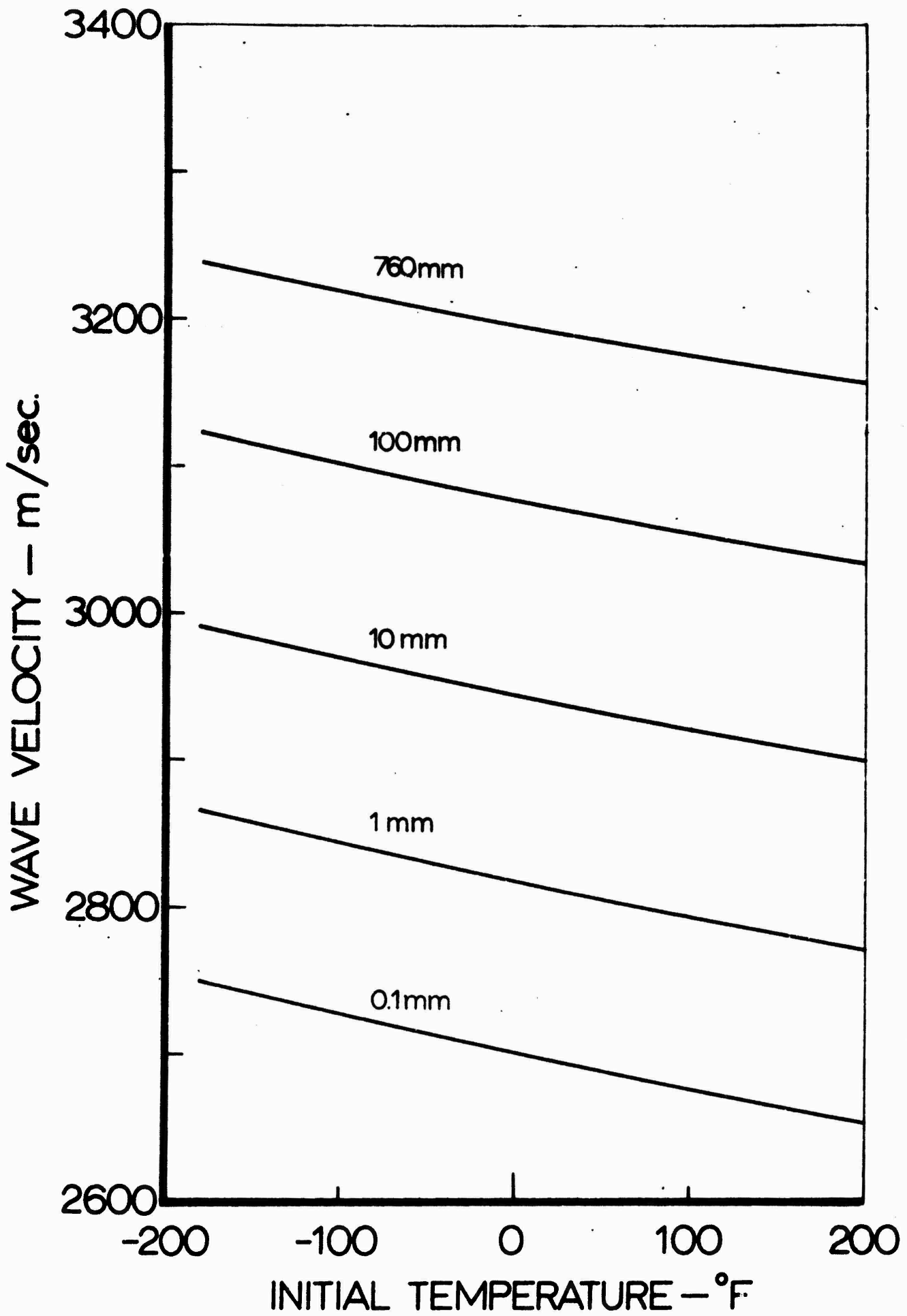


Fig. 16: Influence of Initial Temperature on CJ Detonation Velocity for $3\text{H}_2 + \text{O}_2$ Mixture

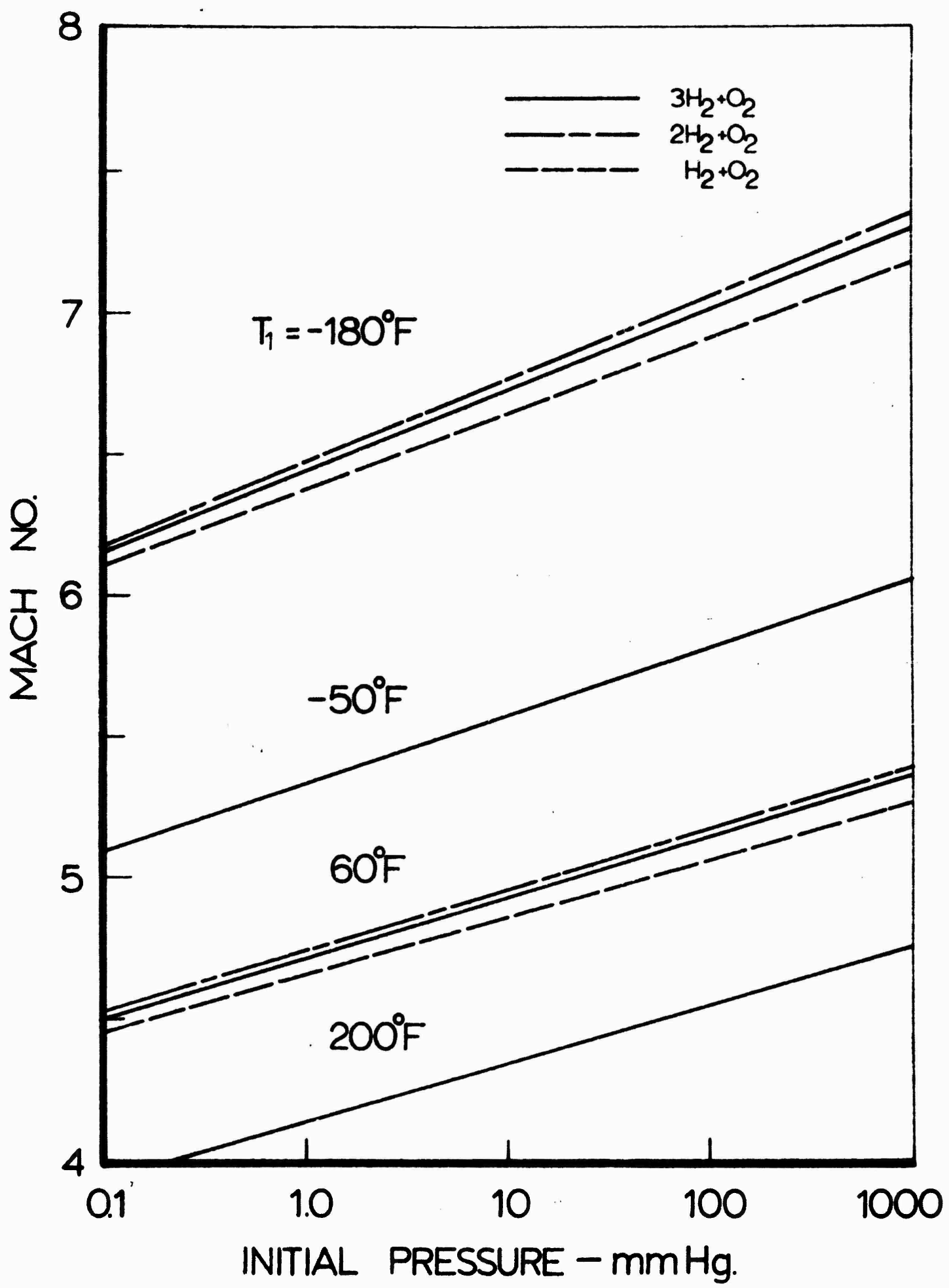


Fig. 17: Influence of Initial Pressure on CJ Detonation Mach Number

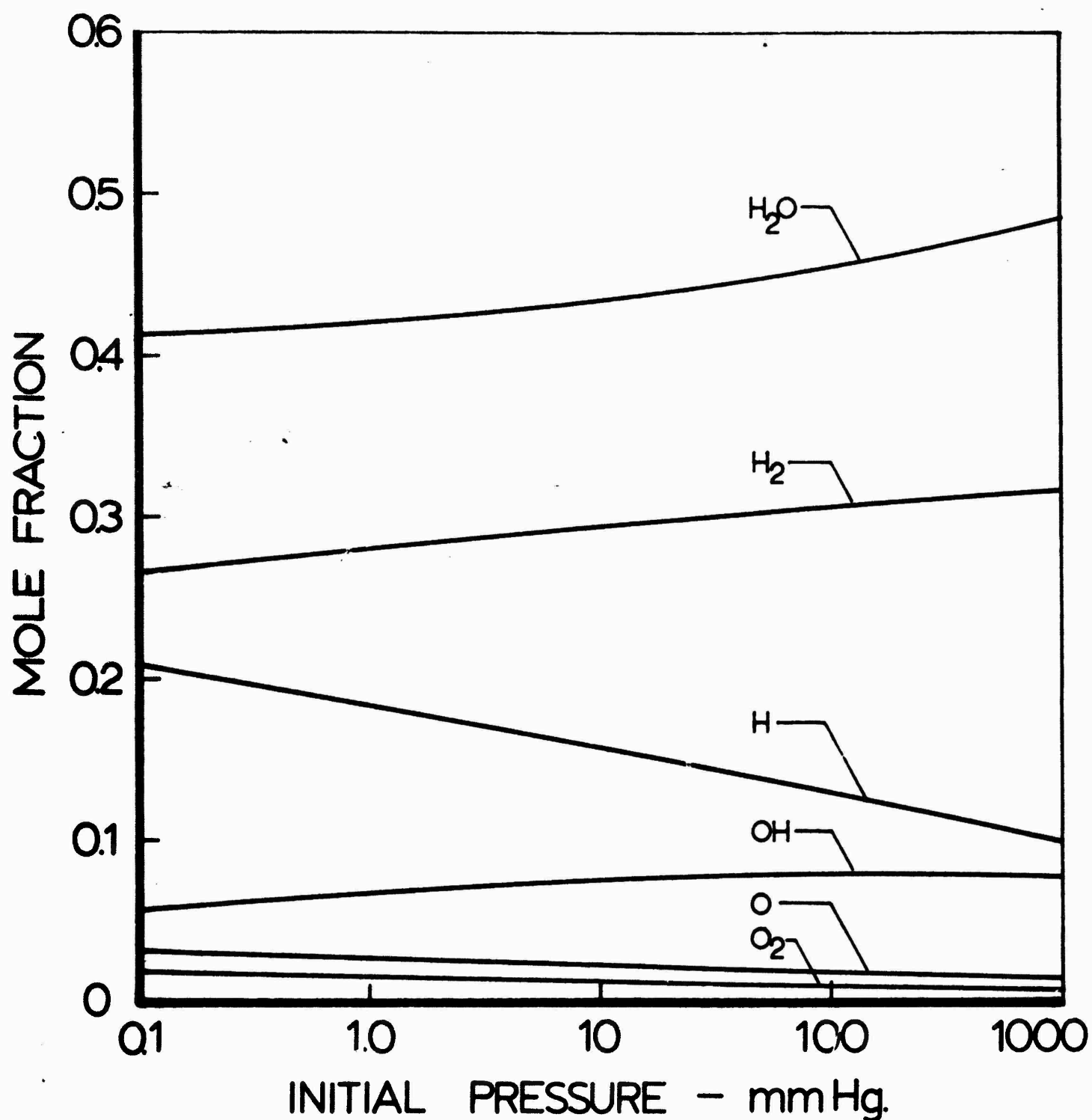


Fig. 18: Influence of Initial Pressure on Equilibrium Composition of Product Gases for $3H_2 + O_2$ Mixture Initially at $200^{\circ}F$

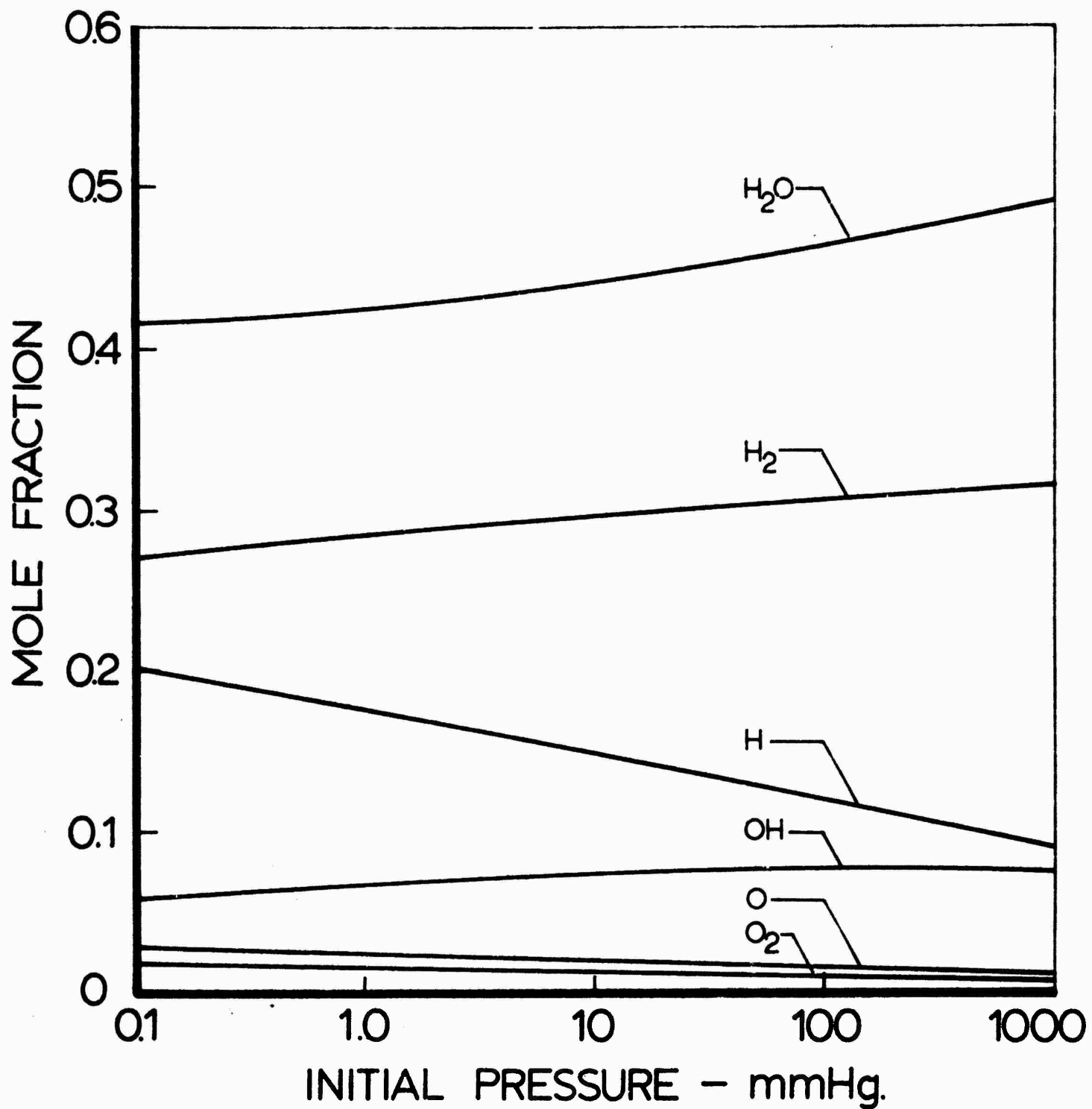


Fig. 19: Influence of Initial Pressure on Equilibrium Composition of Product Gases for $3H_2 + O_2$ Mixture Initially at $60^{\circ}F$

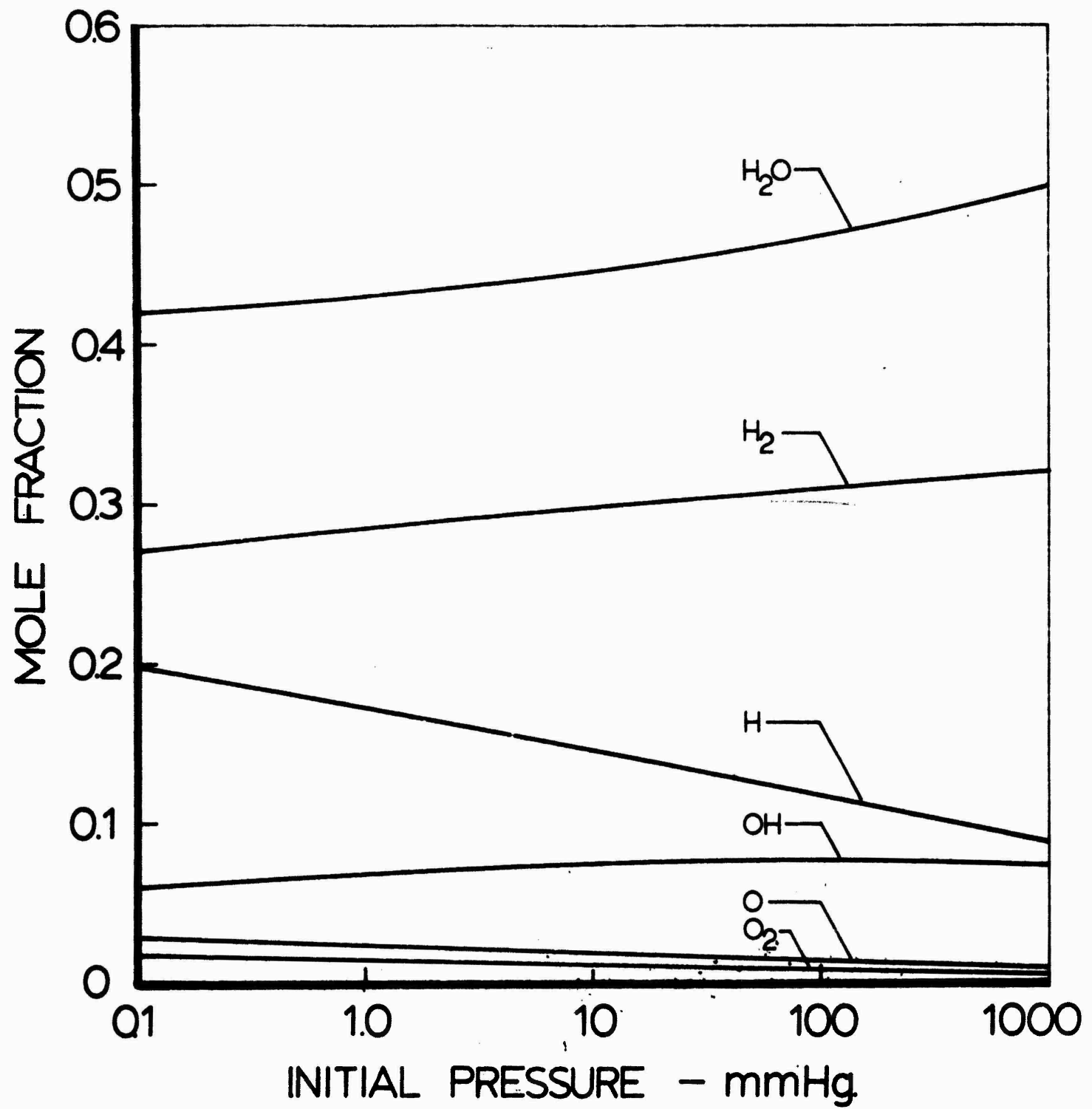


Fig. 20: Influence of Initial Pressure on Equilibrium Composition of Product Gases for $3\text{H}_2 + \text{O}_2$ Mixture Initially at -50°F

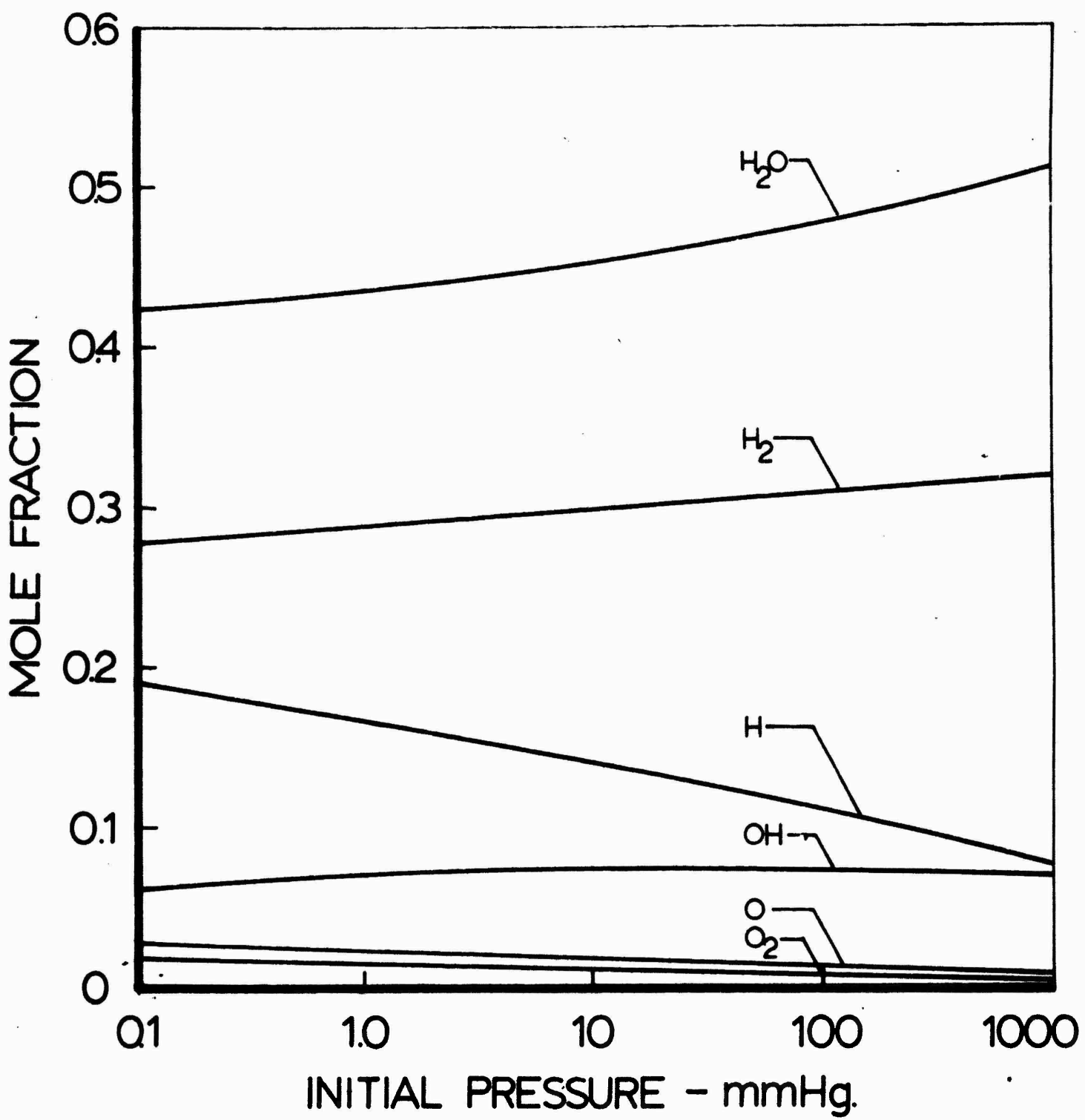


Fig. 21: Influence of Initial Pressure on Equilibrium Composition of Product Gases for $3\text{H}_2 + \text{O}_2$ Mixture at -180°F

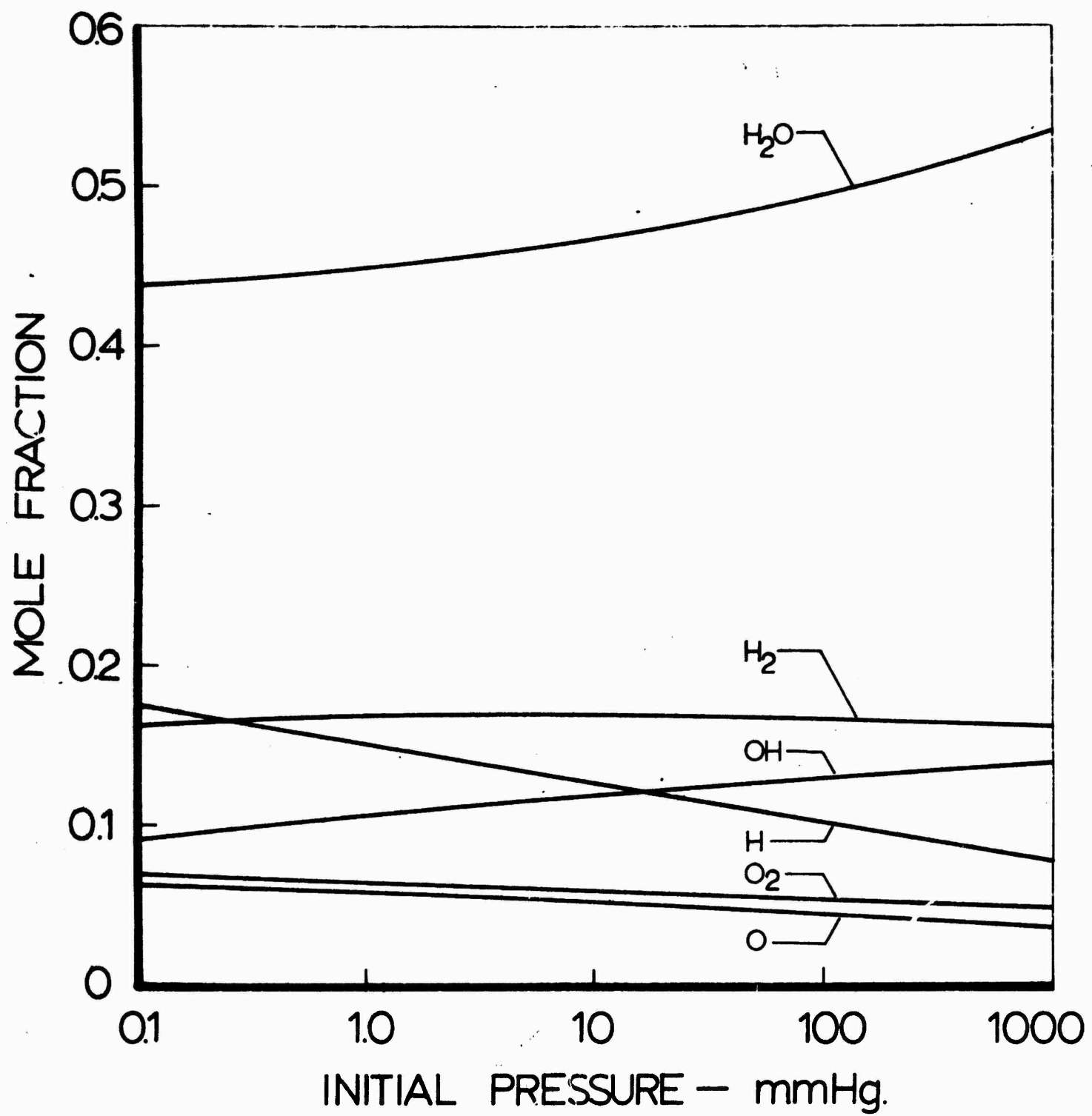


Fig. 22: Influence of Initial Pressure on Equilibrium Composition of Product Gases for $2\text{H}_2 + \text{O}_2$ Mixture Initially at 60°F

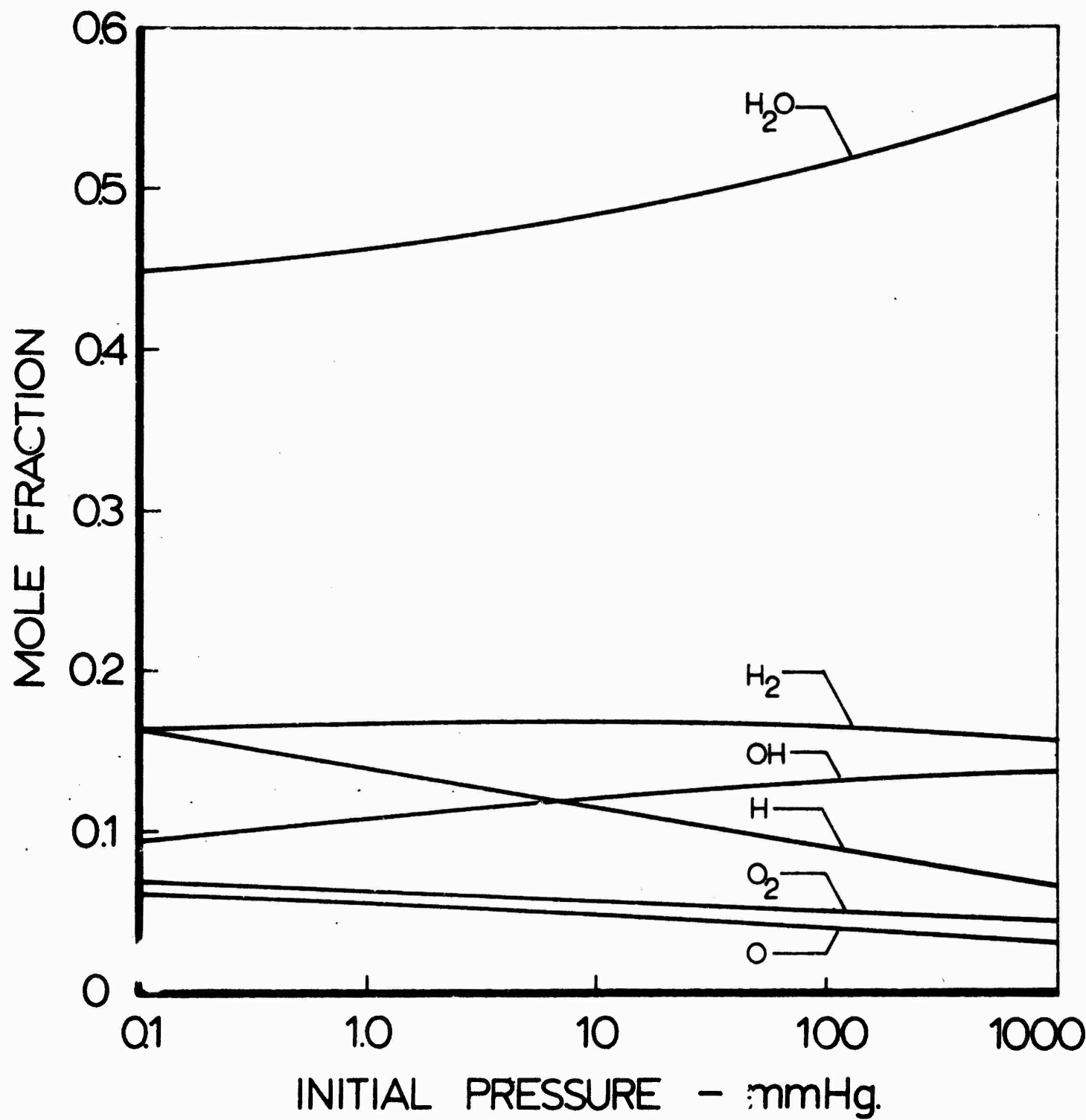


Fig. 23: Influence of Initial Pressure on Equilibrium Composition of Product Gases for $2\text{H}_2 + \text{O}_2$ Mixture Initially at -180°F

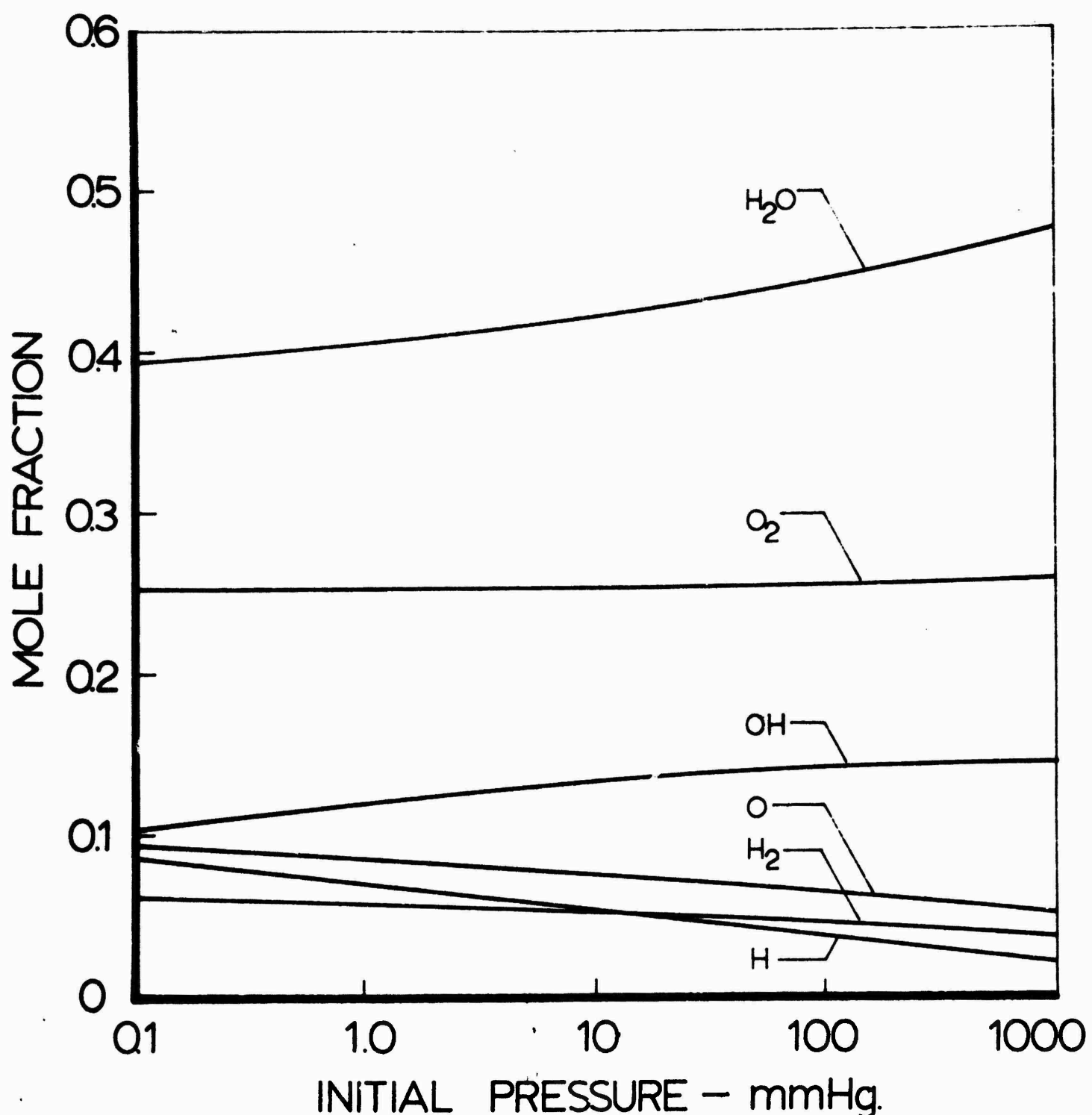


Fig. 24: Influence of Initial Pressure on Equilibrium Composition of Product Gases for $\text{H}_2 + \text{O}_2$ Mixture Initially at 60°F

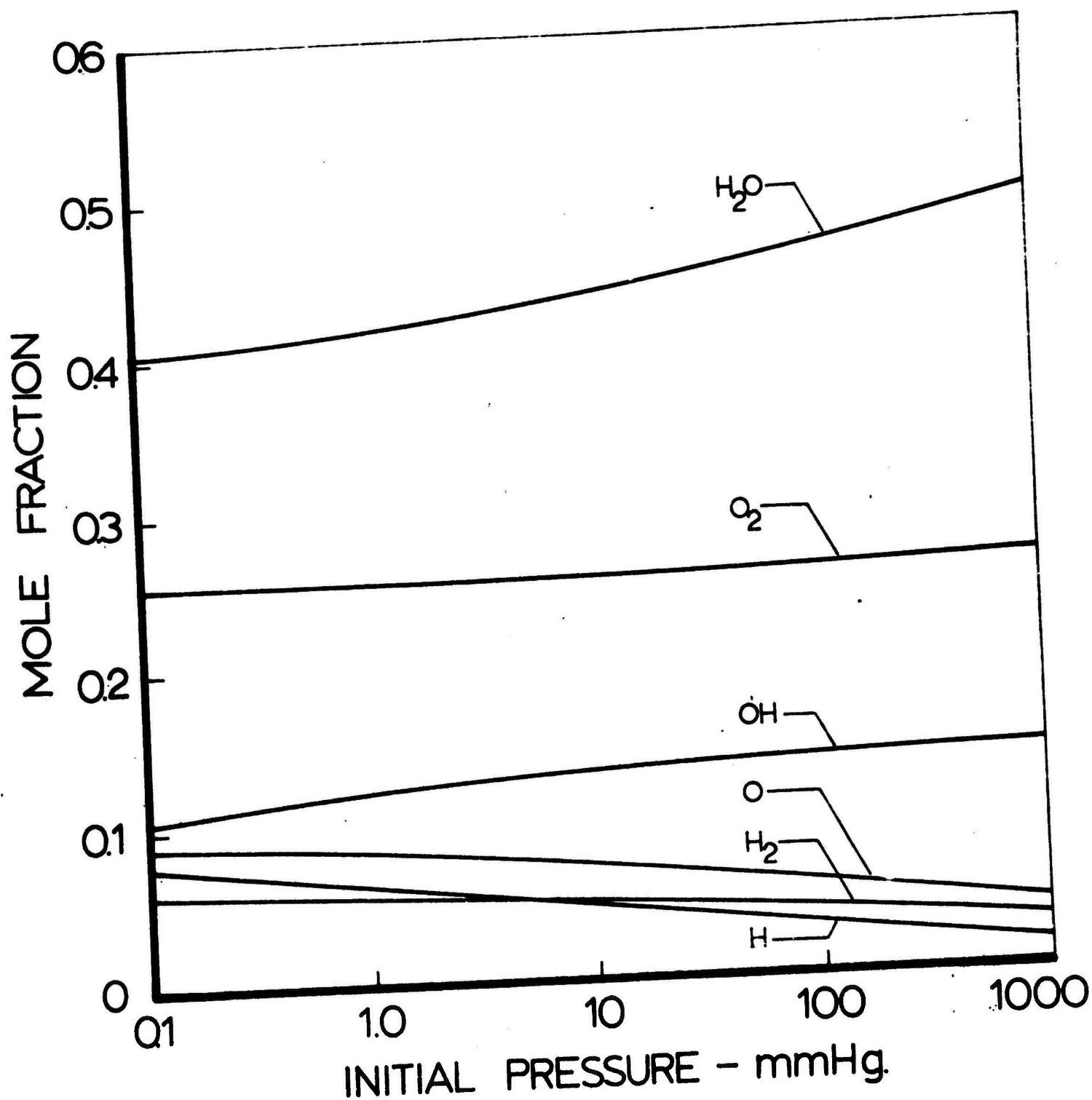


Fig. 25: Influence of Initial Pressure on Equilibrium Composition of Product Gases for $\text{H}_2 + \text{O}_2$ Mixture Initially at -180°F

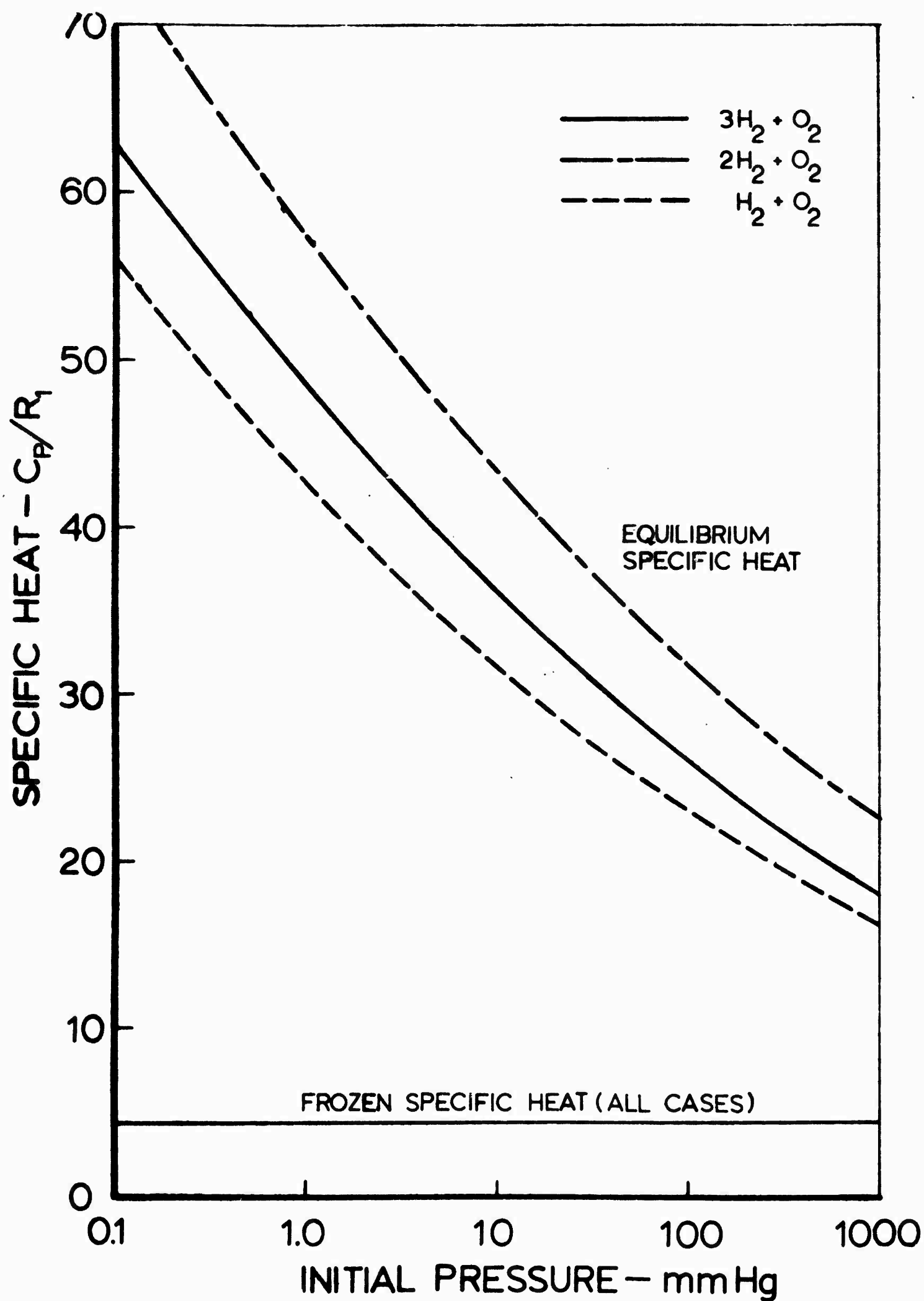


Fig. 26: Influence of Initial Pressure on Specific Heat at the Constant Pressure of Products at CJ State. Initial Temperature 60°F

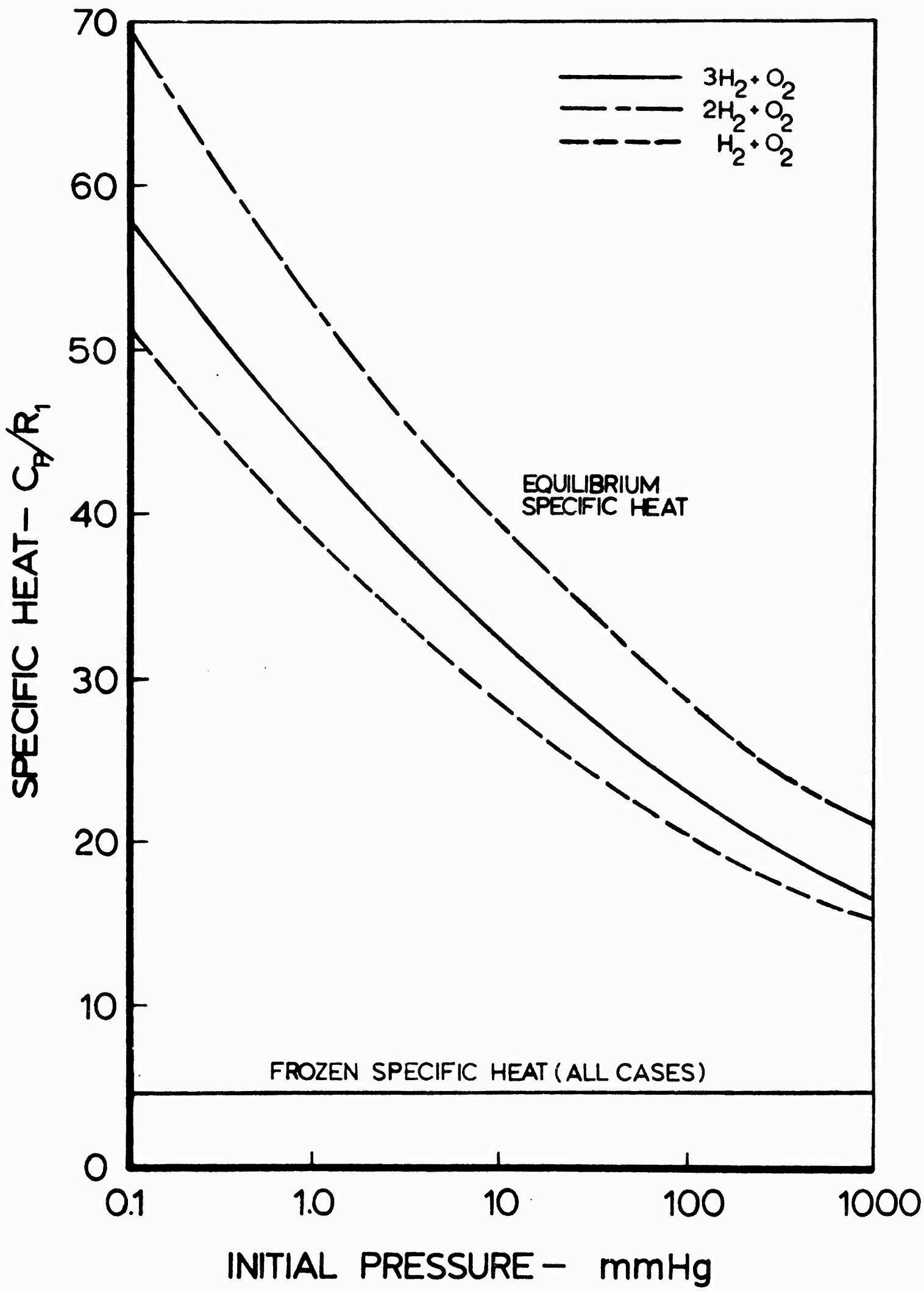


Fig. 27: Influence of Initial Pressure on Specific Heat at the Constant Pressure of Products at CJ State. Initial Temperature -180°F

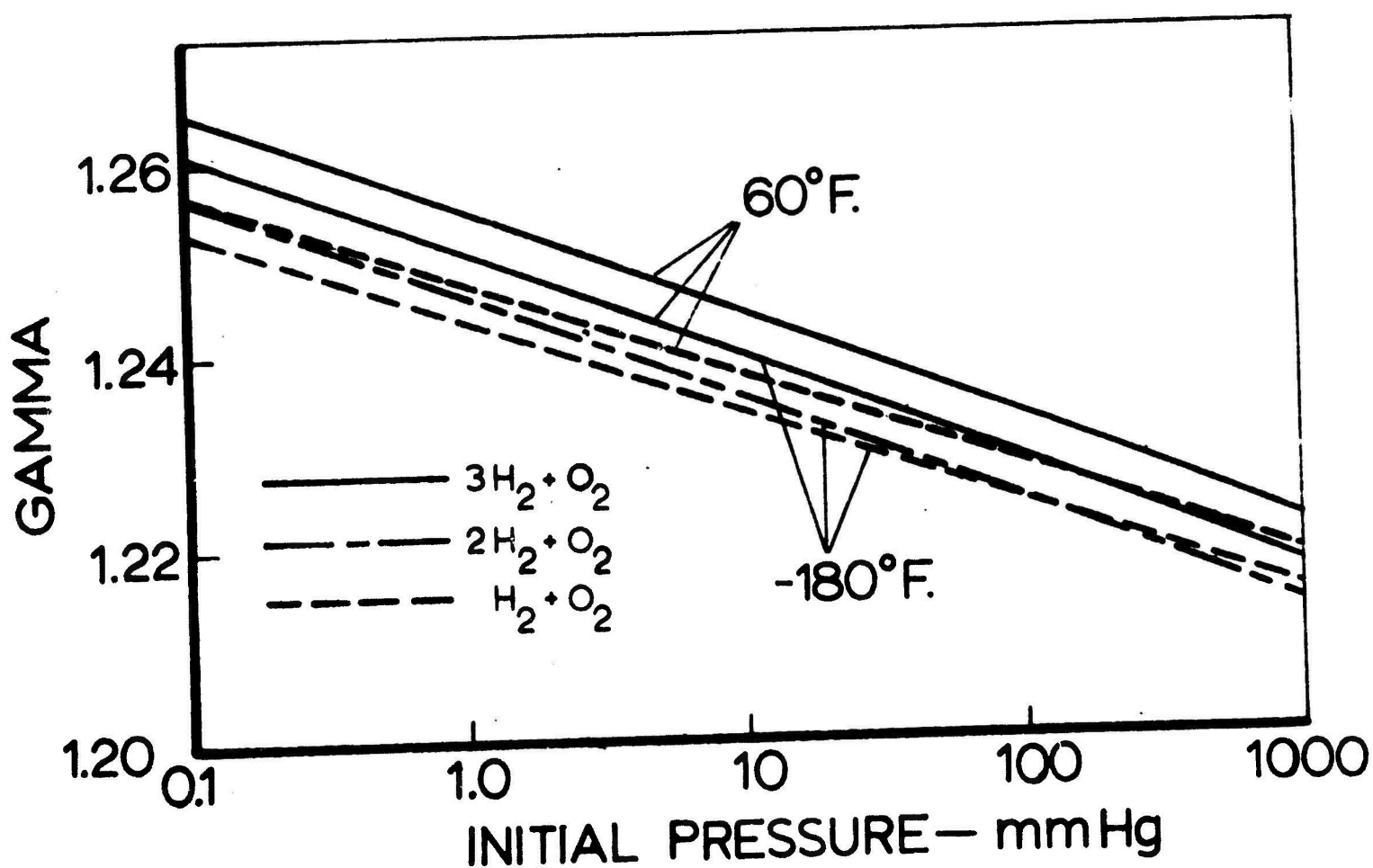
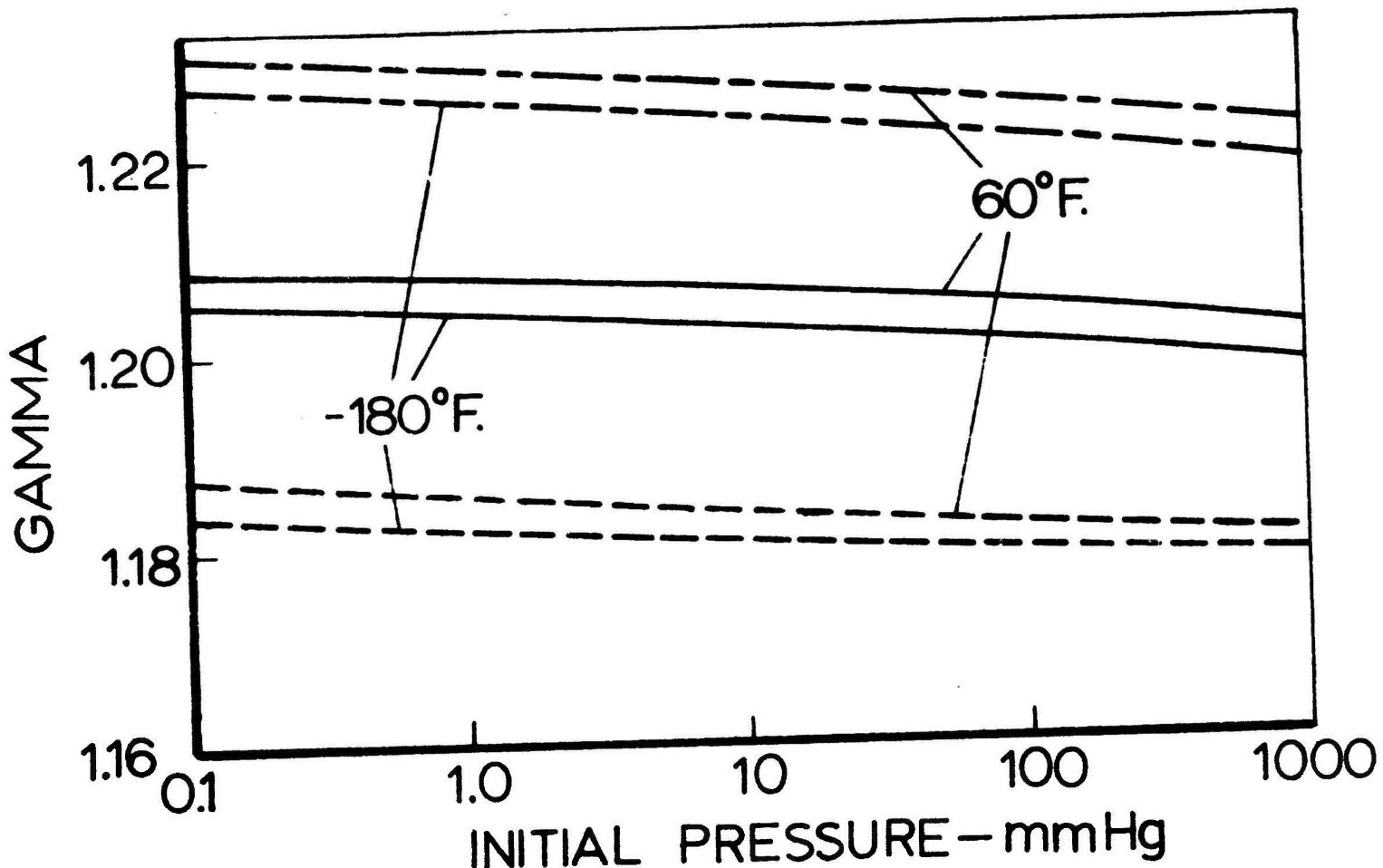


Fig. 28: Influence of Initial Pressure on Specific Heat Ratio of Products at CJ State. The Upper Graph is for Frozen Composition and the Lower Graph is for Equilibrium Composition.

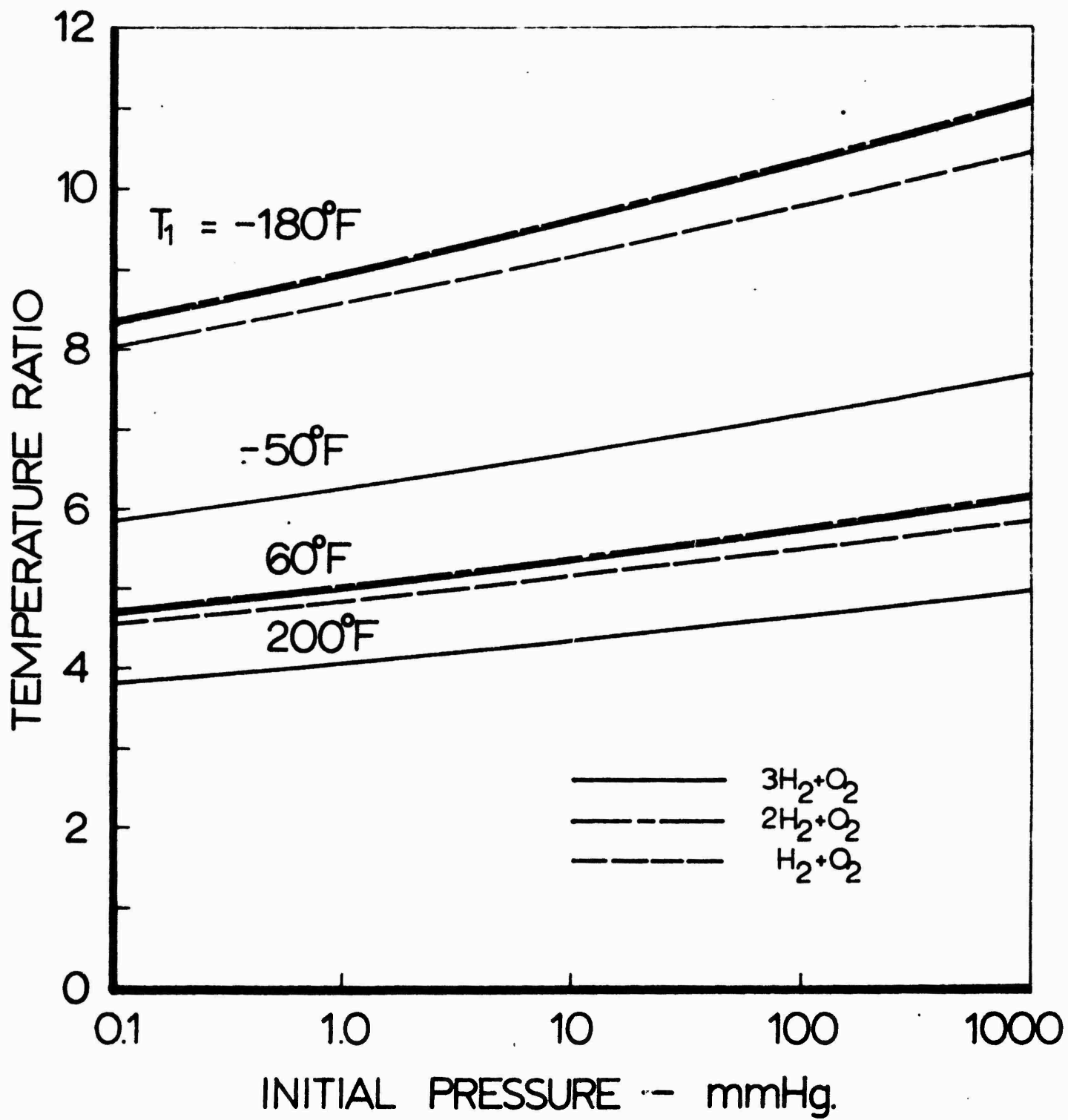


Fig. 29: Influence of Initial Pressure on Von Neumann Spike Pressure Ratio

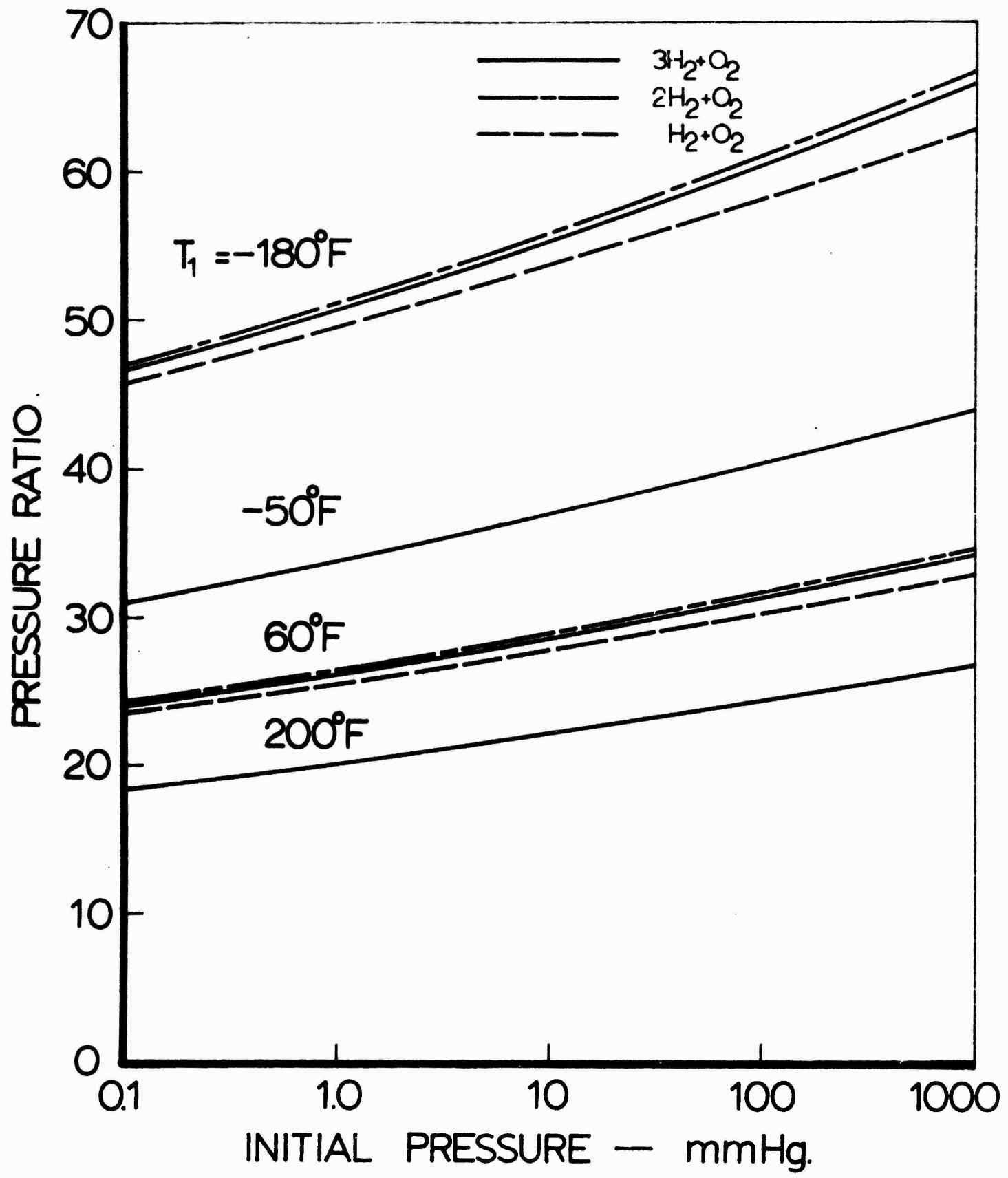


Fig. 30: Influence of Initial Pressure on Von Neumann Spike Temperature Ratio

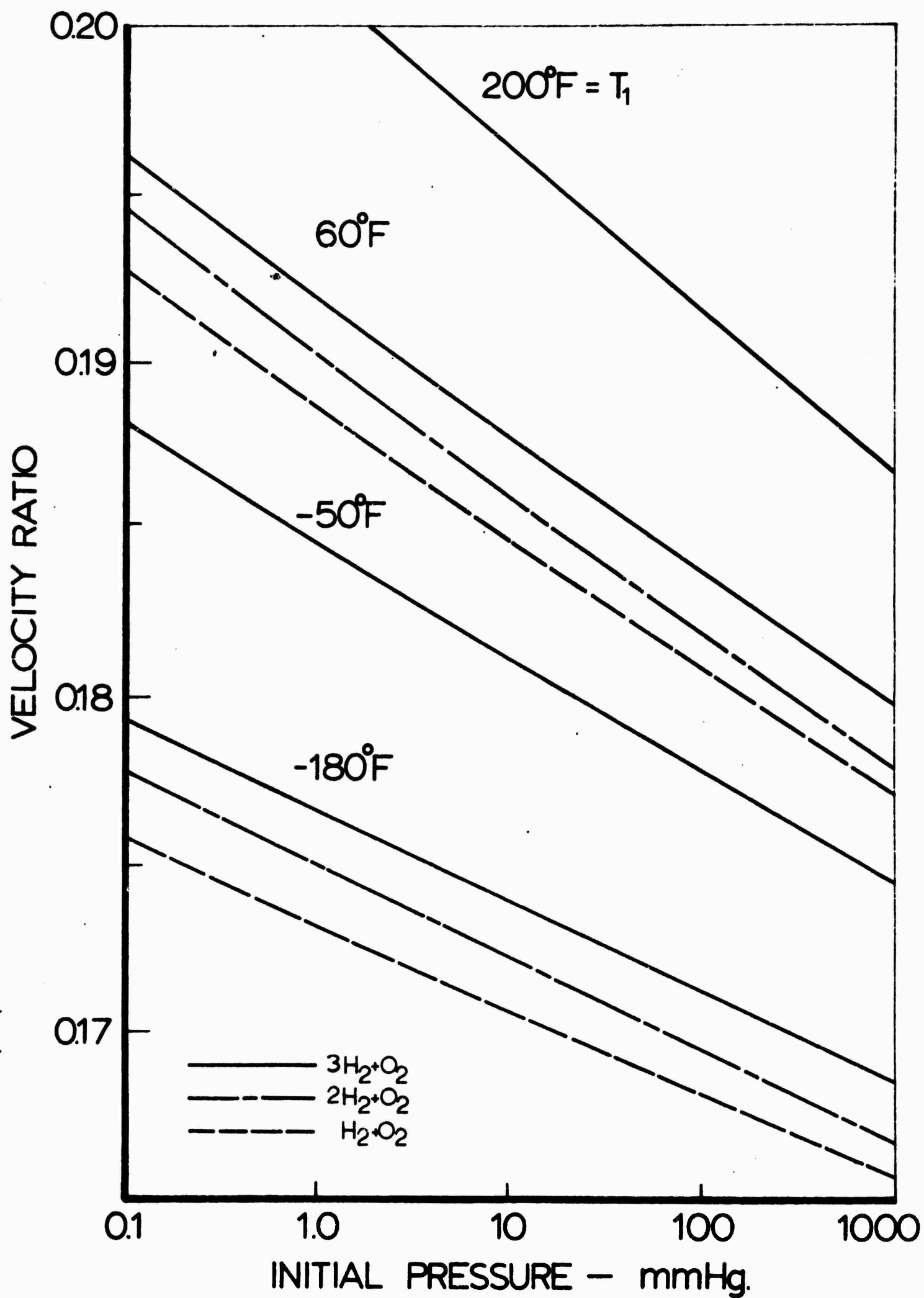


Fig. 31: Influence of Initial Pressure on Von Neumann Spike Velocity Ratio